PhD degree in Molecular Medicine, curriculum in Molecular Oncology
European School of Molecular Medicine (SEMM)
University of Milan and University Federico II of Naples
Faculty of Medicine

Unraveling Molecular Mechanisms Underlying *Meis1* Oncogenic Activity; Possible Competition With *Prep1*

Leila Dardaei Alghalandis
IFOM-IEO campus, Milan, Italy

Supervisor: *Prof. Francesco Blasi*
IFOM-IEO campus, Milan, Italy

Co-supervisors:
Prof. Stefano Casola
IFOM-IEO campus, Milan, Italy

Prof. Eric CW So
King's College, London, UK

Academic year 2011-2012

To the memory of a friend

Table of Contents

ABBREVIATIONS

293 cells	human embryonic kidney 293 cell line
ACN	acetonitrile
ALL	acute lymphoblastic leukemia
AML	acute myeloid leukemia
APS	ammonium persulphate
AR	androgen receptor
bp	base pair
BSA	bovine serum albumin
CBB	calmodulin binding buffer
CBP	calmodulin binding protein
CDK	cyclin dependent kinase
ChIP	chromatin immunoprecipitation
CTD	C-terminal domain
DAPI	4′, 6-diamidino-2phenylindole
DMs	double-minute chromosomes
DMSO	dimethyl sulfoxide
DOT1L	disruptor of telomeric silencing like 1
dpc	days post coitum
EMT	epithelial-mesenchymal transition
emPAI	exponentially modified protein abundance index
ER	estrogen receptor
ESCC	esophageal squamous cell carcinoma
FACS	fluorescence activated cell sorter
FLT3	Fms-like tyrosine kinase 3
FSHβ	follicle stimulating hormone
GM-CSF	granulocyte-macrophage colony-stimulating factor
GSK-3	glycogen synthase kinase 3
GST	glutathione S-transferase
HCC	hepatocellular carcinoma
HCV	hepatitis C virus
HD	homeodomain
ΔHD	homeodomain-less
HIFs	hypoxia inducible factors
HIV	human immunodeficiency virus
HP	hexapeptide motif
HR	homology region
ΔHR	homology region-less
HSRs	homogeneously staining regions
IBB	IgG binding buffer immunoprecipitation
Im	immortalized
IP	immunoprecipitation
IPTG	isopropyl-β-D-thiogalactopyranoside
kb	kilobase
KD	knock down
KO	Knockout

MEFs	mouse embryonic fibroblasts
MLL	mixed-lineage leukemia
NES	nuclear export signal
NLS	nuclear localization signal
NP-40	noyl phenoxypolyethanol-40
NTD	N-terminal domain
OD	optical density
PBS	phosphate-buffered saline
PBX	pre-B cell leukemia homeobox
PDGF	platelet-derived growth factor
PI	propidium iodide
PREP1	PBX regulating protein1
***Prep1*$^{i/i}$**	hypomorphic Prep1
Ras	rat sarcoma
RB	retinoblastoma-associated
RSV	rous sarcoma virus
SD	standard deviation
SDS-PAGE	sodium dodecyl sulphate polyacrylamide gel
TALE	three aminio acid loop extension
TAP	tandem affinity purification
TCB	TEV Cleavage Buffer
TEV	tobacco etch virus
TF	transcription factor
TGFα	tumor growth factor α
Tm	melting temperature
VEGF	vascular endothelial growth factor
WB	western blot
WT	wild-type

Figures and Tables Index

Figures Index

Tables Index

Abstract

Meis1 and *Prep1* homeodomain-containing transcription factors are essential for the normal embryonic development of several tissues and organs. Although they both can recruit Pbx at least for some of their biological function using the same homology region, the Meis1-Pbx and Prep1-Pbx complexes bind different DNA sequences and play opposite roles in tumorigenicity. In cancer, *Meis1* has been extensively implicated in leukemia and neuroblastoma. Overexpression of *Meis1* greatly shortens the latency and affects the penetrance of myeloid leukemia induced by *Hox* genes retroviral transduction. Furthermore, *Meis1* has essential oncogenic function in all human leukemic *MLL*-translocation. Although, *Meis1* is strongly suggested for involvement in human neuroblastoma and glioma, its function in non-hematological malignancies and solid tumors remains poorly defined. In contrast, Prep1 does not accelerate *Hox*-induced leukemogenesis. In fact heterozygous or homozygous *Prep1*-deficient mice develop tumors at high frequency. In mice, *Prep1* haploinsufficiency causes spontaneous tumor formation and accelerates development of tumors in *EμMyc* transgenic mice. In human tumors, PREP1 is absent or downregulated in a large fraction of tumors including lung, breast and colon cancers. Therefore, *Prep1* exerts tumor suppressor function in the cell by maintaining genomic stability and hence preventing neoplastic transformation.

Here I show that Meis1 is involved in malignant transformation of *Prep1*-deficient MEFs and that this can be partially rescued by re-expression of Prep1. I demonstrate that the Pbx-interacting domain of Prep1 is involved in its tumor suppressor function. Moreover, Both Meis1 and Prep1 require Pbx1 for their oncogenic and tumorsppressive functions, respectively. Therefore Meis1 and Prep1 do compete for Pbx1 in the context of tumor development. Furthermore, I find Meis1 interacts with Ddx3x and Ddx5 RNA helicases,

which is perturbed in the presence of Prep1. Together, the presented results suggest that *Meis1* is a bona-fide oncogene also in non-hematic cells and that *Prep1* impairs *Meis1* tumorigenicity by either competing for Pbx1 or preventing its interaction with transcriptionally relevant partners.

Chapter 1: *Introduction*

1.1. The Evolution of Cancer

Cancer (neoplasm) is a family of genetic diseases that results from uncontrolled cell division and tissue invasiveness (metastasis). The failure to regulate cell proliferation and consequent metastasis is caused by dynamic alterations in the genome and epigenome of the cancer cells. Somatically acquired abnormalities in DNA sequence and selection lead to the alterations of the cancer cell genome. These somatic mutations according to their contribution in cancer development may be classified into driver and passenger mutations. Driver mutations confer growth advantages to the cancer cells and are positively selected during the evolution of the cancer. They tend to cause clonal expansion of cancer cells. Passenger mutations are present in a cancer genome as a by-product of cancer cell development and do not contribute to the cancer development. However, they may be associated with a clonal expansion caused by driver mutations [1,2,3,4,5,6].

A growing body of evidence resulting from the study of epigenetic mechanisms in cancer has shown that cancer is not solely a consequence of genetic alteration of the cancer-critical genes. Cancer cells have a different epigenome compared to their normal counterparts. For instance hypomethylation of cancer cells was one of the first epigenetic alterations found in human cancers [6]. Cancer development is a multistep process and it requires the accumulation of different mutations during the lifetime of the cancer patient. During each step, cells acquire genetic alterations that progressively transform normal cells into more malignant ones (Figure 1.1) [1,2,5].

Cancers are classified into different types according to the type of their original cell, including carcinoma (epithelial cell), glioma (glial brain cell), sarcoma (mesenchymal cell), lymphoma and leukemia (bone marrow and blood cells), mesothelioma (mesothelial

cells that cover the peritoneal and pleural cavities), choriocarcinoma (placenta), and germinoma (germ cell of the testes or ovary) [1].

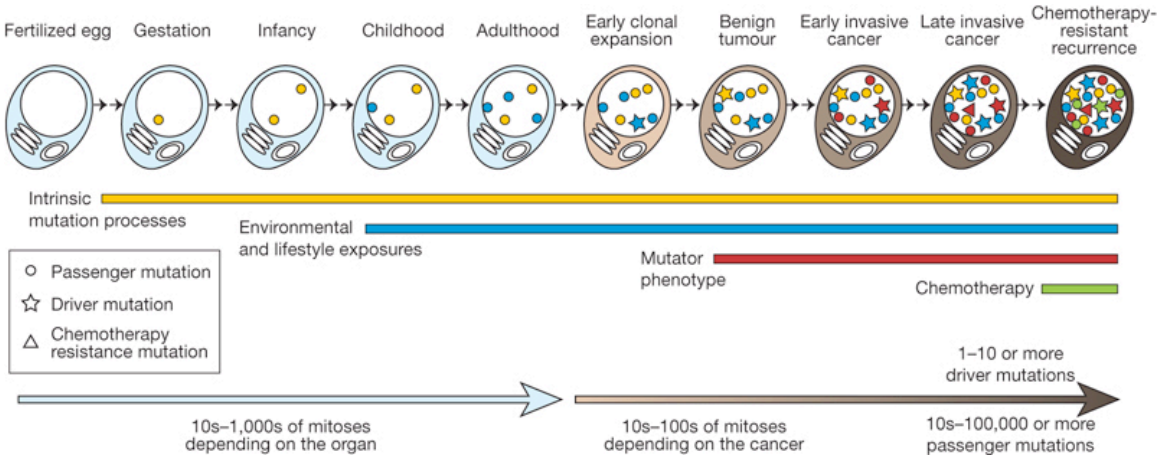

Figure 1.1. Somatic mutations occurring from a fertilized egg to a single cell within a cancer. Mutations accumulate because of the intrinsic mutation rate during normal cell divisions and of the formation of mutations because of exogenous mutagens. Other processes may contribute to the cancer development by mutational burden. Passenger mutations may be acquired while the cell lineage is phenotypically normal. Driver mutations will cause a clonal expansion and resistance to chemotherapy [5].

1.2. Cancer Critical-Genes

The term " cancer-critical genes" includes all genes whose mutations contribute to the tumorigenicity. The affected genes are divided into two broad categories, according to their functions. Cancer risk may arise either from the activation or inactivation of the cancer-critical genes. Genes of the first category, for which a gain-of-function mutation drives a cell towards cancer, are called proto-oncogenes; their mutant overactive forms are called oncogenes. Genes of the second category, for which a loss-of-function mutation impacts normal cellular mechanisms, are defined as tumor suppressor genes [1,7].

1.2.1. Oncogenes

1.2.1.1. Discovery of Oncogenes

In the 1960s, it was realized that some animal cancers were caused by viruses. These observations led to the discovery of the first oncogene from the Rous Sarcoma Virus (RSV) called *v-src* (the viral oncogenes are called v-oncogenes) in 1970. Studies of RSV mutant revealed that RSV did not require *v-src* gene for its replication. Further studies showed that *v-src* was homologous to a host cellular gene (*c-src*) that was widely conserved in eukaryotic species. Studies of other transforming retroviruses from various species have led to the discovery of different retroviral oncogenes. The retroviral oncogenes are copies of normal cellular genes, the proto-oncogenes, that are captured from the genome of the host through a process known as retroviral transduction [7,8,9].

1.2.1.2. Function of Oncogenes

Proto-oncogenes encode proteins that control cell proliferation, apoptosis or both. They can be activated to become oncogenes through alteration of the structure and/or amplification. The activated oncogenes which are capable of inducing neoplastic phenotypes in the cells, can be divided into six different groups based on the function and biochemical characteristics of protein products of their normal counterparts (proto-oncogene): transcription factors, chromatin remodelers, growth factors, growth factor receptors, signal transducers, apoptosis regulators [7,10]. In section 1.4, I will discuss the oncogenic functions of transcription factors with the specific focus on the TALE family of homeodomain containing transcription factors.

1.2.1.3. Oncogene Activation

Oncogenes can be activated through genetic alterations of cellular proto-oncogenes, which involve a gain of function. This can be mediated through three different genetic

mechanisms in human neoplasms: (1) mutation, (2) gene amplification, and (3) chromosome rearrangements. All these changes lead to either a change in the structure of proto-oncogene or deregulation of its expression [7]. Different types of mutations, such as base substitutions, deletions, and insertions are able to activate proto-oncogenes through alterations in the structure of their encoded proteins. These alterations, which usually impact critical regulatory regions of a protein; enhance the transforming activity of the mutated protein [11]. For example, point mutations in key codons are frequently detected in the *RAS* family of proto-oncogenes. The mutated *RAS* encodes a protein that remains in the active state, which leads to continuous signal induction. The incessant signal transduction induces continuous cell growth [12].

Many cancer cells contain several copies of structurally normal oncogenes. The increased copy number of a gene due to genomic changes is called gene amplification. It was first discovered in some tumor cells, which acquire resistance to anti-growth treatments. The process of gene amplification, which takes place through redundant replication of genomic DNA, often creates chromosomal abnormalities called double-minute chromosomes (DMs) and homogeneously staining regions (HSRs) [7,13,14]. The high frequency of DMs and HSRs in human tumors suggests that the amplification of specific proto-oncogenes may be a common occurrence in malignancies. Studies then showed that three proto-oncogene families including *MYC*, *ERBB*, and *RAS* are usually found amplified in a large number of human tumors [13].

Chromosomal rearrangements are more common in hematological malignancies than solid tumors. These cytogenetic abnormalities consist mainly of chromosomal translocations. Chromosomal rearrangements increase or deregulate transcription of the oncogenes by transcriptional activation of proto-oncogenes or the creation of fusion genes. For example, transcriptional activation occurs when a proto-oncogene is moved

next to an immunoglobulin or T-cell receptor gene. In this condition, regulatory elements of the immunoglobulin or T-cell receptor locus control the transcription of the proto-oncogene [7]. The t(8;14)(q24;q32) translocation found in Burkitt lymphoma is one of the well studied examples of proto-oncogene activation. This chromosomal rearrangement brings the c-*Myc* gene under control of regulatory elements of the immunoglobulin heavy chain locus [15,16]. Gene fusions sometimes form chimeric transcription factors. For example, the E2A/PBX1 fusion protein found in childhood pre-B-cell ALL results from t(1;19)(q23;p13) translocation [16].

1.2.2. Tumor-Suppressor genes

The discovery of the oncogenes fueled the idea that different classes of genes must exist to carry out tumor-preventing functions. In fact, somatic cell fusion and chromosomal segregation experiments confirmed the existence of such genes involved in tumor suppression [17]. Over the years many such tumor suppressor genes have been identified based on the fact that only one single functional allele of the gene is sufficient to manifest cancer-preventing effects. These prototypic tumor suppressor genes are recessive and follow the "two-hit hypothesis" proposed by A.G.Knudson [18]. This hypothesis implies that biallelic gene inactivation is required before an effect is observed [18]. Further studies showed that not all tumor suppressor genes follow this hypothesis. Some tumor suppressors are haplo-insufficient for tumor progression; meaning that inactivation of a single tumor suppressor gene either by mutation, deletion or methylation-mediated transcriptional silencing provides a selective advantage during tumorigenesis. For example, inactivation of a single allele of the genes encoding *Prep1*, *p53*, *TGF-β*, *27kip1* and *Dmp1* is sufficient to predispose mice to tumor development [19,20,21].

More than 30 tumor suppressors have been identified [22] that control a broad range of critical and highly conserved normal cellular activities including cell cycle checkpoint control, apoptosis, control of genomic integrity and repair of DNA damages, signal transduction, cell differentiation and adhesion, and angiogenesis. These functions can be deregulated in cancer cells [23]. Thus, tumor suppressor genes can be divided into gatekeepers, caretakers and landscapers based on their primary functions [24].

The "Gatekeeper" term was first proposed to explain the role of adenomatous polyposis coli tumor suppressor gene, which is consistently found mutated in colorectal tumorigenesis. Gatekeeper genes encode proteins that act directly to inhibit tumor growth by either suppressing proliferation, inducing apoptosis or promoting differentiation. Since, the loss of function of these genes is the rate-limiting event in tumorigenesis, the restoration of their function suppresses neoplasia. Each cell type has few gatekeepers, which are specific to the tissue in which they reside. Individuals with a hereditary mutation in one of two alleles of a gatekeeper gene are disposed to neoplasia [24,25].

"Caretaker" genes help to maintain genomic stability by encoding proteins that act in DNA repair and mitotic checkpoint pathways such as *MLH1, BRCA1, MYH, and XPA*. They indirectly suppress cell proliferation by ensuring the fidelity of DNA. Caretakers do not directly contribute to cancer development but their loss of function increases the DNA mutation rate, raising the probability that gatekeeper gene function will be lost. These alterations in caretaker genes will increase cancer development risk by 5 to 50 fold [24,25].

The products of third class of tumor suppressor genes, the "landscapers", act by modulating the microenvironment of the tumor cells. These genes regulate extracellular matrix proteins, cell surface receptors, adhesion proteins or secreted growth factors. Loss

of function mutations of landscapers generate aberrant microenvironment that prompts the neoplastic transformation of the adjacent epithelia [24,26].

1.3. " The Hallmarks of Cancer"

12 years ago, Hanahan and Weinberg [2] enumerated six "Hallmarks of Cancer" which provided a logical framework to summarize and understand several decades of intense research dedicated to cancer. These six common traits ("Hallmarks"), which govern the transformation of normal cells to cancer cells, are essential for a cell to acquire a cancer phenotype by a multistep process. In 2011, they added two emerging hallmarks to this list due to the conceptual progress in the last decade. The complexity of the more than 100 different types of human cancers arises from disruption of the distinct regulatory circuits of the cells that govern normal cell proliferation and homeostatsis. Hanahan and Weinberg proposed that this complexity can be explained by a small number of traits that are common between most and perhaps all types of human tumors [2,27]. In the following sections these traits are discussed.

1.3.1. Sustaining Proliferative Signals

Tumors arise from unconstrained proliferation of cells harboring oncogenic activating or tumor suppressor inactivating mutations. Thus, uncontrolled proliferation is one of the fundamental features of cancer development. Normal cells require mitogenic growth signals to exit from a quiescent state and enter into active proliferation state. The growth-promoting signals released from a cell are transmitted through transmembrane receptors to its neighbors. Cell proliferation relies on the availability of growth promoting signals and normal cells stop proliferating in the absence of these signals. Cancer cells

develop a number of alternative ways to grow and proliferate independent of the absence of exogenous mitogenic signals [2,27]. Some cancer cells produce their own growth factors. The production of tumor growth factor α (TGFα) and platelet-derived growth factor (PDGF) by sarcomas and glioblastomas, respectively, are two representative examples [7]. They can also stimulate normal cells present in the tumor microenvironment to produce different growth factors [28]. The cell surface receptors that bind to the growth factors and transmit the growth signals inside the cell are often overexpressed in many cancer types. This elevation of the receptors makes cancer cells hypersensitive to a minimal amount of the growth factor which normally would not trigger proliferation [7]. For instance, the *HER2/neu* is overexpressed in stomach and mammary carcinomas [29]. Additionally, structural alterations of the receptor can also lead to ligand-independent signaling. Furthermore, growth factor autonomy may be achieved by constitutive activation of components of signaling pathways operating downstream of these receptors [30].

1.3.2. Evading Growth Suppressors

Cells have evolved stringent mechanisms to control proliferation and tissue homeostasis via positively and negatively acting growth signals. Like the growth-promoting signals, which were discussed in the previous section, the growth-inhibitory signals are transmitted through transmembrane cell surface receptors. These signals block proliferation either by transiently forcing cells out of the proliferative state into the quiescent state or by permanently preventing their proliferative ability by driving cells into a postmitotic state. The growth suppressor program is usually governed by tumor-suppressors that act in different ways to inhibit cell growth and proliferation. The inactivation of these tumor suppressors conveys various capabilities to the cancer cells to

evade the anti-proliferative signals [2,27]. RB (retinoblastoma-associated) and p53 proteins are the typical examples of the key tumor suppressors that control cell proliferation decision or activation of senescence and apoptosis programs. They are frequently inactivated in cancer by loss of function mutations [31,32,33].

1.3.3. Resisting Cell Death

Normal tissues maintain their homeostasis by balancing the rates of cell proliferation and cell death. Programmed cell death known as apoptosis plays a major role in maintaining cell population in the different tissues. Apoptosis can be triggered either by an extrinsic pathway mediated by cell surface death receptors bound by extracellular ligands, or by an intrinsic pathway mediated by mitochondria. The latter is triggered in response to different extracellular and intracellular stresses, such as growth factor depletion, hypoxia, DNA damage and oncogene induction. The ability of transformed cells to bypass the apoptotic barrier is widely implicated in the pathogenesis of cancer. Tumor cells develop different strategies to attenuate or escape apoptosis including the loss of *p53* tumor suppressor, increasing expression of anti-apoptotic regulators and survival signals or down regulating the pro-apoptotic signals [27,34].

1.3.4. Enabling Replicative Immortality

Normal cells have a finite replicative capability and are able to pass through certain and limited number of cell growth and division cycles. Mammalian cells in culture stop growing and go into senescence after 60-70 doublings. Some cells succeed to bypass this barrier and go into a crisis phase, which involves apoptosis and karyotypic abnormalities. Rarely, cells from a population in crisis acquire indefinite replicative potential. This

transition is called immortalization, which is one of the characteristics of the tumor cells [35]. In non-immortalized cells, the telomeres protecting the ends of chromosomes progressively shorten with each cell division, which leads to the end-to-end fusions of chromosomes, karyotypic disarray, crisis and cell death. Telomerase, which is responsible to maintain telomeric DNA is mainly absent in non-immortalized cells but is expressed at high level in a large majority of immortalized cells including human cancer cells [2,27].

1.3.5. Inducing Angiogenesis

Inducing and sustaining of angiogenesis in tumors are crucial for their growth. In the adult angiogenesis is only transiently turned on in response to physiological processes such as wound healing. But during neoplastic growth an "angiogenic switch" is activated which remains on. This forces the normal quiescent vasculature to generate new vessels that helps to expand tumor growth by supplying nutrients and oxygen. The activation of the angiogenic switch is mediated by changing the balance of angiogenic inducers and inhibitors. For instance, vascular endothelial growth factor (VEGF) that induces angiogenesis is over expressed in tumors compared to their normal tissue counterparts. On the other hand, the angiogenic inhibitor thrombospondin-1, positively regulated by p53 tumor suppressor protein, is down regulated in tumors [2,27].

1.3.6. Activating Invasion and Metastasis

Metastasis, the dissemination of cancer cells from their primary site to adjacent and distant organs, is the leading cause of death in patients with solid cancers. Invasion and metastasis are multistep process. This process begins with local invasion followed by intravasation of cancer cells in the nearby vessels and circulation of the cells through the

lymphatic and hematic systems. This process will end up with the extravasation of the cancer cells to the distant tissues and with the formation of micrometastatic lesions. At the molecular level, proteins involved in cell-to-cell and cell-to-matrix adhesion are important. E-cadherin, an important Ca(2+)-dependent cell-to-cell adhesion molecule, is a key suppressor of metastasis. This protein along with other adhesion molecules involved in cell-to-matrix adhesions is down regulated in cells possessing invasive or metastatic capabilities [2,27].

1.3.7. Reprogramming Energy Metabolism

Under normoxic conditions, cells normally process glucose through glycolysis followed by oxidation of pyruvate in mitochondria. In anaerobic condition, however, glycolysis occurs in the cytosol and is followed by lactic acid fermentation. However, malignant cells usually limit their energy metabolisms mainly to glycolysis, even under normoxic conditions. This phenomenon is known as the Warburg-effect. There are several explanations for the Warburg-effect such as mitochondrial damage, adaptation to hypoxic environments, and shut down of mitochondria because of their involvement in apoptosis. Glycolysis provides most of the intermediates necessary for the production of nucleosides and amino acids, which facilitates biosynthesis of the macromolecules and organelles required for active cell proliferation. Therefore, Cancer cells often switch their metabolic pathways to anaerobic glycolysis to support the uncontrolled and continuous cell proliferation [27].

1.3.8. Evading Immune Destructions

Multiple line of evidence point out that the immune system plays an important role in the recognition and eradication of malignant cells. The cancer immunosurveillance theory proposes that immune cells which constantly monitor cells and tissues, recognize and eliminate continuously arising, nascent transformed cells by immunoediting. Immunoediting is a process, which protects the individual from cancer growth and the development of tumor immunogenicity. It is composed of three major phases including, elimination, equilibrium, and escape. Although both innate and adaptive immune systems contribute significantly to immunosurveillance, many tumors manage to escape the immune barrier and drive immunological tolerance. This may lead to tumor progression by mimicking immune signaling pathways that impact the tumor microenvironment and activate immunosuppressive cells such as regulatory T (Treg) and myeloid-derived suppressor cells (MDSCs) [27].

1.4. Transcription Factors

Transcription factors are sequence-specific DNA binding factors that regulate the transcription of target genes at the level of regulatory regions such as promoters or enhancers [36]. Most of the approximately 2600 proteins in the human genome that contain DNA-binding domains are thought to act as transcription factors. Therefore, almost 10% of the protein-coding genes in the human genome encode proteins that regulate transcription, which makes this family the single largest family of human proteins [37,38]. Multigene families of transcription factors share common DNA-binding domains such as zinc finger, leucine-zipper, helix-loop-helix and homeodomain motifs [39]. Transcription factors usually act in complex by binding to other proteins. They

operate as final link in the signal transduction pathway that translates cellular signals by alteration of gene expression [1].

Proto-oncogene transcription factors were discovered through their retroviral homologs. Chromosomal translocations often activate transcription factors in haematological and solid malignancies [40]. Examples of proto-oncogene transcription factors include *Hoxa9, Meis1, Pbx1, erb A, ets, fos*, *jun*, *myb*, and c-*myc*. For example, *Hoxa9* transcription factor cooperates with *Meis1* transcription factor in the induction of acute myeloid leukemias (AML) [41,42,43]. E2A-PBX1 chimeric protein which results from chromosomal translocation of the basic helix-loop-helix transcription factor *E2A* with the gene encoding the homeodomain protein *PBX1* can cause pre-B cell acute lymphoblastic leukemias (ALL) [16].

1.4.1. Homeodomain Family of Transcriptional Regulators

Homeobox was independently identified by two different groups in 1984 as a sequence motif shared between the Antennapedia and the Bithorax complexes, two homeotic loci in *Drosophila*. The mutations of these homeotic genes result in conversion of one body part to another [44,45]. Homeobox is an evolutionarily conserved 180-base-pair sequence motif located in a large number of genes virtually in all eukaryotic species. The homeobox encodes a 60 amino acids DNA binding domain known as the homeodomain. The helix-turn-helix structure of the homeodomain is composed of three α-helices around a hydrophobic core that are essential in maintaining the structural integrity and in making essential contacts with DNA (Figure 1.2). Homeobox genes play critical roles in different cellular processes, including body plan specification, pattern formation, and cell fate determination during development [46,47]. These “master

regulators" of development also control various cellular processes including proliferation, differentiation, apoptosis, cell shape, cell adhesion and migration [48].

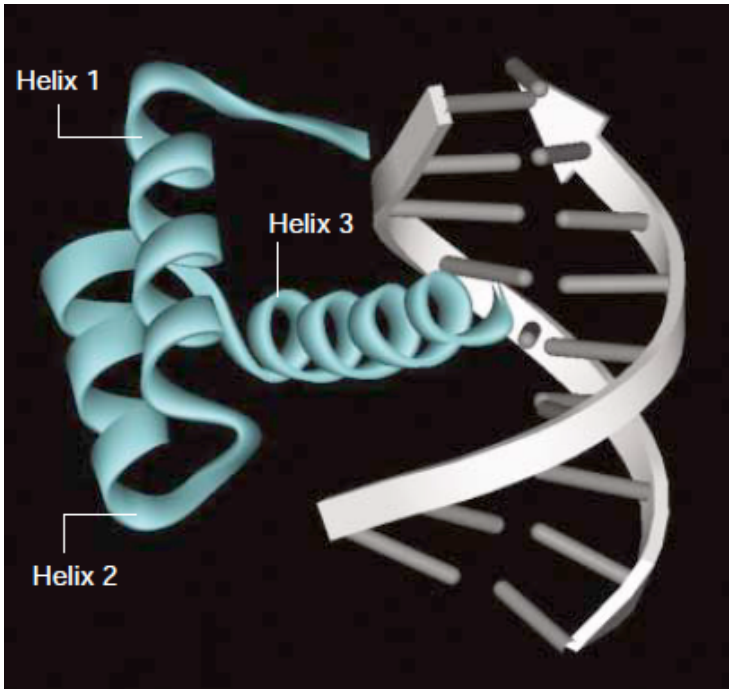

Figure 1.2. Homeodomain-DNA complex [49]. To form this complex the N-terminal tail of helix 1 inserts into the minor groove of DNA and helix 3 lies in the major groove.

The high number of homeodomain containing genes sometimes cause difficulty in their classification. In the human genome at least 200 homeobox genes have been estimated [50]. These genes are divided into nine superfamilies on the basis of the level of similarity among their respective homeodomains. These superfamilies include the ANTP (including the HOX and NKL families), PRD (including the PAX family), POU, HNF, LIM, SINE, CUT, ZF, PROS and TALE groups (Figure 1.3) [50] .

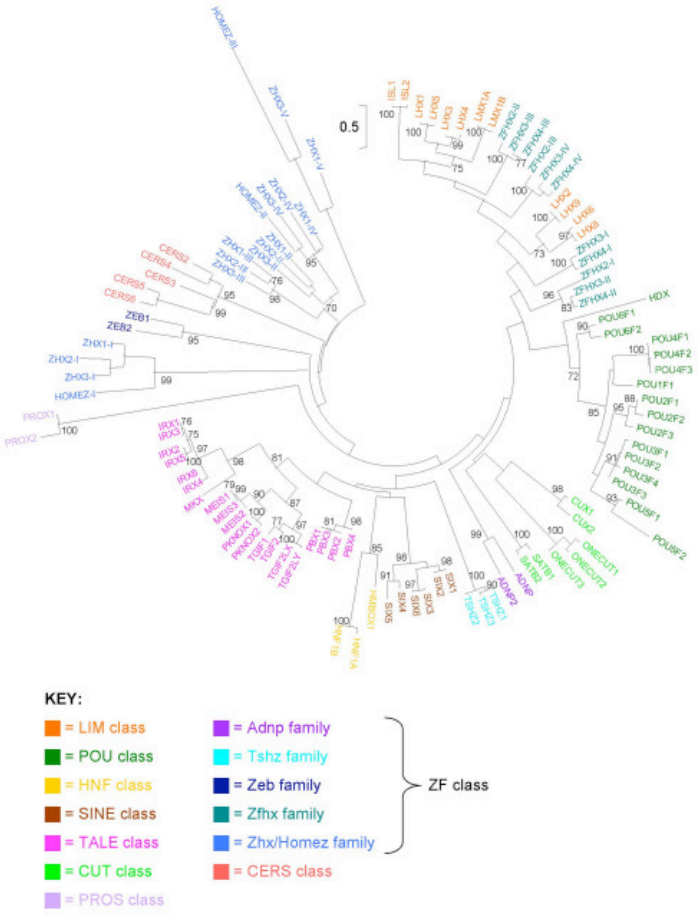

Figure 1.3. Phylogenic tree of human homeodomain proteins excluding ANTP and PRD classes is constructed using maximum likelihood method [50].

1.5. *HOX* Genes and Their Role in Cancer

In contrast to most homeobox genes, which are dispersed throughout the genome, *HOX* genes are organized in chromosome clusters. In man, 39 *HOX* genes are organized in 4 clusters (A-D). They are expressed in an orderly manner corresponding to their positions from the 3′ to the 5′, within each cluster. *HOX* genes function to pattern the anterior-posterior body axis of embryos. They are also involved in various processes including limb bud axis patterning, hematopoiesis, organogenesis, apoptosis, receptor signaling, differentiation, motility, and angiogenesis [51,52].

The homeobox motif of *HOX* genes is located in exon 2, placing the homeodomain

in the C-terminal half of the protein. In addition to the homeodomain, HOX proteins contain a short conserved tryptophan-containing hexapeptide motif (HP) that is required to mediate specific interactions with the TALE motif (Three Amino acid Loop Extension) of PBX homeodomain proteins [53]. HOX proteins can regulate the transcription of downstream targets by acting as monomers, homodimers or heterodimers with the TALE family of cofactors or with the non-homeodomain proteins such as CBP and SMAD [52].

This subgroup of the homeobox superfamily not only is crucially important in developmental regulation, but also is implicated in a growing number of diseases, including cancer. Aberrant expression of *HOX* genes has been described in many solid tumors and leukemias. The deregulated expression of *HOX* genes perturbs the fine balance between cell proliferation and differentiation that is essential for the normal development and differentiation. Different mechanisms can alter this balance leading to malignancies. The first mechanism is "temporospatial deregulation". In this case the expression pattern of *HOX* genes in tumors arising from a specific tissue temporospatially differs from that in normal tissue [49,52]. For instance, the expression levels of all *HOX* genes in 48 primary esophageal squamous cell carcinoma (ESCC) and 7 normal esophagus specimens were quantified by qRT-PCR. The results showed that in normal esophagus more 3′ *HOX* genes are expressed compared to the 5′ genes. However, in tumor samples the expression of 5′ *HOX* genes was significantly increased [54]. The second is "gene dominance", in which *HOX* genes are overexpressed in tumors compared to the normal tissues [49,52]. *HOXA9* is overexpressed in acute myeloid leukemia (AML) that is correlated with poor prognosis and treatment failure in AML patients [55]. Moreover, the chromosomal translocation between *HOXA9* and other *HOX* genes with the nucleoporin protein NUP98 leads to the formation of fusion proteins, which inhibit differentiation and induce transformation of hematopoietic progenitor cells [56,57,58].

The last mechanism is "epigenetic deregulation" in which *HOX* genes are aberrantly silenced or downregulated due to promoter methylation in the tissues in which they are normally expressed [49,52].

The perturbation of normal *HOX* gene expression affects different pathways that induce tumorigenesis. Some result in the maintenance of more embryonic state through the suppression of differentiation or activation of anti-apoptotic pathways. For instance, *HOXC8* overexpression in prostate cancer specimens correlates with loss of differentiation and androgen-independent proliferation [59,60]. Downregulation of *HOXA5* and *HOXA10* perturbs the balance between apoptosis and proliferation. In this case, downregulation of these genes leads to the suppression of *p53* expression and therefore to the block of apoptosis in a breast cancer cell line [61,62]. In some tumors altered receptor signaling pathways due to the deregulation of *HOX* genes drives tumor growth. For example in ovarian and breast cancer *HOXB13* exerts oncogenic activity by ER upregulation and tamoxifen resistance [63]. The involvement of *HOX* gene in the pathogenesis of different cancer has been summarized in table 1.1 [52].

Table 1.1. Overview of *HOX* genes dysregulation in tumorigenesis [52]

Tumour type	Hox gene	Mechanism of Hox effect	Change in Hox gene	Effect
Oesophageal squamous cell carcinoma	5′ Hox genes[41]	Temporospatial deregulation	Overexpression	Associated with primary tumours
Lung carcinoma	5′ HOXA, 5′ HOXD, *HOXA1* and *HOXC5* (REF. 124)	Gene dominance	Overexpression	Associated with primary tumours
	HOXA7 and *HOXA9* (REF. 21)	Epigenetic deregulation	Promoter methylation	Associated with primary tumours
Neuroblastoma	*HOXD1* and *HOXD8* (REF. 61)	Temporospatial deregulation	Expression	Expressed in differentiated cell lines
	HOXC6 and *HOXC11* (REF. 14)	Temporospatial deregulation	Expression	Causes differentiation of S-type GOTO cell line
Ovarian carcinoma	*HOXB13* (REF. 16)	Gene dominance	Overexpression	Associated with primary tumours; upregulation of ER; and tamoxifen resistance *in vitro*
	HOXA7 and *HOXA9–11* (REF. 66)	Temporospatial deregulation	Expression	Associated with primary tumours and specific histological subtypes
Cervical carcinoma	HOXC cluster[125]	Gene dominance	Overexpression	Associated with primary tumours
	HOXC10 (REF. 18)	Gene dominance	Overexpression	Increased invasion; necessary for transition of HGSIL to squamous cell carcinoma
Prostate carcinoma	*HOXB13* (REFS 10,62)	Temporospatial deregulation	Downregulation	Loss of differentiation; allows transactivation of AR and proliferation
	HOXC8 (REF. 64)	Gene dominance	Overexpression	Associated with primary tumours; loss of differentiation and AR-independent growth
Breast carcinoma	*HOXA5* (REFS 15,78,79)	Epigenetic deregulation	Promoter methylation and downregulation	Downregulation of p53; decreased RARβ-driven apoptosis through caspase 2 and caspase 8
	HOXA10 (REF. 81)	Temporospatial deregulation	Downregulation	Downregulation of p53 in ER-positive primary tumours
	HOXB7 (REFS 17,72,73)	Gene dominance	Overexpression	Upregulation of FGF2 in cell culture; associated with bone metastases when compared with primary tumours or other metastases; increased invasion and vascularization *in vitro*; increased and larger metastases in cell lines with *ERBB2* (also known as *HER2*) amplification
	HOXB13 (REFS 12,75,76)	Gene dominance	Overexpression	Associated with tamoxifen resistance in ER-positive primary tumours; increased migration and invasion *in vitro*; downregulation of ER and tamoxifen resistance *in vitro*
Leukaemia	*HOXA9*, *HOXA10*, *HOXC6* and *MEIS1* (REF. 70)	Gene dominance	Overexpression	Upregulated by *MLL* translocations in acute leukaemias; associated with aggressive ALL
	HOXA9 (REFS 27,28,43,47)	Temporospatial deregulation	Overexpression	Poor prognostic indicator for AML; increased proliferation alone, with increased phenotype when expressed in NUP98-HOXA9 fusion protein; upregulates MEIS1 and FLT3

ALL, acute lymphoblastic leukaemia; AML, acute myeloid leukaemia; AR, androgen receptor; ER, oestrogen receptor; FGF2, fibroblast growth factor 2 (also known as basic FGF); FLT3, fms-related tyrosine kinase 3; HGSIL, high grade squamous intraepitheliel lesion; MLL, myeloid/lymphoid or mixed-lineage leukaemia; RARβ, retinoic acid receptor-β.

1.6. The TALE Family of Homeobox Genes

TALE superclass of homeodomain proteins is characterized by a divergent homeodomain harboring three extra amino acids in the loop between helix 1 and helix 2 of the DNA binding domain. This loop is crucial for the interaction with other homeodomain proteins [64]. This family forms an ancient subclass within the homeodomain transcription factors and plays crucial roles in the development of animal, plant, and fungi [64].

1.6.1. Classification

The TALE superclass of transcription factors is divided into five classes of genes in animals (*PBC*, *MEIS*, *TGIF*, *IRQ* and *MKX*), two in fungi (*M-ATYP* and *CUP*) and two in plants (*KNOX* and *BEL*) [64,65]. The PBC class in animals includes *PBX1*, *2*, *3* and *4* in mammals, Extradenticle (ExD) in *Drosophila* and Ceh-20 in C. elegans. The MEIS class is subdivided into two sub-families; the MEIS sub-family itself includes *MEIS1*, *2*, *3* in mammals, Homothorax (Hth) in *Drosophila* and unc-62 (ceh-25) in C. elegans. The PREP sub-family includes *PREP1/PKNOX1* and *PREP2/PKNOX2* in mammals and psa3 in C. elegans. There is no *PREP1* homolog in *Drosophila* but in other insects such as the malaria mosquito, the honeybee, and the red flower beetle there is both a *MEIS* and a *PREP* Homolog [64].

1.6.2. Evolution and Structure of *PBX*, *MEIS*, and *PREP* genes

In addition to the TALE homeodomain, there is another domain upstream of the TALE homeodomain that is conserved between animal *MEIS* genes and plant *KNOX* genes, which is called MEINOX [64,65]. A similar MEINOX domain is also present within the PBC domain of PBC class genes [66]. The significant sequence similarity between MEIS and KNOX and PBC domains indicates that they are derived from an ancient MEINOX domain already present when plants and animal diverged (Figure 1.3). The MEINOX domain is split into two subdomains, joined by a flexible linker. Secondary structure predictions suggest that the MEINOX domain is constituted of α helical structures [64]. However, no structural study is available. The PBX MEINOX domain is composed of two motifs, PBC-A and PBC-B, which together are known as the PBC domain. There is a third conserved motif downstream of the homeodomain that is called

PBC-C composed of 15 conserved residues which is essential for the interaction with HOX proteins on DNA (Figure 1.4) [64].

The MEINOX domain of MEIS and PREP proteins is also split into two motifs called HR1 (Homology Region 1) and HR2 or MEIS A and MEIS B motifs (together known as MEIS domain). The MEIS A motif of *PREP* genes is shorter than in *MEIS.* In addition, other structural differences between *MEIS* and *PREP* genes arise from three other motifs (MEIS C, MEIS D and MEIS N) present only in MEIS (Figure 1.4) [64].

The Prep1 homeodomain sequence has 44/60 (70% identity) identity and 54/60 (86% similarity) similarity to Meis1. However, Pbx1 homeodomain has 22/60 (35% identity) identical and 41/60 (65% similarity) similar residues with Prep1. Although Prep1 and Meis1 are highly homologous all over the homeodomain, this homology is mainly concentrated (16/18 residues) in the third helix (the DNA recognition helix). In addition to the homeodomain, Prep1 and Meis1 display strong homology over the HR1 and HR2 regions. Moreover, the position of HR1 and HR2 relative to the homeodomain is conserved between Prep1 and Meis1 proteins. Beside the homeodomain and HR1 and HR2 domains, these two proteins do not share high sequence similarity [67].

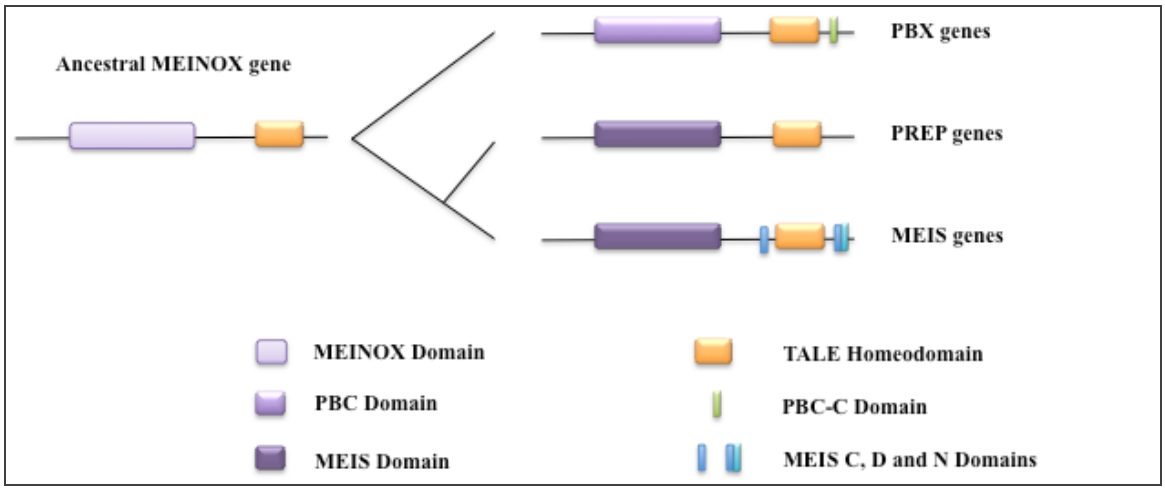

Figure 1.4. Evolutionary relationship between *Pbx*, *Meis* and *Prep* genes. Adapted from [64].

1.6.3. The Pbx Interaction with Meis/Prep Regulates their Sub-Cellular Localization.

The regulation of transcription factor activity plays an important role in various biological processes. Different mechanisms regulate the transcription factor activity such as post-translational modifications, expression level and protein stability. In addition, since a transcription factor exerts its transcriptional regulation role in the nucleus, the control of its nuclear localization plays a crucial role in this regulation [68]. Therefore the presence of Pbx1, Meis1 and Prep1 transcription factors in the nucleus of cells is determinant for the regulation of the appropriate target genes. Numerous studies have shown that Pbx1 nuclear/cytoplasmic distribution is tightly regulated through different mechanisms [69]. Now, I will focus on the role of Meis/Prep and Pbx interactions on their nuclear translocation (Figure 1.5). For this interaction, the PBC-A domain of Pbx1 [70,71] and the HR1 and HR2 domains of Meis1/Prep1 [67,71] are required. The LFPLL motif in HR1 is essential for Pbx1 binding [72]. Pbx1 and Meis1/Prep1 bind cooperatively to DNA, although they interact efficiently in the absence of DNA as well

[70,71,73]. Their interaction in the absence of DNA regulates the subcellular localization [74,75] and stability [74,76] of Pbx proteins.

Pbx1 has a dynamic subcellular localization. It contains two cooperative NLS (nuclear localization signal) [77] and two independent NES (nuclear export signal) [78]. The first NLS is located in the N-terminal arm of the HD (amino acids 234-239) and contains the consensus RRKRR sequence. The second, less conserved (KRIRYKKNI), is located in helix 3 (amino acids: 285–294) [77]. The two NES are located within the PBC-A domain spanning amino acids 45-72 and 73-90 respectively [78]. The two NES can mask and inhibit the NLS by an intramolecular interaction between the N-terminus and homeodomain of Pbx1. The conformational change of Pbx1 due to the interaction with Meis/Prep exposes the Pbx1 NLS, which causes their (Meis/Prep in complex with Pbx1) nuclear translocation [77]. The NES of Pbx1 mediates interaction with the nuclear export receptor Crm1 that exports Pbx from the nucleus. Interestingly, the two NESs are located within the domains required for the interaction with Meis/Prep and deletion of either of the two NESs impairs this interaction. Since the contact domain for Crm1 and Meis/Prep overlap, therefore the interaction of Pbx1 with Meis/Prep masks the NESs and allows Pbx-Meis/Prep to stay in the nucleus as heterodimers [68,75,78]. Pbx1 nuclear localization is not only dependent on the Meis/Prep interaction but there are other mechanisms, which regulate its subcellular distribution. However, Prep1 does not have its own NLS and mainly relies on Pbx-Prep interaction for its nuclear translocation [75].

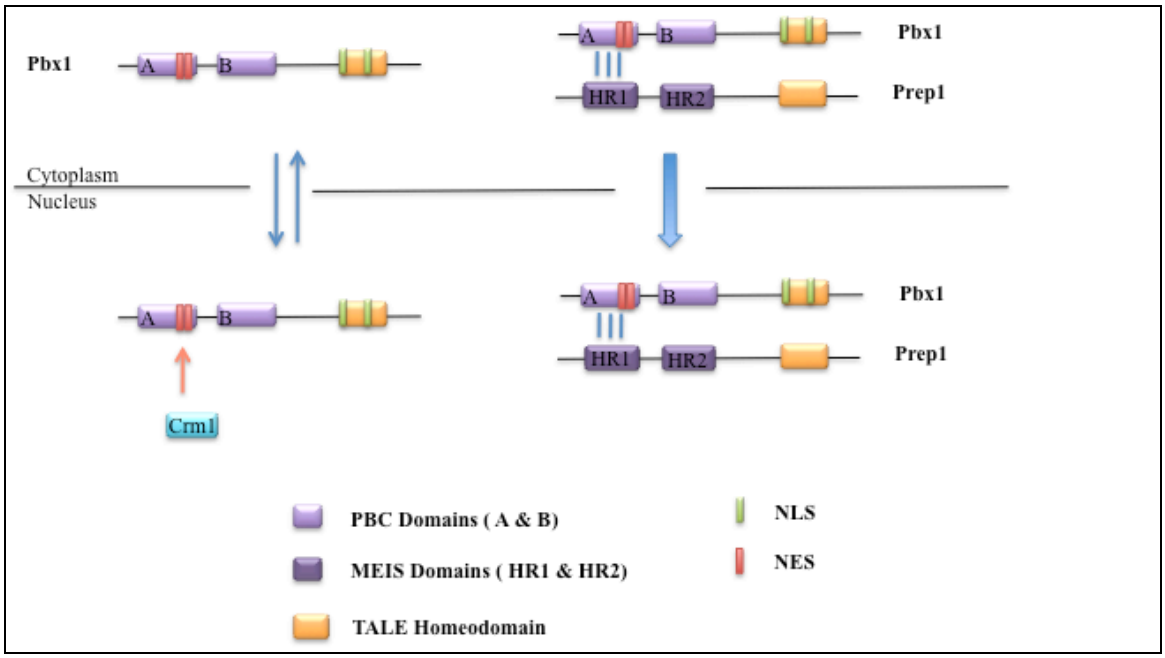

Figure 1.5. Pbx1 and Prep1 interaction and subsequent translocation to the nucleus. Pbx also interacts with Meis through the same domain and the subsequent complex translocates to the nucleus as shown in this figure. Adapted from [68,75,78].

1.6.4. The PBC Family in Mammals

The PBC family contains four members in mammals; *PBX1*, *PBX2*, *PBX3,* and *PBX4*. *PBX1* (Pre-B cell leukemia homeobox 1) was initially identified as E2A-Pbx1 oncogenic fusion protein resulting from chromosomal translocation t(1;9) in human pre-B cell acute lymphoblastic leukemia (ALL) [79,80]. *PBX2* and *PBX3* were identified based on their extensive homology to *PBX1*. Overall, PBX2 and PBX3 proteins have 92 and 94% identity to PBX1 over the 266 amino acids within and flanking their homeodomain. But they have significant differences in amino acid composition close to their amino and carboxy termini [81]. *PBX1* and *PBX3*, and not *PBX2*, have two isoforms with different carboxy termini due to alternative splicing: PBX1a, PBX1b and PBX3a, PBX3b [51,81]. *PBX2* and *PBX3* are expressed in embryonic and adult tissues as well as different cell lines and their expression is not restricted to the specific stage of the embryo development. However, *PBX1* is not expressed in lymphoid cell lines [81]. Also different

isoforms of *PBX1* show different expression patterns. For example, Pbx1a expression is restricted to neural tissues while Pbx1b exhibits widespread expression patterns in the mouse embryo [51]. Finally, the fourth mammalian *PBX* family member, *Pbx4*, is only expressed in testis, especially in spermatocytes in the pachytene stage of the first meiotic prophase [82]. The *PBX* genes are not clustered and map to different chromosomes: *PBX1* is mapped to the first chromosome in mouse and man, *PBX2* to chromosome 17 in mouse and 6 in man, *PBX3* to chromosome 2 in mouse and 9 in man [81], *PBX4* to chromosome 8 in mouse and 19 in man [82].

Since *PBX* genes show extensive sequence identity, their functional differences are not due to their biochemical functions but more likely to their different expression patterns [83]. For example the different PBX proteins show very similar DNA binding properties in *in vitro* assays [84]. Thus, PBX proteins might have at least partially redundant functions where their expression overlap. In general Pbx proteins are involved in diverse developmental processes. For instance Pbx1 is implicated in hematopoiesis, skeleton patterning, pancreas, and urogenital systems organogenesis [85,86,87].

1.6.4.1. Pbx Proteins as Hox Cofactors

Pbx proteins interact with Hox proteins from paralogue groups 1 to 10 to increase their DNA affinity and specificity [88]. This interaction is mediated by the binding of the Hox hexapeptide motif located in the N-terminal arm of the homeodomain to a hydrophobic pocket formed between the three amino acid loop extension and helix 3 of the Pbx homeodomain. This interaction is DNA-dependent [89]. Also the PBC-C domain of Pbx has been shown to be involved in Hox-DNA complex formation [64].

The identification of Hox/Pbx regulatory elements in the promoters of mammalian Hox genes was the first evidence that Pbx proteins function as Hox cofactors. This

regulatory element consists of paired Hox/Pbx binding sites and mutating either the Hox or the Pbx binding sequence abolishes its function [90,91]. The second piece of evidence came from the *Pbx* loss of function mice. *Pbx1* and *Pbx3* mutant mice are reminiscent of late stage *Hox* loss-of-function phenotype. *Pbx1* deficient mice develop normally till E11.5. But later display severe organ hypoplasia (lungs, liver, stomach), ectopia (thymus and kidneys) or aplasia (spleen), which lead to the death of the embryos at E15.5 [86]. For example, impaired hematopoiesis in *Pbx1*$^{-/-}$ embryos [92] resembles the *Hoxa9*$^{-/-}$ mutant phenotype [93] and the cervical vertebral malformations of *Pbx1*$^{-/-}$ embryos [86] recapitulate *Hoxa3*$^{-/-}$ and *Hoxd3*$^{-/-}$ loss-of-function phenotypes [94]. *Pbx3*$^{-/-}$ mutants die within few hours after birth due to central respiratory failure resulting from abnormal activity of inspiratory neurons in the medulla where this gene is highly expressed [95]. The congenital apnea phenotype seen in *Pbx3*$^{-/-}$ mice resembles *Rnx*$^{-/-}$ mutants phenotype. *Pbx2*$^{-/-}$ mice are instead viable and do not show obvious phenotypic anomalies [96]. This suggests that another member of PBC family compensates for the loss of *Pbx2* as observed by the phenotype of the double mutants [51].

In vivo observations, such as genetic interaction between Pbx1 and Hoxa2 to pattern branchial arch 2-derived craniofacial structures, suggest that Hox proteins act together with Pbx proteins to regulate developmental processes [51]. Finally Pbx presence is essential for Hox activity. For example anterior *hox* genes overexpression in zebrafish leads to a posterior transformation of segment identities in the hindbrain in *Pbx* wild-type background, but in the *pbx4* mutants this effect is strongly suppressed [97].

1.6.4.2. Hox-independent Functions of Pbx Proteins

A growing body of evidence suggests that Pbx proteins may act broadly to modulate non-Hox proteins and non-homeodomain proteins functions and indeed 12% of Pbx1 putative partners are non-homeodomain transcription factors [69]. In vitro studies of muscle differentiation have shown that Pbx1-Meis complexes are constitutively bound to the myogenin gene marking the region where MyoD will be recruited. MyoD indirect promoter interaction through Pbx1, recruits the chromatin-remodeling SWI/SNF enzymes of the chromatin-remodeling complex. This facilitates the binding of other regulators, which finally leads to transcriptional activation of the myogenin gene. These findings suggest a critical role of *Pbx1* in marking specific genes for activation [98]. Furthermore, Pbx1 and Prep1 proteins bind to the *FSHβ* (Follicle-stimulating Hormone) promoter and recruit Smad proteins regulating *FSHβ* gene response to activin. This study highlights the link between *Pbx* and TGFβ signaling [99].

1.6.4.3. PBX Proteins in Cancer

Pbx genes are normally involved in developmental processes and cell fate determination during organogenesis. However, the accumulating evidence shows that they are also involved in the development of human cancers [16,92,100]. Pbx1 has been implicated as a proto-oncogene in human leukemia. The t(1;19) chromosomal translocation detected in almost 23% of all pediatric pre-B cell ALL patients forms an oncogenic fusion protein, so called E2A-PBX1, which correlates with poor response to standard chemotherapeutic protocols [101]. In the resulting fusion protein, the DNA binding domain of E2A is replaced by the DNA binding domain of PBX1. So, the E2A-PBX1 fusion protein contain the E2A activation domain and the homeodomain of PBX1

[16]. Two alternatively spliced isoforms of *PBX1* are detected as a fusion protein with E2A, E2A-PBX1a and E2A-PBX1b in human primary tumor cells [79].

E2A belongs to the class I family of basic helix-loop-helix (bHLH) proteins and contains two activation domains called AD1 and AD2. The B cell development blockage at the early pro-B cell stage in E2A-deficient mice points out the importance of E2A as a B lymphopoiesis regulator [102]. It also carries out various functions from regulation of Ig class switch recombination in peripheral mature B cells [103] to T cell development [104]. Although the underlying mechanisms by which E2A-PBX1 causes pre-B cell ALL are not clear so far, the main contributions of this oncoprotein to the pathogenesis of ALL are summarized in this section. E2A can act as a tumor suppressor to suppress the tumorigenic cell growth both *in vitro* and *in vivo* [16]. The t(1;19) chromosomal translocation disrupts one allele of both *E2A* and *PBX1*. This may lead to a decrease in the amount of functional E2A acting as a tumor suppressor. On the other hand the cooperation of the E2A activation domain with the DNA binding domain of PBX1 activates transcription through PBX1 binding sites [105] which can alter the regulation of HOX/PBX target genes. These alterations seem to be oncogenic. For instance, E2a-Pbx1a can collaborate with *Hoxa9* to cause AML [106]. PBX1 binding to MEIS/PREP proteins is one of the mechanisms that regulate its nuclear-cytoplasmic localization (reviewed in section 1.6.3). But in the fusion form the MEIS/PREP interaction domain of PBX1 (PBC-A and PBC-B domains) is disrupted which leads to the constitutive presence of the fusion protein in the nucleus. Hence the E2A-PBX1 protein is always available for dimerization with HOX proteins [16,107]. A screening to identify other factors involved in E2A-PBX1-induced transformation revealed that *Pim1* and $Notch^{\Delta C}$ enhance E2A-PBX1 tumorigenicity [16,108].

In addition to the role of Pbx1 in leukemogenesis, it also has been implicated in the pathogenesis of different human solid cancers including breast, ovarian and prostate cancers [85,100,109]. Two-thirds of all breast cancers are estrogen receptor alpha (ERα) dependent. Following estrogen stimulation, ERα binds to DNA and promotes a pro-tumorigenic transcriptional response. *PBX1* acts as a pioneer factor in ERα positive breast cancer. It opens the chromatin by recognizing and binding to the chromatin harboring the H3K4me2 epigenetic modification, which leads to chromatin remodeling and the recruitment of ERα [85].

In the pathogenesis of ovarian cancer not only the highly deregulated expression of *HOX* genes is important, but also the PBX1-HOX heterodimer complex contributes to the oncogenic activity in this cancer. The disruption of the interaction between HOX proteins and PBX1 induces apoptosis in the ovarian cancer derived line SK-OV3, and significantly reduces tumor growth *in vivo* [110]. Functional inactivation of *NOTCH3* that is amplified in ovarian cancer identified PBX1 as a downstream effector of the Notch signaling pathway. This finding suggests that *NOTCH3* activation and the subsequent activation of *PBX1* potentially modulates the function of HOX proteins, which are deregulated in ovarian cancer [100]. However the molecular mechanism of how *PBX1* promotes tumorigenesis remains unclear. An integrated approach overlapping PBX1 ChIP-chip with the *PBX1*-regulated transcriptome in ovarian cancer cells has identified the genes whose transcription is directly regulated by *PBX1*. Among these target genes, a homeodomain protein, MEOX1, was identified and its interaction with PBX1 demonstrated. The suppression of MEOX1 caused a similar growth inhibitory phenotype similar to PBX1 inhibition and its ectopic expression functionally rescued the *PBX1*-deficient effect, suggesting that MEOX1 mediates the cellular growth signal of PBX1. This study also revealed potential cis-regulatory cofactors of PBX1, which include

GATA1, FOSL1, MEIS1, JUNB, and a ‘‘TAATTA’’ motif for MEOX1 and HOX. The motifs of these transcription cofactors were significantly enriched in PBX1-bound sequences, suggesting that these proteins may work in concert with PBX1 to facilitate transcriptional regulation [111].

The role of other PBX proteins in human cancers remains mysterious and needs to be studied. There is only one recent study that showed the correlation of high level *PBX2* expression with a poor prognosis in gengival squamous cell carcinoma [112]. Another recent study showed the upregulation of *PBX3* in prostate cancer and its post-transcriptional regulation by androgen through Let-7d [113].

1.6.5. The *MEIS* Family

The *MEIS* or *MEINOX* family in mammals is divided into two subclasses, *MEIS* and *PREP*. *MEIS* subclass is composed of *MEIS1*, *MEIS2* and *MEIS3* [114,115,116]. *PREP* subclass has two paralogs in man, *PREP1* and *PREP2*, with 60% sequence identity [67,117,118]. *MEIS1* is mapped to chromosome 11 in mouse and 2 in man. *MEIS2* is located on the chromosome 2 in mouse and 15 in man. *MEIS3* is on the chromosome 7 in mouse and 19 in man. *PREP1* is located on the chromosome 17 in mouse and 21 in man and *PREP2* is mapped on chromosome 9 in mouse and 11 in man. The *Drosophila* ortholog of *MEIS1* is called *homothorax (hth)*. HTH is required for the nuclear localization of EXD, the *PBX* ortholog in *Drosophila*. HTH and EXD have many functions in *Drosophila* including the regulation of eye development, patterning the embryonic peripheral nervous system and proximal-distal limb development [119].

Like Pbx, Meis/Prep proteins are also well known as Hox cofactors. They are required for the normal function of the Hox-Pbx complex. Their interaction with Hox-Pbx complex increases Hox DNA binding specificity (Hox-Pbx binding sites occur once every

8200 bp and Hox-Pbx-Meis/Prep once every 420000 bp [69]) [51]. The tripartite Hox-Pbx-Meis/Prep complex is formed by the interaction of HR1 of either Meis or Prep with PBC-A of Pbx. The subsequent complex can form a ternary complex through the Homeodomain of Pbx bound to the hexapeptide motif of Hox [71,73,120]. The consensus Hox/Pbx binding site, ATGATTGATGA, is often associated with essential binding sites for the Meis/Prep proteins [51,120]. Trimeric Hox-Pbx-Meis/Prep complexes were shown to be crucial in the early development of the vertebrate hindbrain. For instance Prep1, Pbx1 and Hoxb1 form a ternary complex on the rhomobomere 4 enhancer of the *Hoxb2* gene [90,121]. In the following sections the different biological functions of Meis/Prep proteins, especially their role in tumorigenicity will be reviewed in detail.

1.6.6. The *Meis* Subclass Discovery and Mutant Phenotypes

Meis1 (Myeloid Ecotropic viral Integration Site 1) was isolated as a site of viral integration in 15% of the leukemias arising in BXH-2 mice. It is located on proximal mouse chromosome 11 and human chromosome 2p23-p12, in a region known to contain translocations found in human leukemias. *Meis1* has two alternatively spliced isoforms in mammals: Meis1a and Meis1b [114,115]. *Meis2* and *Meis3* were identified by DNA cross-hybridization with a *Meis1* probe under low stringency conditions [116]. A screen for genes involved in retinoic acid differentiation in P19 embryonic carcinoma cells also led to the isolation of *Meis2* [122].

Meis1$^{-/-}$ embryos die around E14.5. They exhibit a variety of malformations including severe hemorrhage because of the lack of well-formed capillaries, although the larger blood vessels are normal, anemia, liver hypoplasia, the complete absence of megakaryocytes, decreased number of hematopoietic stem cells and eye defects (Figure 1.6) [119,123]. *Meis1* is strongly expressed in hematopoietic stem cells and is essential

for the proliferation and self-renewal of these cells. *Meis2* seems to be involved in the control of chick limb outgrowth [124,125]. No *Meis2* and *Meis3* KO mice have been described.

In the mouse embryo, *Meis1* and *Meis2* show region-specific expression patterns from E10.5 until birth, defining distinct sub territories in the developing telencephalon. *Meis* genes are highly expressed in the subventricular zone and mantle regions of the ventral telencephalon [126]. *Meis1* is required for the regulation of *Pax6* expression during vertebrate lens development [127]. Moreover *Meis* genes are involved in patterning of the hindbrain [128,129]. In general, *Meis1* and *Meis2* are expressed in the following tissues: hematopoietic, central nervous system (CNS), liver and pancreas, gastrointestinal tract, respiratory (lung), cardiovascular, female tissue, male tissue, urinary tract (kidney), skin and soft tissues [130] [131].

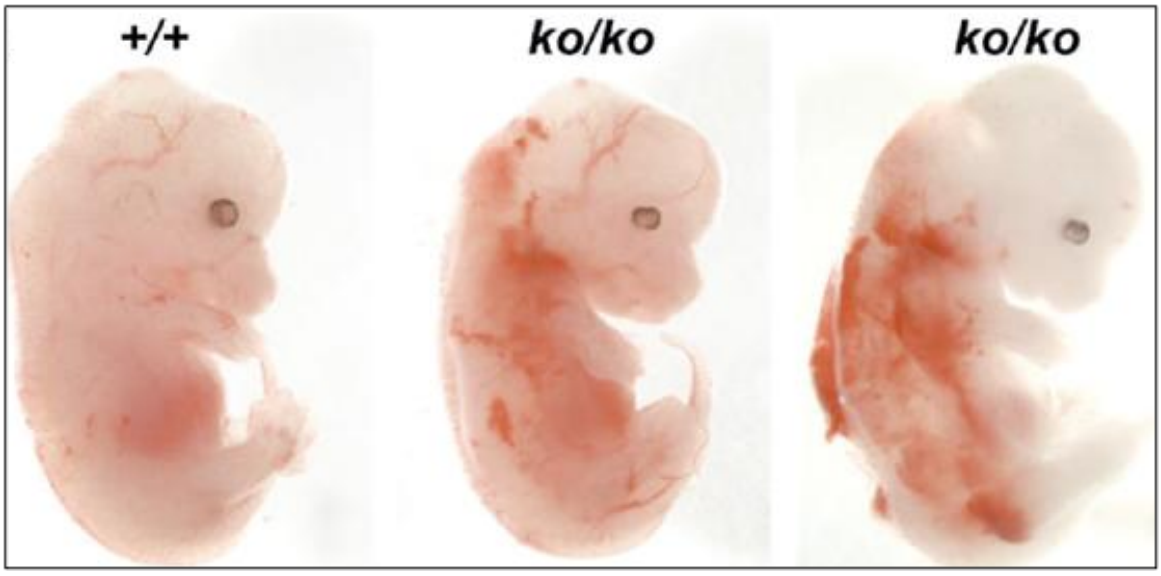

Figure 1.6. Morphology of *Meis1*-deficent embryo compared to the wild-type at E13.5 [119].

1.6.7. Meis proteins in cancer

1.6.7.1. Role of *Meis1* in leukemogenesis

An oncogenic collaboration between Hox and Meis proteins has been established both by proviral insertion [116] and by retroviral overexpression studies [41]. Retroviral insertions induce myeloid leukemia in BXH-2 mice by deregulating the expression of proto-oncogenes and tumor suppressor genes. Proviral tagging was used to identify common viral integration sites in the leukemias derived from BXH-2 mice. This led to the identification of *Hoxa7*, *Hoxa9* and *Meis1* genes whose expression was activated by proviral integration. Strong correlation between proviral activation of *Hoxa7* and *Hoxa9* with proviral activation of *Meis1* implies that *Hoxa7* and *Hoxa9* cooperate with *Meis1* in leukemogenesis [115,116]. Indeed, overexpression of *Hoxa9*, *Meis1* or *Pbx1 per se,* is not sufficient to efficiently transform murine primary bone marrow cells. Furthermore, *Meis1* overexpression in hematopoietic progenitors not only does not immortalize these cells but also induces apoptosis, which is caspase-dependent, and can be abrogated by *Hoxa9* coexpression [132].

Although *Hoxa9* overexpression induces leukemia after long latency [43], overexpression of *Meis1,* but not *Pbx1* [41] or *Prep1* [43], drastically lowers the latency of *Hoxa9*-induced AML. Thus *Hoxa9* selectively cooperates with *Meis1* in leukemic transformation in mice and human AML. *Hoxa9* and *Meis1* are expressed in more than 80% of human AML [133] and their expression levels are correlated with poor prognosis in AML [134].

Although Meis1 and Prep1 can interact with Pbx and Hox family members, they play opposite roles in tumorigenesis. In fact, *Prep1* overexpression is not capable of accelerating *Hox*-induced leukemia. Indeed, in agreement with its tumor suppressor function [19], *Prep1* marginally increases the latency of leukemia formation [43].

Molecular dissection of Meis1 showed that three different domains of Meis1 including the Pbx-interacting domain, the DNA binding homeodomain and the C-terminal domain (CTD), are required for its oncogenic activity [42,135,136]. In agreement with these data, chimeric Prep1 carrying the C-terminal domain (the transactivating domain) of Meis1 acts as a *Hoxa9*-collaborating oncogene and accelerates the onset of *Hoxa9*-induced leukemia by regulating expression of genes involved in chromatin accessibility and cell cycle progression. So, chimeric Prep1 is capable of inducing a distinct gene expression profile that is associated with wild-type *Meis1* overexpression [137].

Meis1 fusion to Vp-16 trans-activating domain (Vp16-Meis1) forms a chimeric oncoprotein, which induces leukemia in the absence of coexpressed *Hox* genes. Vp16-Meis1 induced leukemias exhibit longer latency than observed with *Hoxa9-Meis1* coexpression. Vp16-Meis1-induced transformation requires the Pbx and DNA binding domains of Meis1. The CTD of Meis1 and the N-terminal domain (NTD) of Hoxa9, which is required to cooperate with wild-type Meis1, are dispensable in Vp16-Meis1 mediated transformation. The fact that the Vp16 domain replaces the function mediated by the Meis1 CTD and the Hoxa9 NTD, suggests that the Meis1 CTD and the Hoxa9 NTD might recruit cofactors containing HAT activity. Thus, Meis1-Pbx, Hox-Pbx and Meis1-Hox-Pbx complexes co-occupy the promoters of leukemia-associated genes using the Meis1 CTD and the Hoxa9 NTD for transcription activation [138].

Characterization of leukemic cells overexpressing *Hoxa9* and *Meis1* revealed that they are poorly differentiated myeloid lineage cells. Since hematopoietic stem cells (HSC) have both myeloid and lymphoid potential [41], the myeloid feature of *Hoxa9-Meis1*-induced leukemia suggests that HSCs are not the target of *HoxA9-Meis1* transformation.

Study of the mechanisms underlying *Hoxa9* and *Meis1* cooperation showed that *Meis1* suppresses myeloid differentiation pathways that are not altered by *Hoxa9*. Constitutive expression of *Hoxa9* immortalized bone marrow cells by blocking the macrophage and neutrophil differentiation of primary myeloid progenitors cultured in granulocyte-macrophage colony-stimulating factor (GM-CSF). However, the monocyte differentiation in response to macrophage CSF (M-CSF) and granulocytic differentiation in response to granulocyte CSF (G-CSF) were not impaired. In *Hoxa9*-immortalized progenitors, *Meis1* suppresses differentiation in response to G-CSF and promotes self-renewal [139]. Therefore complementary differentiation pathways targeted by *Hoxa9* and *Meis1* regulate progenitor abundance by blocking differentiation and promoting self-renewal in response to the different subsets of cytokines during myelopoiesis. Moreover, *Meis1* up-regulates *Pbx2* by 3-fold in AML cells and prevents transcription of genes which are normally activated in neutrophil differentiation such as Egr-1, neutrophil gelatinase B and CD14 [139].

The other mechanisms by which *Meis1* cooperates with *Hoxa9* to induce AML are regulated through Meis1-Pbx complexes. These mechanisms include increased expression of *Flt3* (Fms-like tyrosine kinase 3) proto-oncogene, a receptor for FL (Flt3 ligand), and other genes involved in short-term HSCs (ST-HSCs), such as *Cd34* and *Sox4* proleukemic transcription factor [140]. It has also been shown that both Meis1 and Hoxa9 bind to the *Flt3* promoter. Flt3 expression is associated with ST-HSCs and *Flt3*-deficient stem cells are impaired in lymphoid and myeloid reconstitution potential [141]. However, *Flt3*-deficient hematopoietic cells are efficiently transformed by *Hoxa9-Meis1* coexpression, suggesting that *Flt3* is not the only essential mediator of leukemogenesis and therefore other genes must be involved in leukemic transformation [142].

Trib1 and *Evi1* have been identified as putative cooperative genes located close to the common retroviral integration sites in *Hoxa9-Meis1* induced AML and their overexpression accelerates AML formation through cooperation with *Hoxa9* and *Meis1*. One possible model for this interaction is the involvement of the Flt3/MAPK pathway, which is important in leukemogenesis. On one hand, *Meis1*-mediated *Flt3* upregulation leads to MAPK phosphorylation. On the other hand Trib1 interaction with MAPKKs enhances MAPK phosphorylation. The consequence of these phosphorylations force the MAPK signaling leading to leukemia [143].

In search of other *Hoxa9-Meis1* target genes involved in leukemogenesis and to shed more light in the field, the *c-Myb* proto-oncogene was found to be essential but not sufficient for the transformation [144]. *c-Myb* is a key regulator of normal hematopoiesis which is frequently altered in lymphomas and leukemias. The mechanisms underlying this alteration are poorly documented. One recent study showed the role of *Hoxa9* and *Meis1* in *c-Myb* gene regulation in AML. Hoxa9 and its cofactors Meis1, Pbx1 and Pbx2 directly regulate the expression of the c-*Myb* gene by binding to the *c-Myb* locus on consensus HoxA-TALE sequences in normal and *Hoxa9-Meis1* transformed hematopoietic cells [145].

The identification of different *Meis1* target genes such as *Flt3*, *Cd34*, *Erg1*, *c-Myb*, and *Trib2* suggests that *Meis1* functions to modulate multiple pathways in leukemogenesis. In this regard, cell-cycle analysis using the M33-Meis1 fusion, which suppresses the upregulated *Meis1* target genes in normal and malignant hematopoiesis, revealed that *Meis1* induces proliferation of normal and malignant HSCs by modulating G-1 phase regulators. In fact, *Meis1* promotes G1-to-S phase progression by direct transcriptional regulation of cyclin D3 and subsequent hyperphosphorylation of Retinoblastoma (pRb) [135].

Hoxa9 and *Meis1* are reported overexpressed not only in human AML [133] but also in acute lymphoid leukemia (ALLs) harboring *MLL* (mixed lineage leukemia) chromosomal translocations [146]. In hematopoiesis, *MLL* regulates *Hox* gene expression by methylation of histone H3 at lysine 4 through its intrinsic histone methyltransferase activity [146]. The constitutive expression of *Hoxa9* and *Meis1* in immortalized myeloid progenitors by MLL fusion oncoproteins such as MLL-ENL suggests that *Hoxa9* and *Meis1* are crucial targets for *MLL-ENL*-induced cellular transformation [147]. Since myeloid progenitors cells from *Hoxa9*$^{-/-}$ mice failed to be immortalized by MLL-ENL, the *MLL-ENL*-induced immortalization is *Hoxa9* dependent [148]. Moreover, using HSCs from *Meis1*$^{-/-}$ embryos in *MLL*-fusion transformation studies revealed that *Meis1* is essential for the transformation [149]. The *Meis1* and *Hoxa9* upregulation can occur through epigenetic alterations as seen in *MLL-AF9*-mediated leukemia. In this leukemia, *Hoxa9* and *Meis1* are upregulated following the H3K79 methylation mediated by DOT1L, an H3K79 methyltransferase [150].

One possible role for *Meis1* in *MLL*-fusion-mediated transformation is through the regulation of the genes associated with cell cycle entry and progression such as *Cdk2*, *Cdk6*, *Cdkn3*, *Ccna2*, *Cdc7*, *Cdc42*, *Rbl1*, and *Wee1*. Indeed, shRNA-mediated depletion of *Meis1* caused the reduction of the expression of these genes, reduced cell growth and promoted differentiation [151]. Also downregulation of *MEIS1*, *HOXA7*, *HOXA9* or *HOXA10* by shRNA impairs the engraftment of *MLL*-induced leukemia and decreases the proliferation rate of the leukemic cells in culture [152].

Pbx proteins are required for *MLL*-induced leukemogenesis and the depletion of Pbx2 and Pbx3 impairs leukemia formation. Moreover, the Pbx interacting domain of Meis1 is required for leukemic transformation mediated by *MLL*-fusions and *Hoxa9*-immortalization [149].

In addition, the maintenance of *MLL*-induced leukemias requires GSK-3 (glycogen synthase kinase 3) function. GSK-3 facilitates *HOX*-mediated transcription and transformation by inducing the conditional association of CREB transcription factor and its co-activators TORC and CBP to MEIS1 [153]. CREB regulates proliferation, differentiation, and survival in different cell types, including hematopoietic and neuronal cells [154]. CREB induces *MEIS1* expression in normal and malignant hematopoietic cells by binding to the CRE sequences in the promoter region of *MEIS1* which in turn leads to the differentiation block of primitive hematopoietic progenitor cells and the development of acute leukemia [155].

1.6.7.2. Role of Meis genes in Non-Hematopoietic Malignancies

The role of *Meis1* in solid tumors is poorly documented. However, the few studies performed to analyze the function of *Meis1* in carcinogenesis suggest that *Meis1* expression in solid tumors is context-dependent. Study of *MEIS* and *PBX* gene expression in public human affymetrix data sets of normal (N353) and tumor (XPO1026) tissue of different origins revealed that in ovarian cancer, the average expression level of *MEIS1* is 3-fold higher than *MEIS2* and that among the four *PBX* genes, *PBX1* is highly expressed. In addition the average expression level of *MEIS1* is high in ovarian and uterine cancers, neuroblastoma and medulloblastoma compared to the other types of tumors. The oncogenic function of *MEIS1* and *PBX1* is not well understood in ovarian carcinogenesis. One possible explanation for the up-regulation of these proteins in ovarian cancer is related to their *HOX* cofactor functions. Since the HOXA9-11 proteins are expressed in ovarian malignancies and not in normal ovary, the overexpression of their cofactors *MEIS1* and *PBX1* may enhance their oncogenic activity by increasing their DNA-binding affinity and specificity [130].

Although the *MEIS* genes are highly expressed in ovarian cancer, their function in ovarian carcinogenesis is still unclear. A recent study has shown that *MEIS3*, and not *MEIS1* and *MEIS2* regulates the survival of pancreatic β-cells and ovarian carcinoma cells through direct modulation of *PDK1* (3-phosphoinositide-dependent protein kinase 1), which is involved in the PI3K-Akt signaling pathway. The frequent impairment of the PI3K-Akt signaling pathway in human cancers raises the possibility that *MEIS3* functions in tumor cell survival through the regulation of *PDK1* [156].

MEIS1 is overexpressed in neuroblastomas [157] and is amplified in the IMR32 neuroblastoma cell line. Analysis of the expression pattern of *MEIS1* and *MEIS2* in a broad panel of neuroblastoma cell lines and in neuroblastoma tumor samples showed moderate to high expression of these genes. The oncogenic role of *MEIS1* in neuroblastoma was studied by interfering with *MEIS1* function with the naturally occurring dominant-negative variant of *MEIS1* (*MEIS1E*). *MEIS1E* lacks the C-terminal part of the homeodomain and therefore cannot contribute to transcriptional regulation. But it can compete with wild-type MEIS1 by binding to other homeobox proteins such as PBX. Neuroblastoma cells transfected with *MEIS1E* showed impaired cell proliferation, acquisition of differentiated phenotype, and increased contact inhibition and cell death which indicates a potential role for *MEIS1* in neuroblastoma cell growth and proliferation [158]. Moreover, gene expression profiling of human sarcomas showed that MEIS1, MEIS2, MEIS3, and PBX1 are upregulated in leiomyosarcoma (LMS) [159]. However, the functional impacts of these alterations to the biology of sarcoma remain unclear.

Although *MEIS1* is implicated in the pathology of ovarian cancer, neuroblastoma, and sarcoma, it has been found hypermethylated or downregulated in the other subset of human solid tumors. But the functional relevance of these alterations and whether *MEIS1* acts as a tumor suppressor in some cellular contexts, remain fully undefined. Aberrant

CpG island methylation in the promoter region of genes is a hallmark of cancer and occurs at early stages of tumorigenesis. Although the impact of the altered CpG methylation on tumor development is not well determined, it is unlikely that all of these methylation alterations play a causal role in tumorigenesis. CpG island hypermethylation silences important tumor suppressor genes and accounts for different cancers including breast, lung and colon cancers. These changes in DNA methylation pattern discriminate tumor from normal tissue. The differently methylated genes can be used as diagnostic biomarkers in the early stages of tumorigenesis. The CpG island of *MEIS1* is methylated in ductal carcinoma in situ, in stage I breast tumors [160], and in squamous cell carcinomas of the lung [161]. *MEIS1* and *MEIS2* transcript downregulation were observed in colorectal adenomas [162] and in genome wide expression analyses of tumor lesions in lung adenocarcinoma induced by c-Raf-1 [163].

1.6.8. The *PREP* Sub-Family and Mutant Phenotypes

Characterization of genes encoded by human chromosome 21 led to the discovery of the *Pbx/KNOX1* (*PKNOX1*) gene [164]. At the same time, studies on the *uPA* (urokinase-type Plasminogen Activator) enhancer in human cell lines [165,166] led to the discovery of the same protein as a component of the regulatory complex of the human transcription factor *UEF3*. Because of its molecular properties, the newly identified protein was named PBX Regulating Protein1 (PREP1) [67,73]. NIH3T3 cells were used to isolate the murine *Prep1* [167], while *Prep2* was isolated by low stringency hybridization due to its similarity to *Prep1* [117,118].

Mouse *Prep1* null embryos have been generated by targeting the DNA-binding homeodomain, which abolishes protein expression. These mutant mouse embryos die before gastrulation at E7.5 because of massive p53-dependent apoptosis of epiblast cells

[168]. Moreover, in the zebrafish down-regulation of *prep1.1* is embryonic lethal [169]. Thus the embryonic lethality of *Prep1* null embryos precludes the study of the *Prep1* deficiency in the later developmental processes and in the adult animals. To overcome this problem, *Prep1* hypomorphic mutant mice (*Prep1*$^{i/i}$) were generated by an enhancer trap strategy [170]. *Prep1*$^{i/i}$ embryos express about 2% of Prep1 mRNA and 2-10% of the protein compared to the wild-type littermates. 75% of *Prep1*$^{i/i}$ embryos die at about E17; but the remaining 25% of the embryos reach term and have an almost normal life span [171,172]. *Prep1*$^{i/i}$ embryos apparently recapitulate in part the *Meis1*$^{-/-}$ embryos phenotypes by exhibiting major defects in hematopoiesis, angiogenesis and eye development. They also show general organ hypoplasia including liver (Figure 1.7) [171,172]. The hematopoietic phenotypes of the *Prep1*$^{i/i}$ embryos are due to deficiency in long term repopulating hematopoietic stem cells and an arrest in erythroid, B- and T-lymphoid differentiations [171,172,173]. No loss of function mutation for *Prep2* has been described.

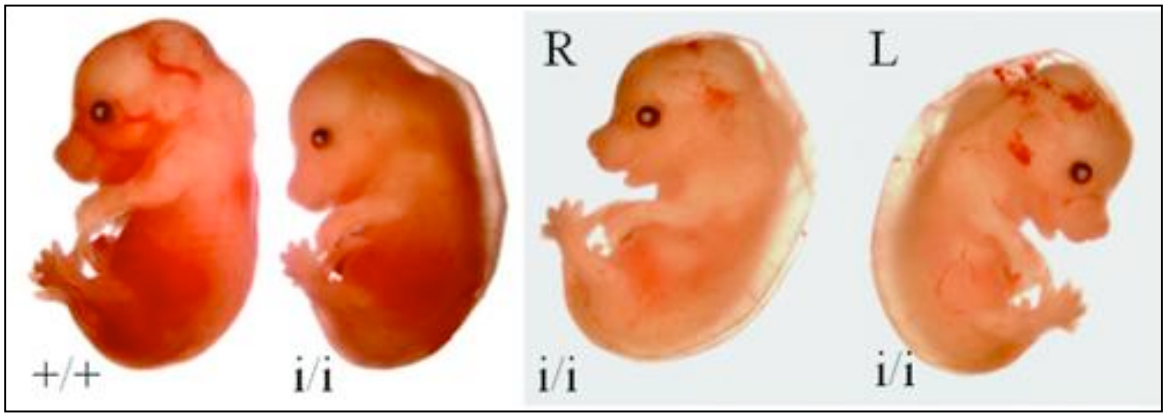

Figure 1.7. Gross morphology of *Prep1*$^{i/i}$ embryos compared to the wild-type littermate. These embryos exhibit edema, pallor, smaller size, small liver spot and hemorrhage. Right (R) and left (L) sides of the embryo are shown.

1.6.9. *Prep1* Implications in Development and Cancer

1.6.9.1. *Prep1* Role in Apoptosis

A balance between proliferation rate and programmed cell death (apoptosis) is crucial for normal development and organogenesis. The normal cellular balance between proliferation and apoptosis rates are usually disrupted in malignant growth. Among the TALE proteins it has been shown that the overexpression of *Meis1* [132] and *Pbx1* [174] causes massive p53-independent apoptosis. In the case of *Prep1* both the depletion [175] and the overexpression [176] cause apoptosis, although by two different mechanisms.

Strong spontaneous apoptosis is observed in $Prep1^{i/i}$ embryos at E9.5 and E11.5 [175]. Moreover, $Prep1^{i/i}$ mouse embryonic fibroblasts (MEFs) from E14.5 embryos display an increase of basal apoptosis and accelerated response to intrinsic, but not extrinsic, apoptotic stimuli compared to those of wild-type littermates. The *p53* transcript and protein level is not significantly altered in $Prep1^{i/i}$ MEFs. However the protein level of the antiapoptotic Bcl-XL protein, a regulator of mitochondrial-membrane permeability, is decreased [175]. Chromatin immunoprecipitation (ChIP) and transient-transfection analysis revealed that *Prep1* directly regulates *Bcl-x* gene expression. The fine balance between pro and antiapoptotic proteins at the mitochondrial outer membrane is needed to regulate its permeability, thus maintaining the mitochondrial homeostasis and controlling apoptosis. Therefore, *Prep1* influences apoptosis and modulates mitochondrial homeostasis by regulating *Bcl-x* gene expression [175].

Like *Prep1* depleted cells, *Prep1* overexpressing cells are also more sensitive to genotoxic stress in a p53-dependent manner. Under these conditions, p53 is a direct transcriptional target of *Prep1* and is up-regulated in the *Prep1* overexpressing cells, indeed, apoptosis is abrogated in these cells upon p53 down-regulation [176]. These data show a defined balance of *Prep1* is crucial in apoptotic homeostasis [175] [176].

1.6.9.2. *Prep1* as a Tumor Suppressor Gene

The role of *Prep1* in cancer is not well documented to date. However, emerging evidence point out that *Prep1* exerts a tumor suppressive function in mouse and man. Almost 40% of *Prep1*$^{i/i}$ mice that survive embryonic lethality develop spontaneous precancerous lesions or solid tumors including lymphomas and carcinomas at different ages, while *Prep1* wild-type mice only develop rare precancerous lesions late in life [19]. Furthermore, transplantation of *Prep1*$^{i/i}$ fetal liver cells induces lymphomas in lethally irradiated recipients. Consistent with the fact that the oncogene-driven tumorigenicity is accelerated in the absence of tumor suppressor genes, *Prep1* haploinsufficiency (loss of one *Prep1* allele) in the *EμMyc* transgenic mouse model strongly accelerates lymphomagenesis and death rate. Therefore *Prep1* functions as a tumor suppressor in mice [19].

The deletion, mutation or silencing of tumor suppressor genes are one of the main features of cancer. In man, *PREP1* is ubiquitously expressed in normal tissues. Its expression is high in breast and skin, intermediate in colon, larynx, lung bronchial epithelium, uterus stroma, and testicular germinal cells and low in lymph-nodes, stomach, kidney tubules, endometrial epithelium, uterine endo- and exocervical epithelia and placenta. Tissue microarray analysis revealed that PREP1 is absent or downregulated in most (70%) human tumors (Figure 1.7) [19]. In addition, *PREP1* is located in a genomic region that experiences loss of heterozygosity in 31% and 50% of informative breast [177] and gastric cancers [178], respectively. Altogether, these pieces of evidence suggest that *PREP1* might act as a tumor suppressor gene in human cancers.

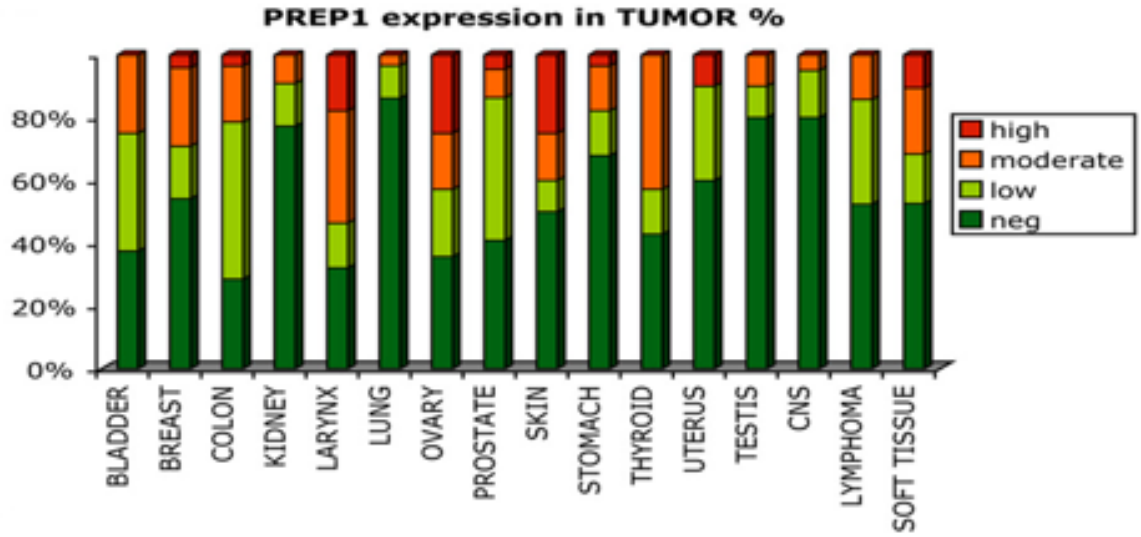

Figure 1.8. Summary of PREP1 expression level in human tissue microarrays analyzed by immunohistochemistry.

Genomic instability, which generates mutations and chromosomal translocations, is an "enabling characteristic" of cancer cells that facilitates the acquisition of cancer hallmarks [27]. The tumor development in *Prep1*$^{i/i}$ mice [19] and apoptosis in *Prep1*$^{-/-}$ epiblasts [168] and *Prep1*$^{i/i}$ MEFs [175], suggests that genetic instability might be a basic cellular phenotype associated with Prep1 depletion or absence. Our study on the role of *Prep1* in maintaining genetic stability unveiled the fact that *Prep1* deficient cells accumulate DNA damage with consequent alterations in chromatin methylation and satellite DNA transcription, chromosomal aberrations, escape from *H-Ras*^{V12}-induced senescence, and increased susceptibility to *H-Ras*^{V12}-dependent neoplastic transformation [179]. These data provide a cellular basis for the tumor suppressor function of *Prep1* [19], suggesting that Prep1 depletion impairs checkpoint mechanisms involved in limiting oncogene-induced transformation and establishing oncogene-induced senescence in human cells.

1.7. DEAD-box RNA Helicases

RNA and DNA helicases are encoded by a large fraction of the eukaryotic and prokaryotic genes. They exert enzymatic activity that unwinds the double-stranded nucleic acids in an energy-dependent manner. RNA and DNA helicases are divided into two main super-families, namely SFI and SFII, based on the occurrence of specific conserved motifs. The human genome encodes 64 RNA helicases and 31 DNA helicases [180]. RNA helicases, which are found in all organisms (from bacteria to humans), mostly reside in the SFII super-family. The DEAD-box (DDX) helicases and the related DEAH, DExH and DExD families, commonly known as the DExD/H helicase family, are members of this super-family and share eight conserved motifs (Figure 1.8). The DEAD-box proteins were identified in the 1980s and the name of the family comes from the amino-acid sequence D-E-A-D (Asp– Glu– Ala– Asp) located on the Walker B motif. DEAD-box proteins are known as the largest RNA helicase family with 38 members in human. The DEAD-box family members are associated with almost all processes involving RNA including ribosome biogenesis, transcription, pre-mRNA splicing, RNA maturation, RNA export, mRNA translation and RNA decay [181,182]. Moreover, members of the DEAD-box family are implicated in human diseases including cancer and viral infections. In the next sections I will focus on two members of this family, DDX3X and DDX5, and their involvement in human carcinogenesis.

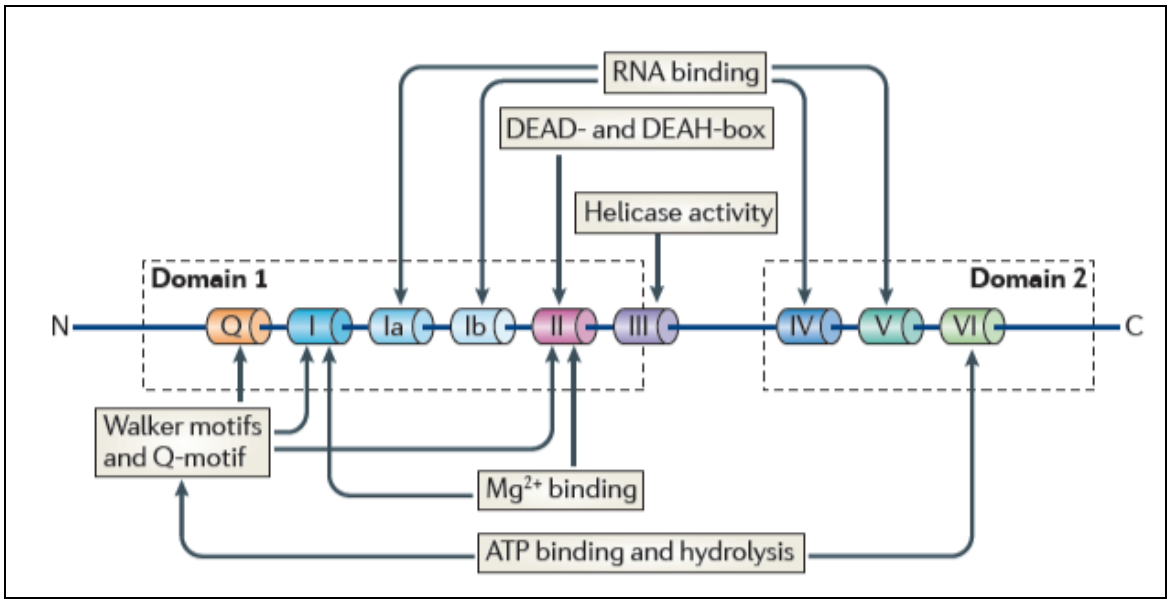

Figure 1.9. DEAD and DEAH helicases contain N-terminal and C-terminal domains (domain 1 and domain 2). Domain 1 and domain 2 are composed of six and three conserved motifs respectively. DEAD- and DEAH-boxes are located inside motif II and are characterized by the presence of an Asp-Glu-Ala-Asp or an Asp-Glu-Ala-His amino acid sequences, respectively [181].

1.7.1. The Role of DDX3 in Cancer

In man and mouse, the *DDX3* gene, also named as *DDX3X*, *CAP-Rf* and *DBX*, maps to the X chromosome and is composed of 17 exons. Human *DDX3* transcript is 5.3 kb in size and encodes a protein of 662 amino acids. Mouse *Ddx3* transcript is 4.7 kb in length and encodes a protein of 662 amino acids. Apart from five different amino acids, human and mouse DDX3 proteins are identical across the entire protein length. A functional homolog of this gene is located on the Y chromosome and is known as *DDX3Y* or *DBY*. The DDX3Y protein sequence is 91% identical with its X-linked homolog [183,184] and is implicated in spermatogenesis [185]. *DDX3* is expressed ubiquitously [183] and shuttles between nucleus and cytoplasm [186].

The DDX3 protein was originally linked to the functions of HCV [187,188] and HIV [186] viruses. HCV and HIV viruses recruit DDX3 to replicate their genome

[186,188]. For instance, the export of HIV RNAs from the nucleus is *DDX3*-dependent [186]. Moreover, *DDX3* is crucial for the HCV life cycle. Its interaction with HCV core protein changes the virus intracellular location [187]. In addition, several studies have linked *DDX3* to the progression of different cancers. The role of *DDX3* is controversial in hepatocellular carcinoma (HCC). Huang and colleagues have reported that the *DDX3* mRNA is upregulated in human HCC and is linked with the pathology of HCC [189]. However, another report has shown that *DDX3* is downregulated in human HCC. Its absence in this cancer is associated with enhanced proliferation and resistance to serum-withdrawal apoptosis induction. In fact, *DDX3* depletion in NIH-3T3 cells increases cyclin D1 and decreases cdk inhibitor $p21^{WAF1}$ levels. This leads to an enhanced transition from G1 to S phase and increased proliferation rate. Moreover, *DDX3* knockdown in NIH-3T3 cells promotes *v-ras*-induced anchorage-independent growth [190].

DDX3 plays an oncogenic role in breast cancer. The exposure of breast epithelial cell line, MCF10A, to benzo[a]pyrene diol epoxide (BPDE) carcinogen, found in tobacco smoke, upregulates *DDX3* expression. Also, the expression level of *DDX3* is increased with the aggressiveness of breast cancer cell lines. The overexpression of *DDX3* induces an epithelial-mesenchymal-like transition in non-tumorigenic MCF10A cells and increases their motility and invasiveness. *DDX3* regulates *E-cadherin* expression and its shRNA-mediated downregulation induces *E-cadherin* expression [191]. *DDX3* functions to modulate Snail transcription factor. Snail promotes epithelial-mesenchymal transition (EMT) by suppressing *E-cadherin* and several other cellular adhesion proteins. *DDX3* and Snail levels are significantly correlated in a panel of glioblastoma multiforme tumor samples. Furthermore, *DDX3* depletion in both MCF-7 and Hela cells decreases Snail levels, resulting in decreased proliferation and cellular migration. Since Snail is involved in EMT, its down-regulation in MCF-7 cells changes the morphology of the cells and

increases cellular adhesion [192]. *DDX3* also exerts anti-apoptotic functions in the MDA-MB-231 breast cancer cell line. It associates with GSK3 and cellular inhibitor of apoptosis 1 (cIAP-1) and prevents death receptor-induced apoptosis. Its depletion by shRNA promotes death receptor-induced signaling. These data suggest that *DDX3* may contribute to resistance to death receptor-induced apoptosis in cancer cells [193].

DDX3 controls translation of cyclin E1 and regulates cell proliferation. *DDX3* knockdown in Hela cells suppresses cell proliferation and delays G1 to S phase transition. Cyclin E1 controls the G1 to S transition through Cdk2 kinase and is upregulated in many cancers. Since *DDX3* modulates cyclin E1 translation, it may be considered as a potential therapeutic target in cancer therapy [194].

Hypoxia, as a main characteristic of solid tumors including breast cancer, changes gene expression programs that efficiently promote survival of cells. Low oxygen conditions affect the expression of hypoxia inducible factors (HIFs). HIFs act as transcriptional factors in the cells and mediate expression of different genes such as *DDX3* in response to the hypoxic condition. In human breast epithelial cells HIF-1α binds to the consensus hypoxic response element (HRE) on the promoter of the *DDX3* gene and increases its expression. This finding suggests that hypoxic conditions in solid tumors activate *DDX3* expression [195]. Altogether these findings suggest that *DDX3* may play essential regulatory roles in the development and progression of certain cancer types.

1.7.2. The Role of DDX5 in Cancer

DDX5, the prototypic member of the DEAD-box RNA helicases family, was one of the first examples of cellular RNA helicases, which was identified by cross-reactivity with PAb204 antibody raised against SV40 large T antigen three decades ago [196]. In

man, DDX5 (also known as p68) protein is encoded by the *DDX5* gene located on chromosome 17 and composed of 614 amino acid residues. *Ddx5* in the mouse maps to chromosome 11 and encodes a protein of 615 amino acids. In both man and mouse the *DDX5* transcripts is split among 13 exons.

Ddx5$^{-/-}$ embryos die at E 11.5, indicating an essential role for *Ddx5* in development. Moreover, down-regulation of *Ddx5* by RNAi reduced cell growth and enhanced apoptosis. Thus, *Ddx5* not only is important in developmental processes but also plays a profound role in cell growth and survival [197].

DDX5 is a multifunctional protein involved in several cellular processes including alternative splicing [198], pre-mRNA processing [199], RNA secondary structure rearrangement [200], ribosomal RNA processing [201], microRNA processing [202] and transcriptional regulation [203]. DDX5 acts as transcriptional co-activator or co-repressor interacting with various transcription factors and nuclear receptors, including the myogenic regulator MyoD [204], the tumor suppressor p53 [205], androgen receptor [206], β-catenin [207], and the osteoblast differentiation factor Runx2 [208]. Although the ATPase and helicase activities of DDX5 seem to be important for its functions in RNA processing, they are not required for most of its transcriptional co-regulator activities [196]. However, p300-dependent transcription requires DDX5 ATPase activity. DDX5 associates with Pol II and CBP/p300 multiprotein complex and promotes transcription [209].

Different studies have shown that *DDX5* expression is growth and developmentally regulated [210,211], suggesting a role for *DDX5* in cell proliferation. *DDX5* is a nucleo-cytoplasmic shuttling protein. The intranuclear localization of *DDX5* is cell cycle-related. *DDX5* is mainly excluded from the nucleoli during interphase, but is transiently

associated with nascent nucleoli in late telophase [212]. This suggests that *DDX5* function is regulated by the cell cycle.

DDX5 is ubiquitously expressed. However, its expression and its post-translational modifications are altered in different cancers, suggesting that DDX5 is associated with cancer development [206,207,213,214,215]. *DDX5* is consistently overexpressed in colorectal tumors and cell lines compared with the corresponding normal tissues and cells [213]. Furthermore, *DDX5* overexpression in NIH-3T3 and NC3H10 fibroblasts results in the tumorigenic transformation of these cells [216], indicating a direct role for *DDX5* in tumorigenesis.

DDX5 is tyrosine-phosphorylated in different cancer cell lines, including colon tumor (Caco-2), lung carcinoma (A549), hepatocellular carcinoma (HepG2), breast cancer (MCF-7), cervix carcinoma (HeLa S3), and leukemia cells (K562). However, DDX5 is not phosphorylated in the cell lines derived from the corresponding normal tissues. Treatment of cancer cells with anticancer agents such as tumor necrosis factor-α decreases tyrosine phosphorylation(s) [214]. Treatment of the hepatic tumor cell lines, HT-29 and HCT116, with platelet-derived growth factor (PDGF) leads to tyrosine phosphorylation of DDX5 at Y593. Phosphorylated DDX5 promotes nuclear translocation of β-catenin by inhibiting its phosphorylation by GSK-3β. The nuclear β-catenin then interacts with LEF/TCF complex and induces EMT [217].

DDX5 is overexpressed in 30 - 58% of breast tumors. Almost 70% of human breast tumors are ERα-positive, and since *DDX5* is a co-activator of ERα, its overexpression may elevate the oncogenic activities of ERα [215]. The upregulation of *DDX5* in breast tumors has been explained by strong sumoylation of the protein, which stabilizes *DDX5* and prevents its degradation [218].

DDX5 acts as an androgen receptor (AR) coactivator in prostate cancer. DDX5 and AR are recruited to the promoter region of the androgen responsive prostate-specific antigen gene. This finding indicates a relationship between *DDX5* and AR signaling in prostate cancer progression [206].

Shin et al have shown that *DDX5* and its closely related homologue *DDX17* (also known as p72) are strongly expressed during the transition from polyp to adenoma and from adenoma to adenocarcinoma in the colon. Moreover, they form complexes with β-catenin and promote β-catenin-mediated transcription, for example of the proto-oncogenes *c-Myc*, *c-jun*, *cyclin D1*, and *fra-1*. Simultaneous depletion of *DDX5* and *DDX17* reduces the expression of these β-catenin-regulated genes. Transcription of the cell cycle inhibitor $p21^{WAF1/CIP1}$, which is suppressed by c-Myc, is increased in *DDX5* and *DDX17* knockdown cells due to the downregulation of c-Myc level. Therefore, *DDX5* and *DDX17* contribute to colon cancer development through direct upregulation of proto-oncogenes and through indirect down-regulation of the growth suppressor $p21^{WAF1/CIP1}$. Accordingly, *DDX5* and *DDX17* depletion in colon cancer cells prevents their proliferation and decreases their tumor formation ability *in vivo* [207].

1.8. Aim of The Thesis

The highly related members of TALE class homeodomain transcription factors, MEIS1 and PREP1, employ their homology domain (HR) to interact with PBX family members. They are also able to interact with HOX family members and bind similar DNA sequences in some cases. However, they have evolved to exert opposite effects in tumorigenesis. The oncogenic member of the family, *MEIS1*, accelerates *HOX*- and *MLL*-induced leukemias and promotes tumor progression in some solid cancers. *PREP1*,

however, appears to have a tumor suppressive function. Accordingly, *Prep1*$^{i/i}$ mice, which escape embryonic lethality, develop tumors or precancerous lesion later in life. Thus, the lack of information on the role of *MEIS1* in non hematological malignancies and its possible competition with *PREP1* in this context prompted me to unravel molecular mechanisms underlying *Meis1* oncogenicity and its possible competition with *Prep1* using MEFs as a model system.

Chapter 2: *Results*

2.1. *Prep1*$^{i/i}$ MEFs are more prone to immortalization by the 3T3 protocol.

I used a 3T3 protocol to analyze the immortalization rate of two *Prep1*^{wt} and two *Prep1*$^{i/i}$ littermate MEF cultures. 3T3 protocol is defined as the passage of 3×10^5 cells every 3 days in 50 mm dishes. Passaging primary cells with a 3T3 protocol maximizes the growth before they develop cellular senescence [219]. The population doubling level (PDL) was identical in the two genotypes up to passage 9 (Figure 2.1). From passage 9 to 34, *Prep1*^{wt} MEFs grew with lower PDL than *Prep1*$^{i/i}$ MEFs. After passage 20, *Prep1*$^{i/i}$ MEFs markedly increased their proliferative capacity [179].

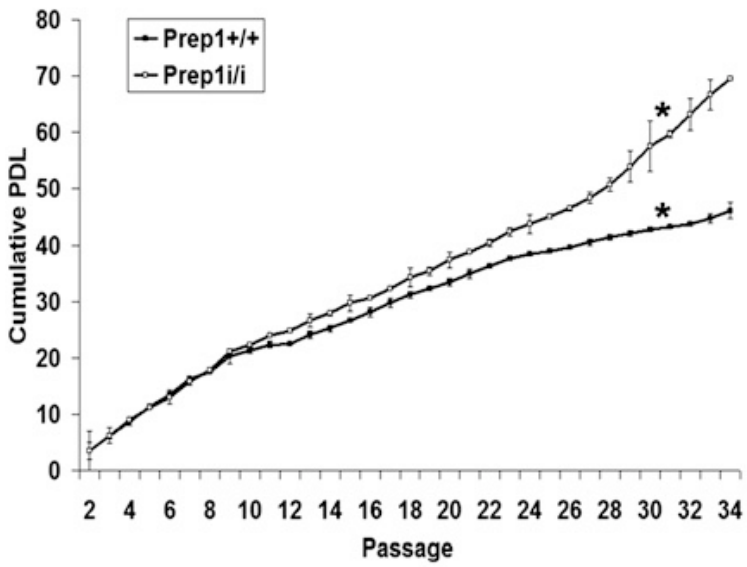

Figure 2.1. Early immortalization in *Prep1*$^{i/i}$ MEFs. 3×10^5 cells from two individually derived primary MEFs of each genotype were plated in 6 cm dishes. Cells were trypsinized and counted every three days based on the 3T3 protocol. Cells were kept in a 3% O_2 incubator during the entire experiment time. Averaged growth curves from two individually derived primary MEFs of each genotype. Error bars indicate SEM; *P < 0.05.

2.2. The growth rate of early passage *Prep1*$^{i/i}$ and *Prep1*^{wt} MEFs is identical but late passage *Prep1*$^{i/i}$ MEFs proliferate faster than their *Prep1*^{wt} counterpart.

To check the effect of Prep1 absence on the proliferation rate of MEFs, I analyzed the growth rate of one primary *Prep1*$^{i/i}$ and two *Prep1*^{wt} littermates MEF cultures at passage 2 (Figure 2.2A, upper panel) or two immortalized *Prep1*$^{i/i}$ and *Prep1*^{wt} MEFs at passage 33 (Figure 2.2B, upper panel). Cells were immortalized using 3T3 protocol (See section 2.1). The proliferation rate of primary *Prep1*$^{i/i}$ and *Prep1*^{wt} cells does not show any difference in early passage cells; however, immortalized *Prep1*$^{i/i}$ cells proliferate faster than WT cells. The protein level of Prep1 in primary (Figure 2.2A, lower panel) and immortalized (Figure 2.2B, lower panel) *Prep1*$^{i/i}$ and *Prep1*^{wt} MEFs was tested by immunoblotting.

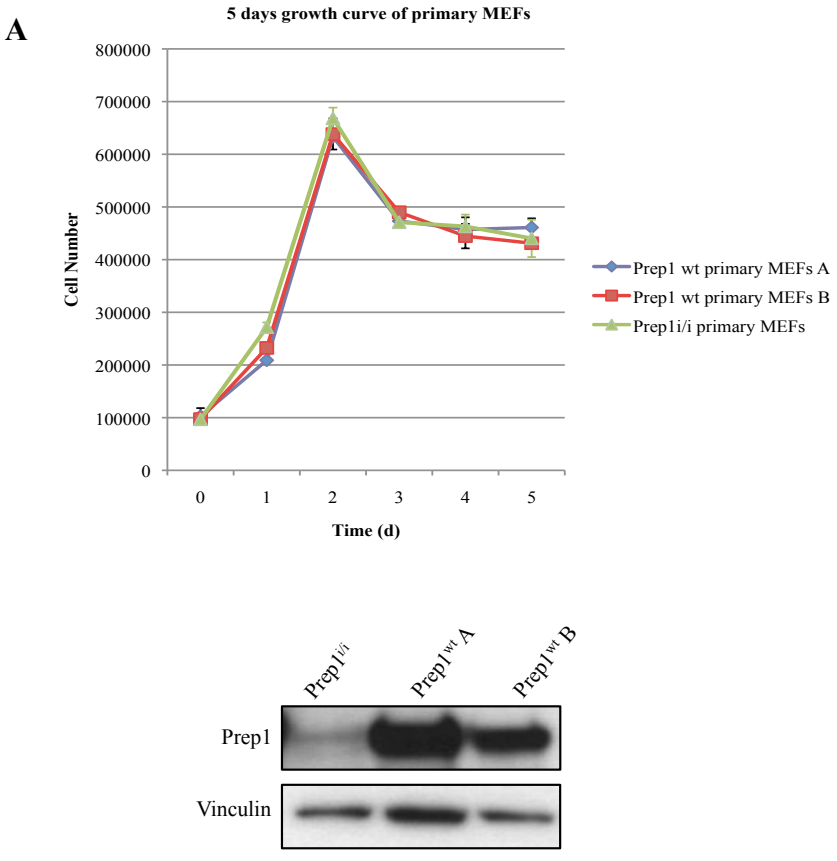

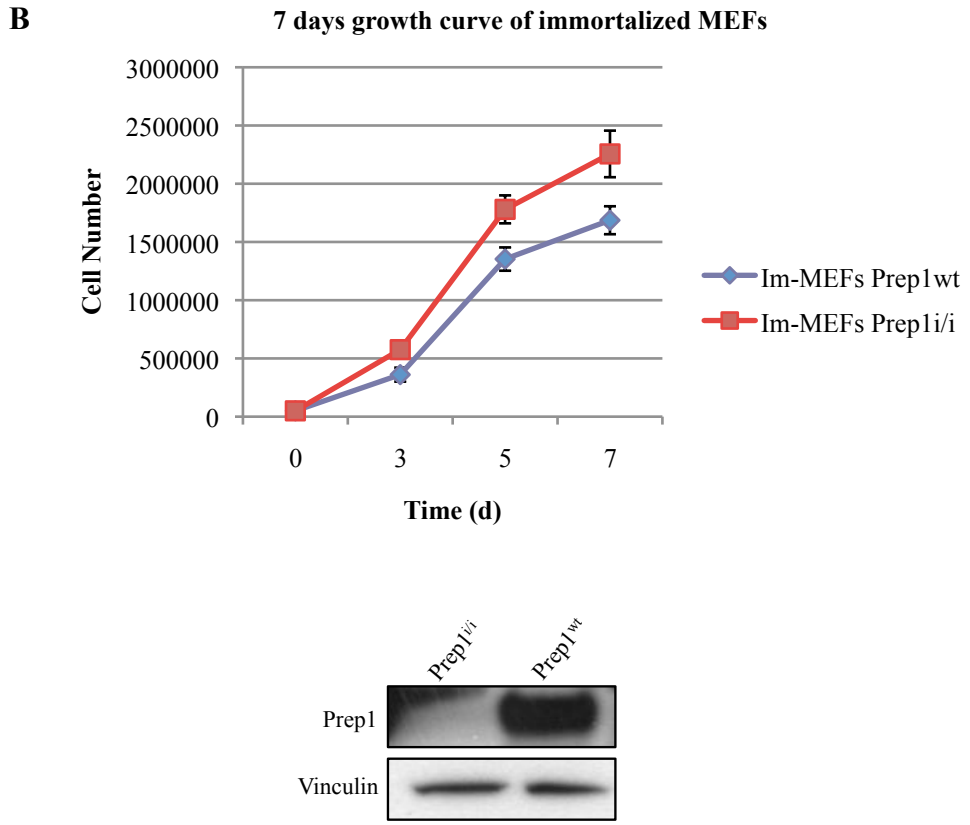

Figure 2.2. Cell proliferation rate of primary and immortalized *Prep1*$^{i/i}$ and *Prep1*^{wt} MEFs. To compare the growth rate between primary *Prep1*$^{i/i}$ and *Prep1*^{wt} MEFs **(A)** and between immortalized *Prep1*$^{i/i}$ and *Prep1*^{wt} MEFs **(B)**, 1 × 10^5 passage-two cells and 5 × 10^4 passage-33 cells were plated in 6-well plates in triplicate. Cells were trypsinized and counted every day or every other day. Data represent the average of three independent wells. Error bars indicate SD. *P > 0.05. Total lysates of primary and immortalized *Prep1*$^{i/i}$ and *Prep1*^{wt} MEFs were analyzed by western blotting using Prep1 polyclonal antibody. Vinculin was used as the loading control.

2.3. *Prep1*-deficiency does not alter *Meis1* mRNA and protein level in primary MEFs, but decreases its protein level in immortalized cells.

Deficiency of *Prep1* affects the stability of Pbx1 and Pbx2 proteins in mouse embryos and therefore decreases their level [171,173]. In this regard, I checked whether the lack of *Prep1* had any effect on the mRNA and protein level of the oncogenic member of the TALE family proteins, *Meis1*. To address this point, qPCR was performed on the

cDNA prepared from 3 different *Prep1*$^{i/i}$ and 3 different *Prep1*^{wt} primary MEFs cultures. I observed no major differences in the levels of expression of the *Meis1* mRNA in *Prep1*$^{i/i}$ compared to *Prep1*^{wt} MEFs (Figure 2.3A**)**. The levels of Meis1a protein also are not particularly changed in these cells (Figure 2.3B**)**. However, in immortalized MEFs, Meis1 protein level is significantly decreased in *Prep1*-deficient cells compared to the WT counterparts (Figure 2.3C). Although its mRNA level is not altered in these cells (data are not shown). Therefore the deficiency of *Prep1* has no significant effect on the expression of *Meis1* in primary cells but it decreases Meis1 protein level in immortalized cells.

A

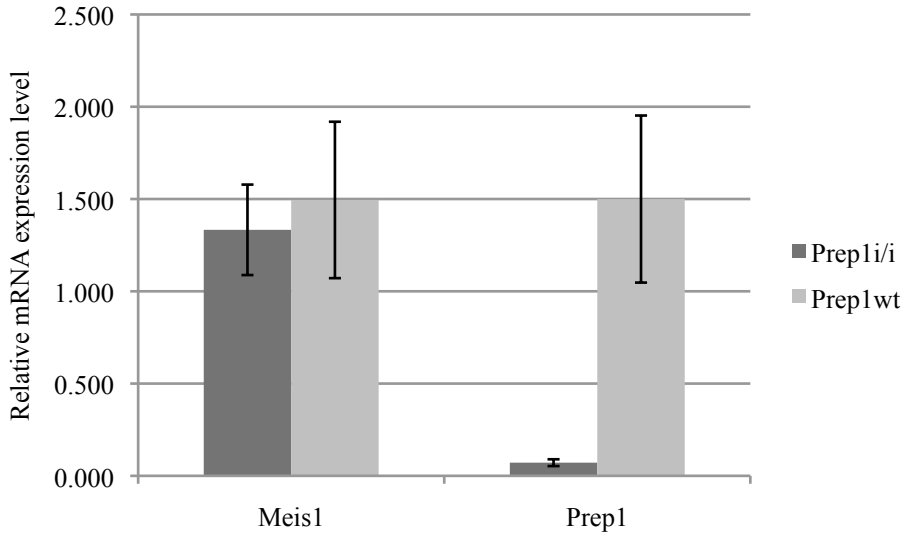

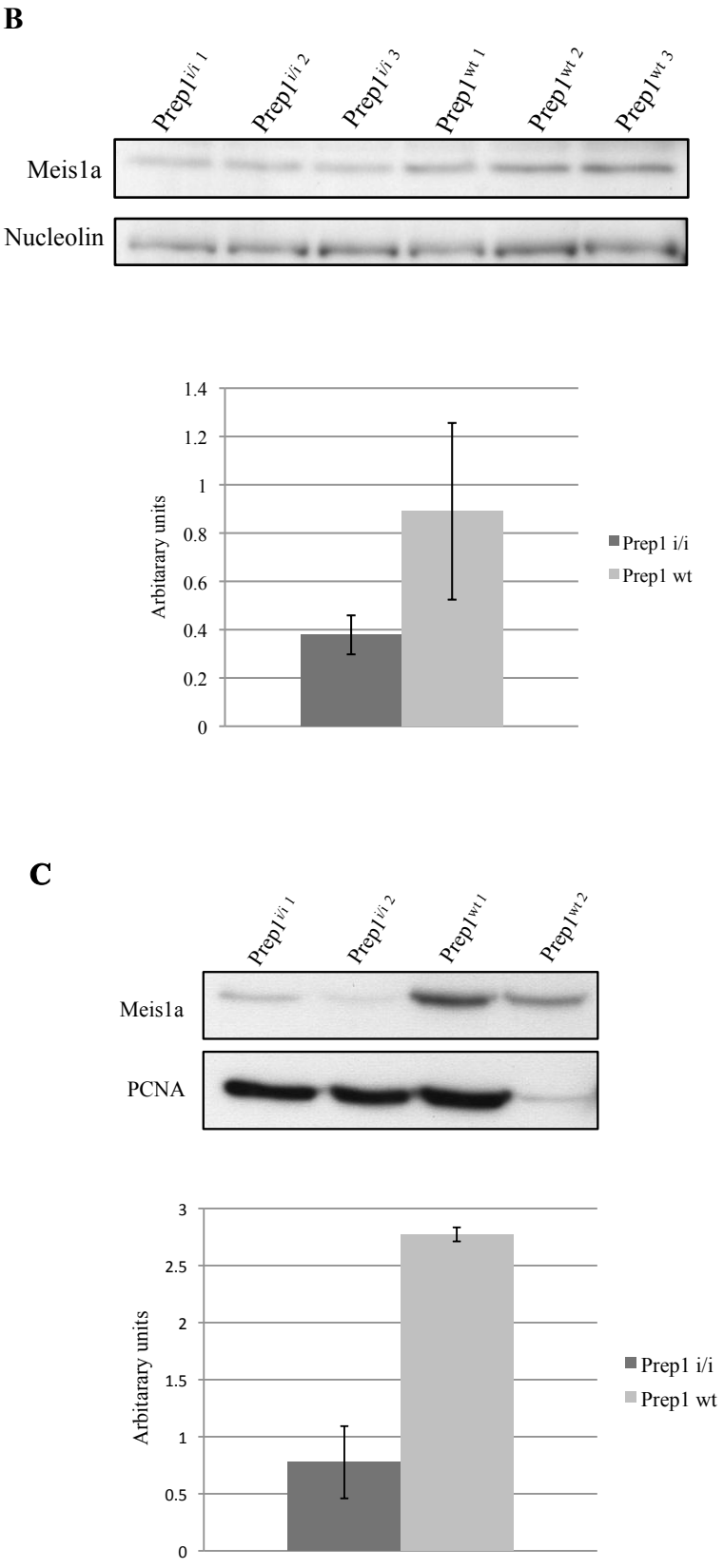

Figure 2.3. Effect of *Prep1* deficiency on *Meis1* expression level (A) Total RNA was extracted from passage-3 MEFs. RNA was retrotranscribed and qPCR analysis performed using specific primers for *Prep1* and *Meis1* genes. GAPDH was used for normalization. The results are plotted as the mean of 3 different $Prep1^{i/i}$ and 3 different $Prep1^{wt}$ MEFs cultures. ($P > 0.05$) **(B)** Nuclear extracts of the same cells were analyzed by western

blotting using Meis1 K845 antibody. Nucleolin was used as the loading control. Quantification of the bands was done by densitometric analysis and plotted as the mean of three different *Prep1*$^{i/i}$ and three different *Prep1*^{wt} MEFs cultures ($P > 0.05$). Error bars indicate SD. **(C)** Nuclear extract of two *Prep1*^{wt} and two *Prep1*$^{i/i}$ immortalized cells was prepared and analyzed by western blotting using Meis1 K845 antibody. PCNA was used as the loading control. Bands were quantified by densitometric analysis and plotted as the mean of two different *Prep1*$^{i/i}$ and two different *Prep1*^{wt} immortalized MEFs ($P < 0.05$). Error bars indicate SD.

2.4. Meis1a induces proliferation in *p53*^{ko} primary and *Prep1*$^{i/i}$ immortalized but not in *Prep1*$^{i/i}$ primary MEFs. Meis1a cooperates with Ras or c-Myc in *p53*^{wt} primary MEFs.

Transformation of primary rodent fibroblasts needs the coexpression of at least two oncogenes or overexpression of one oncogene in the absence of a tumor suppressor gene, whereas a single oncogene is generally sufficient in immortalized cells [219,220]. To check the oncogenecity of *Meis1* in primary MEFs, *p53*^{ko} and WT MEFs at passage-3 were infected with a retroviral vector encoding oncogenic *H-Ras*^{v12}, *Meis1a* or an empty vector as control. Moreover WT cells were infected with a combination of *H-Ras*^{v12}*/c-Myc*, *H-Ras*^{v12}*/Meis1a* and *c-Myc/Meis1a* retroviruses. *H-Ras*^{v12}, *c-Myc* and *Meis1a* expression were confirmed by immunoblotting (Figure 2.4A and 2.4C). I subjected these cells to growth curve assay (Figure 2.4B and 2.4D). Like Ras, Meis1a, did not accelerate the proliferation of *p53*^{wt} primary MEFs, but it did so in *p53*^{ko} cells. The coexpression of *Meis1a* with *H-Ras*^{v12} or with *c-Myc,* however, increased proliferation in the WT cells (Figure 2.4B and 2.4D). Moreover, when *Prep1*$^{i/i}$ MEFs at passage-3 were infected with a retrovirus vector encoding *Meis1a*, I did not observe any proliferation difference between *Meis1a*-overexpressing and control cells (data not shown). I, therefore, used immortalized MEFs to test whether Meis1a alters the proliferation of cells in the absence of *Prep1*. I transduced passage-30 MEFs with a retrovirus encoding *Meis1a*. Infected cells were selected with puromycin, and Meis1a expression level was confirmed by immunoblotting

(Figure 2.4E). *Meis1a* over-expressing *Prep1*$^{i/i}$ cells proliferated faster than WT (Figure 2.4F). Altogether, this data shows that Meis1a alone can accelerate the proliferation of primary MEFs in the absence of p53. However, in the WT cells it requires a cooperating oncogene. Moreover, in the absence of *Prep1,* Meis1a accelerates the proliferation of immortalized MEFs. This agrees with the tumor suppressor function of *Prep1*.

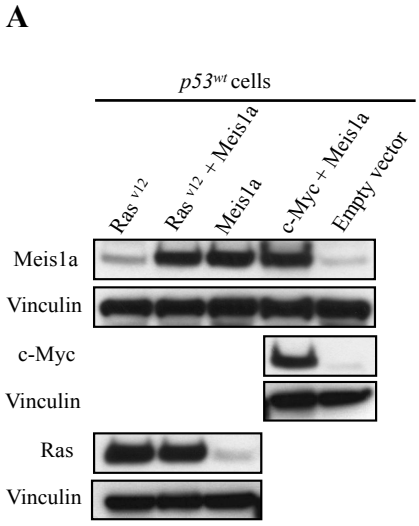

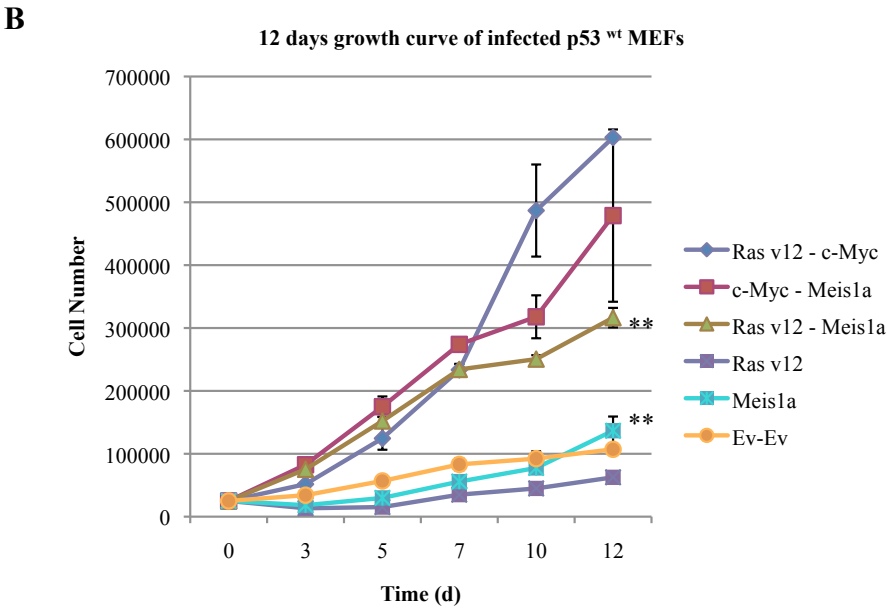

D

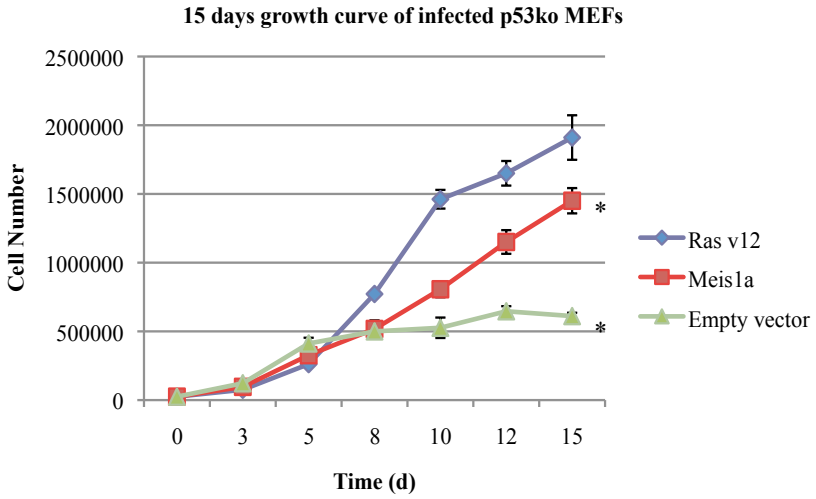
15 days growth curve of infected p53ko MEFs
Cell Number
2500000
2000000
1500000
1000000
500000
0
0
3
5
8
10
12
15
Time (d)
*
*
Ras v12
Meis1a
Empty vector

C

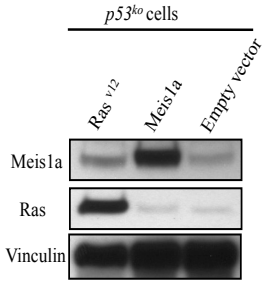
p53ko cells
Ras v12
Meis1a
Empty vector
Meis1a
Ras
Vinculin

E

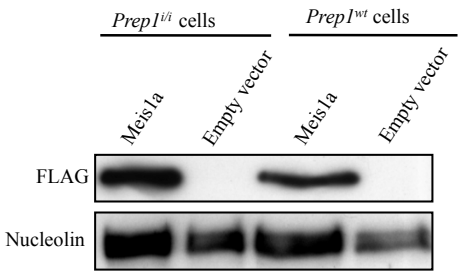
Prep1i/i cells
Prep1wt cells
Meis1a
Empty vector
Meis1a
Empty vector
FLAG
Nucleolin

F

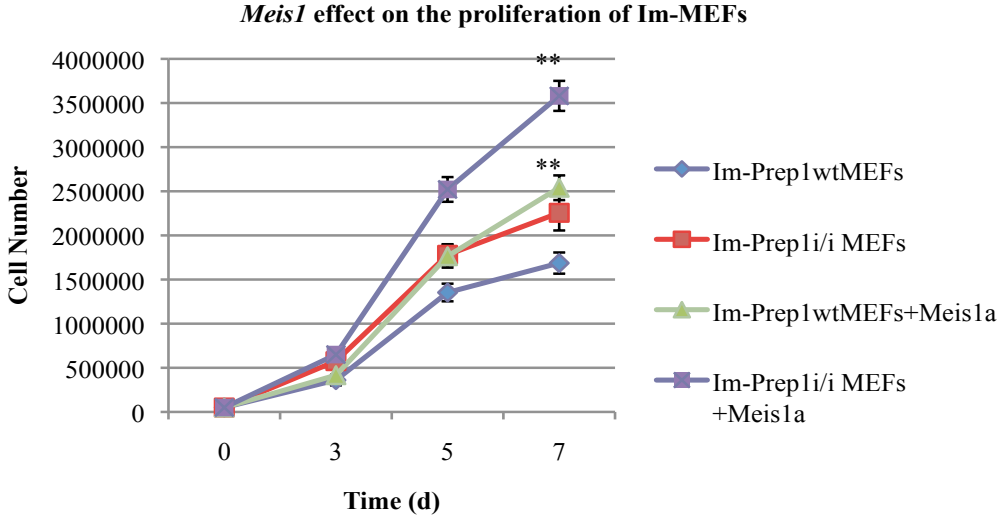
Meis1 effect on the proliferation of Im-MEFs
Cell Number
4000000
3500000
3000000
2500000
2000000
1500000
1000000
500000
0
0
3
5
7
Time (d)
**
**
Im-Prep1wtMEFs
Im-Prep1i/i MEFs
Im-Prep1wtMEFs+Meis1a
Im-Prep1i/i MEFs +Meis1a

Figure 2.4. Meis1a-induced proliferation in MEFs. Passage-3 $p53^{wt}$ **(B)** and $p53^{ko}$ **(D)** cells were infected with *Ras*, *Meis1a*, *c-Myc* or a retroviral combination of *Ras/c-Myc*, *Ras/Meis1a*, c-*Myc/Meis1a* or empty vector as shown. The expression level of the indicated genes was checked by immunoblotting **(A and C)**. 2.5×10^4 infected cells were plated in 12-well plates in triplicate and cells counted at the indicated time points **(B and D).** Passage-33 $Prep1^{i/i}$ and WT MEFs were infected with *Meis1a* and subjected to growth curve assay over a 7-days period. 5×10^4 infected cells were plated in 6-well plates in triplicate and counted at the indicated time points **(F)**. Exogenous Meis1a expression level was checked by western blotting using anti FLAG antibody. Nucleolin was used as a protein loading control **(E)**. Data represent the means of three independent wells. Error bars indicate SD. *P < 0.001; **P < 0.01.

2.5. Meis1a overexpression malignantly transforms $Prep1^{i/i}$ but not $Prep1^{wt}$ immortalized MEFs. The effect is partially reverted by *Prep1* re-expression.

Loss of contact inhibition in monolayer culture and anchorage-independent growth are the characteristics of oncogene-induced cell transformation. They are useful assays *in vitro* to test the tumorigenicity of cells [221,222]. I did not observe formation either of colonies in soft agar or tumors in mice when $Prep1^{i/i}$ or WT passage-3 MEFs were infected with a retrovirus vector encoding *Meis1a* (data not shown). I, therefore, used immortalized MEFs to test whether Meis1a alone transforms *Prep1*-deficient cells. Since *Meis1* and *Hoxa9* cooperate to transform hematopoietic cells [43], I retrovirally infected passage-35 MEFs with *Meis1a*, *Hoxa9* or with a combination of the two retroviruses. The infected cells were first analyzed for foci formation when seeded in low number. *Prep1*-deficent cells formed almost twice more colonies compared to the WT cells when infected with *Meis1a/Hoxa9* or *Meis1a* only retroviruses. However, $Prep1^{i/i}$ and not WT, cells formed few foci when infected with the sole *Hoxa9* retrovirus (Figure 2.5A).

When infected cells were analyzed for anchorage independent growth in semi-solid medium, *Meis1a-Hoxa9* coexpressing $Prep1^{i/i}$ cells formed colonies in agar 3-fold more efficiently than WT. Also the colonies of $Prep1^{i/i}$ cells were bigger than those of WT cells

(Figure 2.5B and 2.5C). Surprisingly, overexpression of *Meis1a* alone in *Prep1*$^{i/i}$ cells induced colony formation in agar. This property was significantly inhibited by *Prep1* re-expression (Figure 2.5B and 2.5C).

Consistent with these data, subcutaneous transplantation of the infected cells into immunodeficient mice revealed a significant difference between the tumorigenicity of WT and *Prep1*$^{i/i}$ cells overexpressing *Meis1a*. Only *Prep1*$^{i/i}$, and not WT, cells overexpressing *Meis1a* formed tumors in mice (Figure 2.5D and 2.5E). In addition, *Prep1*$^{i/i}$ cells coexpressing *Meis1a-Hoxa9* formed more aggressive tumors than WT cells as measured by the volume of the tumor but neither *Prep1*$^{i/i}$ nor WT cells overexpressing *Hoxa9* alone were able to form tumor (Figure 2.5D and 2.5E). I tested whether *Prep1* re-expression can affect the tumorigenic activity of *Meis1*. To this goal, I first overexpressed Meis1a in *Prep1*$^{i/i}$ cells, then divided the cells in two groups re-infecting them with either empty vector or *Prep1* vector. Remarkably *Prep1* re-expression decreased tumor growth of the *Prep1*$^{i/i}$ cells overexpressing *Meis1a* and increased the latency of *Meis1a*-induced tumor (2.5D and 2.5E). Cells transduced with *H-Ras*^{v12} and *c-Myc* retroviruses were used as positive control for tumor formation. The inability of *Hoxa9* to induce tumors in *Prep1*$^{i/i}$ cells is surprising and will deserve further investigation. The overexpression level of the indicated genes is shown in figure 2.5 F.

A

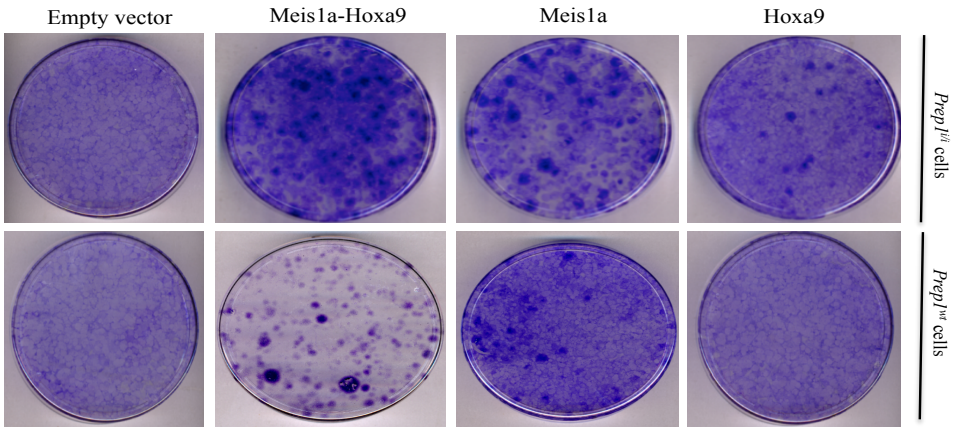
Empty vector
Meis1a-Hoxa9
Meis1a
Hoxa9
Prep1i/i cells
Prep1wt cells

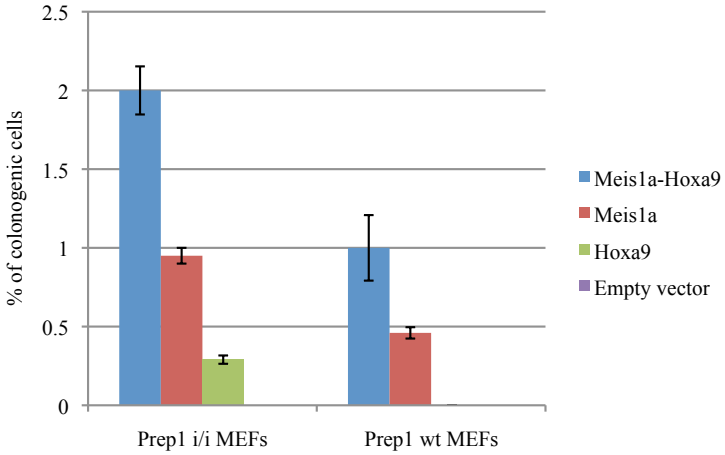
2.5
2
1.5
1
0.5
0
% of colonogenic cells
Prep1 i/i MEFs
Prep1 wt MEFs
Meis1a-Hoxa9
Meis1a
Hoxa9
Empty vector

B

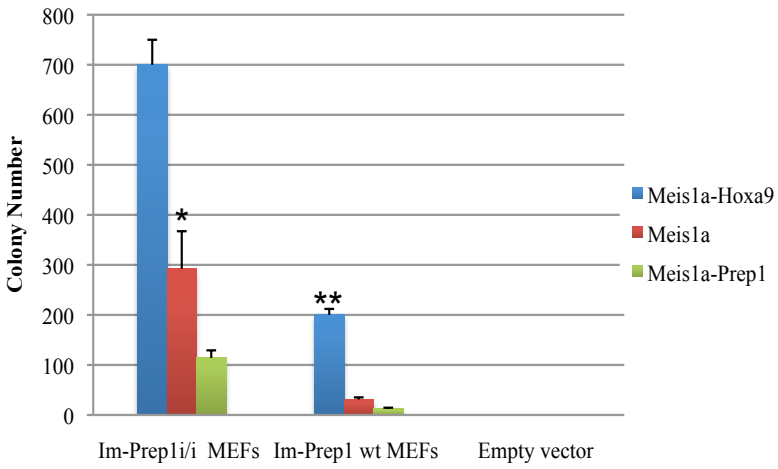
800
700
600
500
400
300
200
100
0
Colony Number
*
**
Im-Prep1i/i MEFs
Im-Prep1 wt MEFs
Empty vector
Meis1a-Hoxa9
Meis1a
Meis1a-Prep1

C

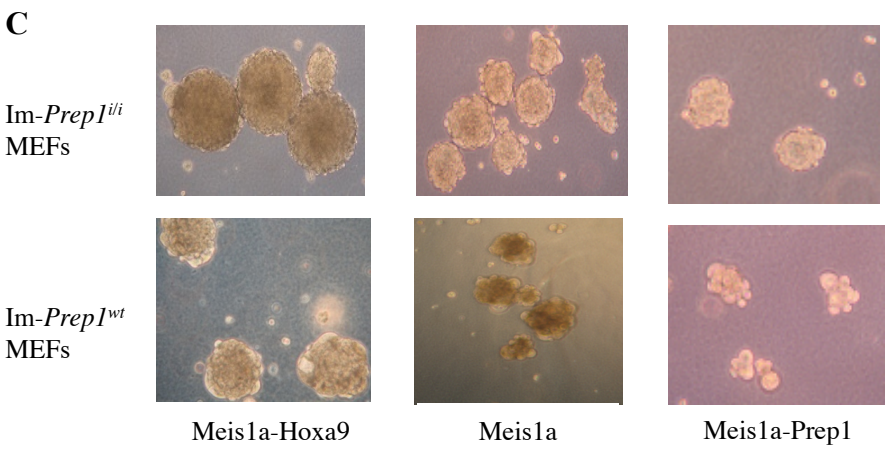
Im-*Prep1*$^{i/i}$ MEFs
Im-*Prep1*^{wt} MEFs
Meis1a-Hoxa9
Meis1a
Meis1a-Prep1

D

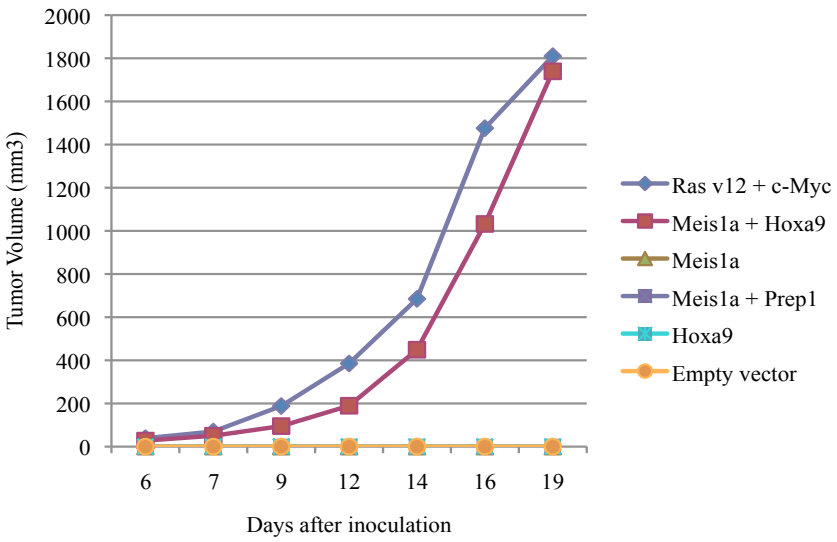
Tumor Volume (mm3)
2000
1800
1600
1400
1200
1000
800
600
400
200
0
6
7
9
12
14
16
19
Days after inoculation
Ras v12 + c-Myc
Meis1a + Hoxa9
Meis1a
Meis1a + Prep1
Hoxa9
Empty vector

E

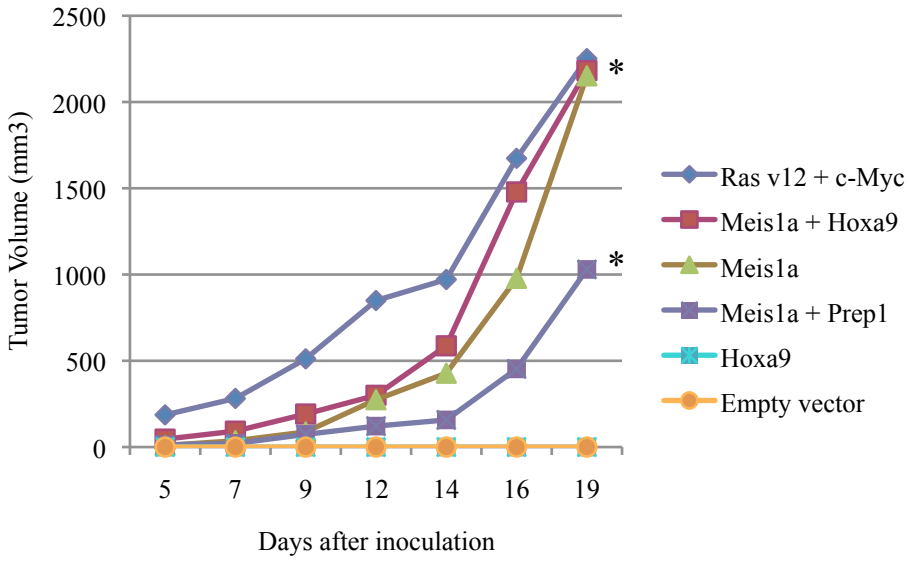
Tumor Volume (mm3)
2500
2000
1500
1000
500
0
5
7
9
12
14
16
19
Days after inoculation
*
*
Ras v12 + c-Myc
Meis1a + Hoxa9
Meis1a
Meis1a + Prep1
Hoxa9
Empty vector

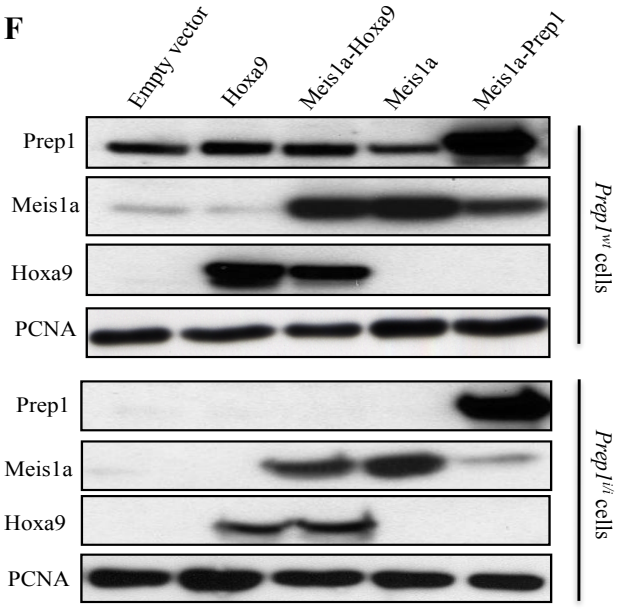

Figure 2.5. Effect of Meis1a on transformation and tumorigenicity of *Prep1*$^{i/i}$ and WT MEFs. Retrotransduced MEFs colony formation assay **(A)** and anchorage-independent soft agar growth assay **(B and C)**. **(A)** The upper panel shows the examples of the plates seeded with 5×10^3 cells. The percentage of the colonogenic cells from two independent experiments, each performed in triplicate, is shown in the lower panel. Error bars represent SD. The number **(B)** and the size **(C)** of colonies formed in soft-agar by 10^5 *Prep1*$^{i/i}$ and WT MEFs per 6cm plate, infected with the indicated retroviruses are shown (*P< 0.001 compared with *Prep1*$^{i/i}$ MEFs re-expressing *Prep1*; **P< 0.001 compared with wt MEFs overexpressing Prep1). Data represent the mean of three independent plates. Error bars indicate SD. WT **(D)** and *Prep1*$^{i/i}$ MEFs **(E)** retrovirally transduced with the indicated vectors were subcutaneously injected into nude mice (1×10^6 cells per animal) and tumor volume was monitored. Lines represent the average of five animals per group. For clarity the SD is not shown. Differences between *Prep1*$^{i/i}$ overexpressing *Meis1a* and *Meis1a* together with *Prep1* groups (*P< 0.05) were statistically significant. **(F)** Immunoblots show the overexpression levels of Prep1, Meis1a and Hoxa9 in cells infected with the indicated retroviruses. PCNA was used as a protein loading control.

2.6. The HR1+2 domain of Prep1 is required to inhibit *Meis1*-induced transformation.

Identification of the domains of Prep1 responsible for the inhibition of tumorigenesis can give information on the mechanism. To identify the domains of Prep1 required to inhibit *Meis1* tumorigenicity, I constructed different Prep1 mutants and tested their effect on *Meis1*-induced cell transformation both in vitro and in vivo. To do so,

several deletion mutants introducing the following modifications were subcloned in pMSCV-hygro vector along with a FLAG-tag: a) deletion of the Pbx interacting domain (Prep1ΔHR1+2, deleted residues: 58-137); b) deletion of the DNA binding homeodomain (Prep1ΔHD, deleted residues: 259-318); c) deletion of the C-terminal domain (Prep1ΔC, deleted residues: 318-436) (Figure 2.6A).

The expression of each Prep1 mutant was checked by semiquantitative RT-PCR and western blotting in infected passage-35 *Prep1*$^{i/i}$ MEFs. The semiquantitative RT-PCR analysis showed that all mutants were well expressed at the mRNA level (Figure 2.6B). The WT and mutated cDNAs produced proteins of the predicted molecular weight as determined by western blotting (Figure 2.6C upper panel). Moreover the subcellular localization of the different mutant proteins was also tested using nuclear and cytoplasmic lysates. Except Prep1ΔHR1+2, which shows both nuclear and cytoplasmic localizations, the other mutants were mainly nuclear (Figure 2.6C upper panel).

To test the effect of different Prep1 mutants on *Meis1*-induced tumorigenesis, I infected passage-35 *Prep1*$^{i/i}$ MEFs with FLAG-tagged *Meis1a* retroviruses. After selection of the infected cells with puromycin, cells were retrovirally infected with different FLAG-tagged *Prep1* mutants and selected with hygromycin B. The expression of exogenous Meis1a and Prep1 mutants was checked by western blotting with an anti-FLAG antibody. Moreover, the Meis1a level was also checked by specific anti-Meis1 antibody (Figure 2.6C middle panel). Unexpectedly, the overexpression of both *Prep1* and *Prep1* mutants except *Prep1ΔHR1+2* decreased Meis1a protein level of almost to 4- to 5-fold depending on the antibody (anti-FLAG versus anti-Meis1) (Figure 2.6C lower panel).

Infected cells were subjected to anchorage independent growth in semi-solid medium and the colonies were scored after 2 weeks. Overexpressed Prep1, Prep1ΔHD and Prep1ΔC proteins significantly reduced Meis1a induced colonies. The full length

Prep1 decreased the number of colonies by almost 3-fold, and the mutants by 2-fold. Prep1ΔHR1+2 did not show any inhibitory effect on the *Meis1*-induced transformation (Figure 2.6D). When cells transduced with *Meis1a* and different *Prep1* mutants were injected in immunodeficient mice, Prep1ΔHD and ΔC mutants still inhibited *Meis1*-induced tumors, whereas Prep1ΔHR1+2 mutant failed to decrease tumor growth (Figure 2.6E). This result indicates that the HR1+2 domain of Prep1 contributes significantly to its tumor suppressive function.

A

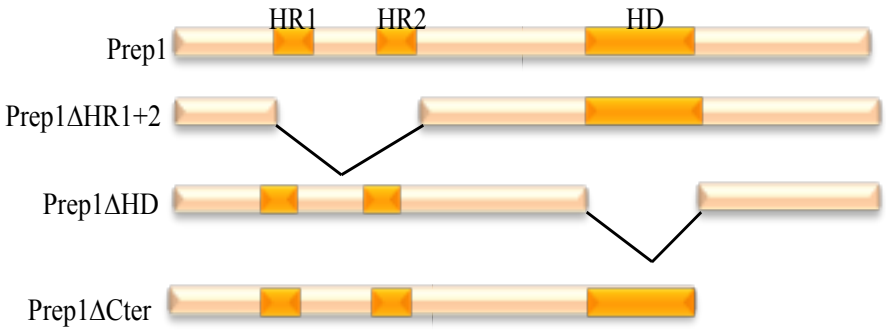

B

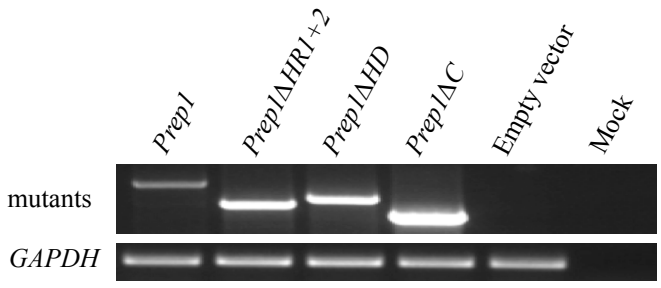

C

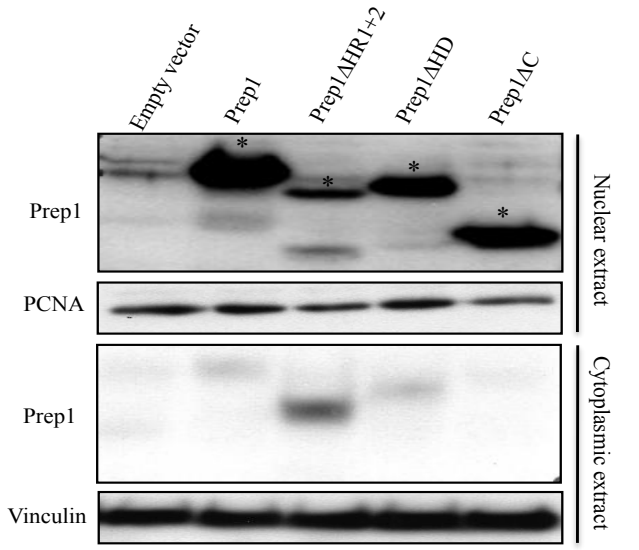
Empty vector
Prep1
Prep1ΔHR1+2
Prep1ΔHD
Prep1ΔC
Prep1
PCNA
Nuclear extract
Prep1
Vinculin
Cytoplasmic extract

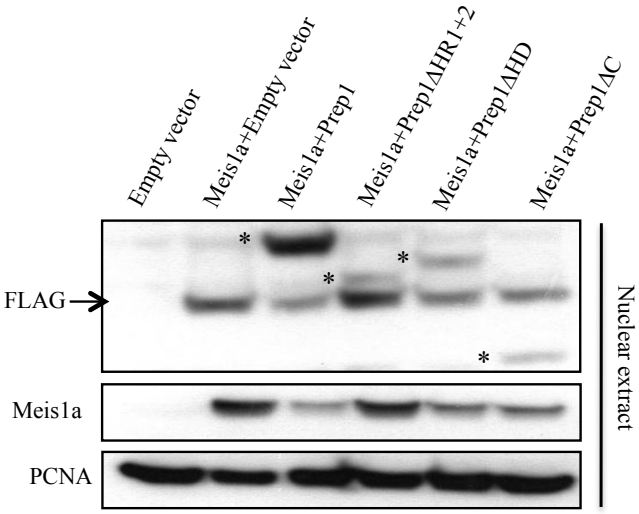
Empty vector
Meis1a+Empty vector
Meis1a+Prep1
Meis1a+Prep1ΔHR1+2
Meis1a+Prep1ΔHD
Meis1a+Prep1ΔC
FLAG
Meis1a
PCNA
Nuclear extract

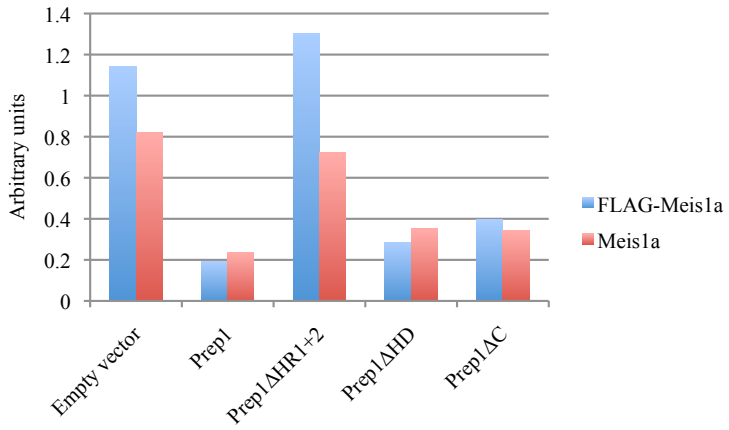
1.4
1.2
1
0.8
0.6
0.4
0.2
0
Arbitrary units
Empty vector
Prep1
Prep1ΔHR1+2
Prep1ΔHD
Prep1ΔC
FLAG-Meis1a
Meis1a

D

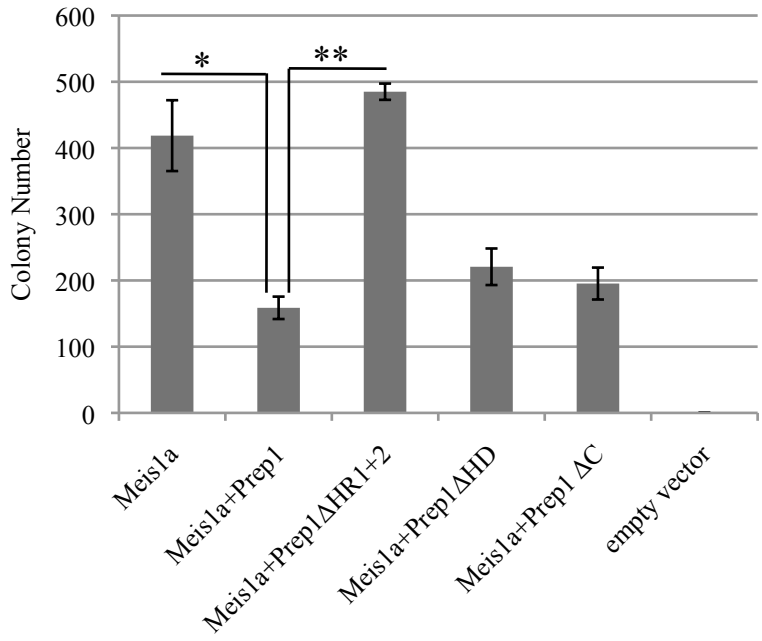

E

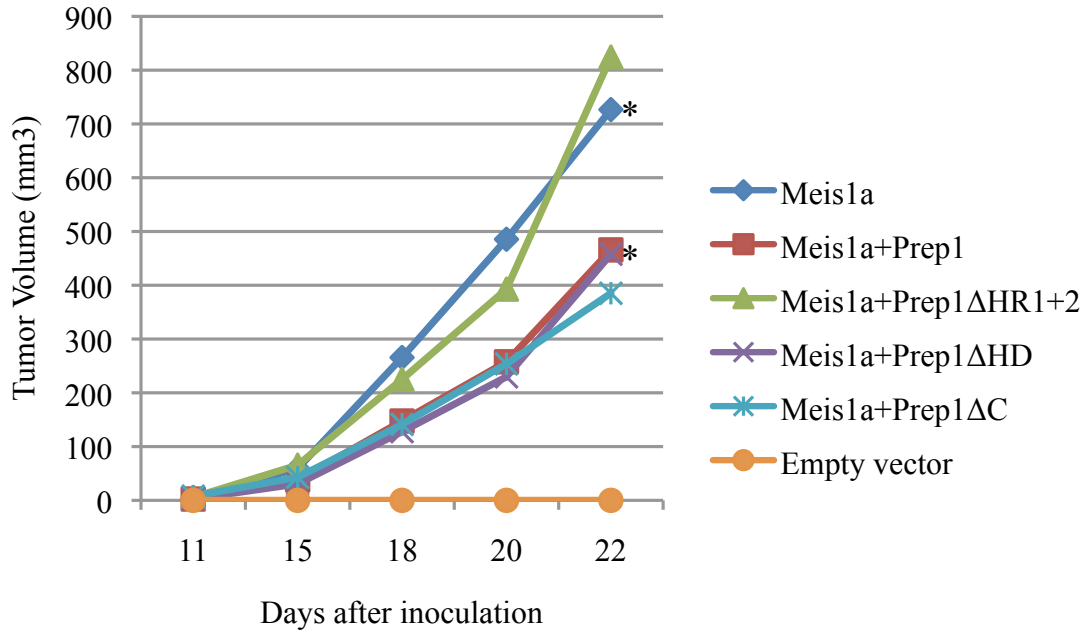

Figure 2.6. Identification of the Prep1 domain involved in inhibiting *Meis1*-induced transformation. (A) Schematic representation of Prep1 and Prep1 mutants, showing the position of the Pbx interacting domain (HR1+2), homeodomain (HD) and C-terminus. Blank spaces represent deletions. **(B)** Total RNA was extracted from passage-35 *Prep1*$^{i/i}$ MEFs stably expressing different *Prep1* mutants. RNA was retrotranscribed and a semiquantitative PCR was performed using specific primers for Prep1 mutants and GAPDH cDNA. **(C, upper panel)** 30 μg of nuclear and 60 μg of cytoplasmic lysates

were analyzed by immunoblotting with Prep1 antibody. PCNA and Vinculin were used as loading control for nuclear and cytoplasmic lysates, respectively. The position of FALG-Prep1 and each mutants is shown by an asterisk. **(C, middle panel)** 30 μg of nuclear lysate was analyzed by immunoblotting with Prep1, FLAG and Meis1 antibodies. PCNA was used as loading control. The position of FLAG-Meis1a is shown by an arrow and the position of FLAG-Prep1 and each mutants is shown by an asterisk. **(C, lower panel)** Densitometric analysis performed using ImageJ (normalized to the level of PCNA). **(D)** 1×10^5 *Prep1*$^{i/i}$ MEFs retrotransduced with *Meis1* and *Prep1* mutants were subjected to anchorage-independent soft agar growth assay. The number of colonies formed after 2 weeks of culturing is shown (*P < 0.01 compared with *Prep1*$^{i/i}$ MEFs re-expressing *Prep1*; **P < 0.0001 compared with *Prep1ΔHR1+2* overexpressing cells). Data represent the mean of three independent wells. Error bars indicate SD. **(E)** *Prep1*$^{i/i}$ MEFs overexpressing *Meis1a* along with *Prep1* or *Prep1* mutants were subcutaneously transplanted into nude mice (1×10^6 cells per animal) and the tumor volume was monitored. Lines represent the average of five animals per group. For the sake of clarity SD is not shown. Differences between *Prep1*$^{i/i}$ overexpressing *Meis1a* and *Meis1a* plus *Prep1*, *Prep1ΔHD* or *Prep1ΔC* groups are statistically significant (*P< 0.05).

2.7. Subcellular localization of WT and mutants Prep1.

Since Prep1ΔHR1+2 mutant is not capable of inhibiting *Meis1*-induced transformation, I wanted to see whether this impairment was due to the inability of this mutant to translocate to the nucleus, since its nuclear translocation depends on the interaction with Pbx [75]. In this regard, I analyzed the subcellular localization of different *Prep1* mutants expressed in MEFs. I retrovirally infected passage-35 *Prep1*$^{i/i}$ MEFs with the different *Prep1* mutants (Figure 2.6A) and checked the expression of each mutant by western blotting on the nuclear extract. (Figure 2.6C). To check the subcellular localization of different mutants by immunoflorescence and confocal microscopy, infected cells were plated on poly-D-lysine treated coverslips. The day after, coverslips were fixed in 4% PFA and stained with Prep1 polyclonal antibody and DAPI. This already known that the deletion of the Pbx interacting domain of Prep1 (HR1+2) impairs its nuclear localization [75]. However, here I observed that Prep1ΔHR1+2, in addition to a clear cytoplasmic localization, could still be detected in the nuclear compartment, possibly indicating that other mechanisms may exist in its nuclear translocation. The

RGB profile of the HR1+2 construct shows only a partial area of co-localization of Prep1 and DAPI. The other mutants did not show any nuclear localization impairment when analyzed by confocal microscopy, as expected (Figure 2.7).

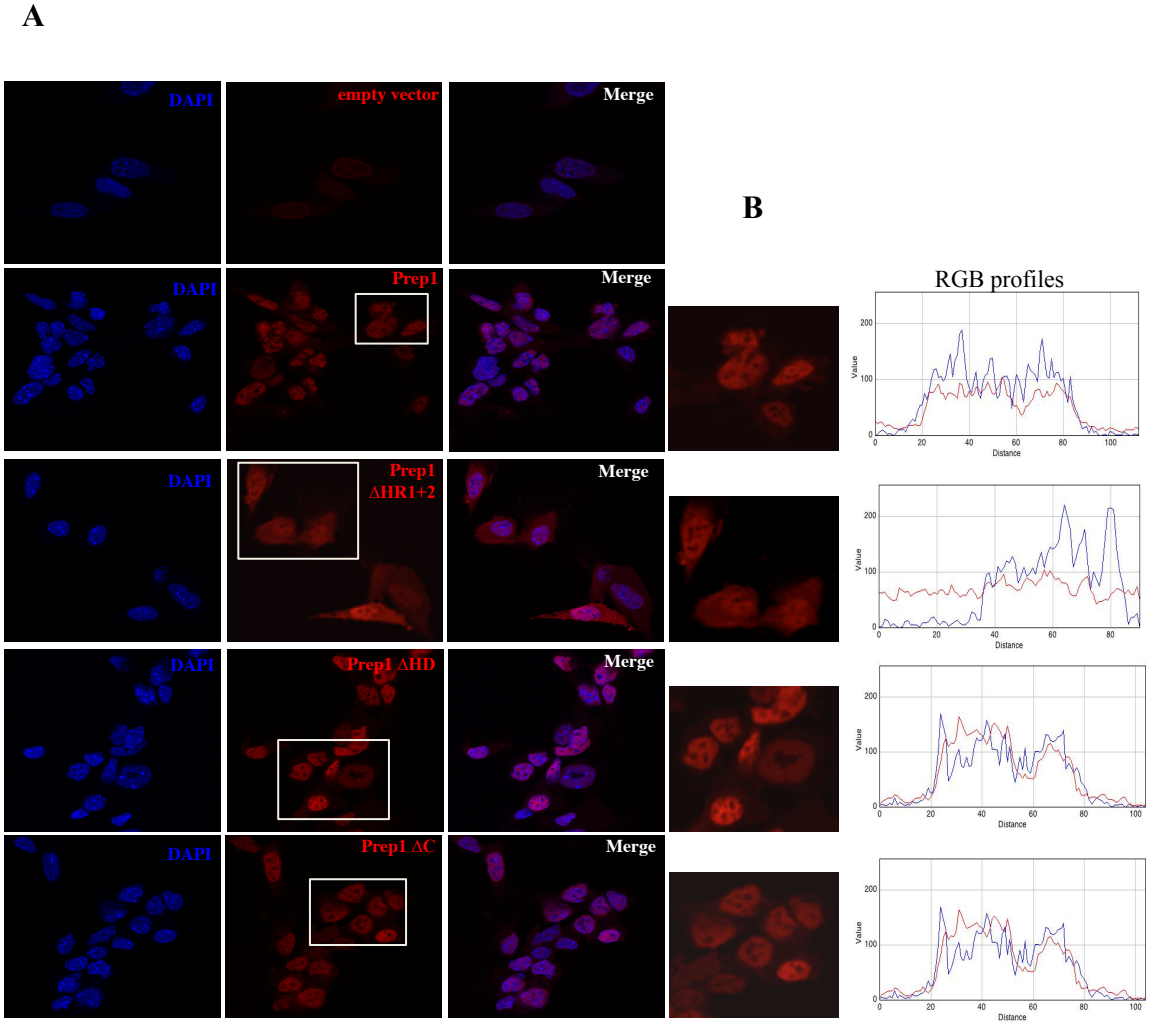

Figure 2.7. Subcellular localization of different Prep1 mutants. (panel A) Cells overexpressing different *Prep1* mutants were analyzed by immunofluorescence and confocal microscopy after fixation and staining with DAPI (blue) and Prep1-Cy5 antibody (Red). Cells infected with empty vector were used as control. The nuclear dye DAPI was used to counterstain nuclei. **Panel B** represents the zoom of the selected areas in the images shown in panel A. The RGB profiles on the right show the extent of co-localization of DAPI (blue line) and Prep1 (red line) staining.

2.8. Prep1ΔHR1+2 mutant does not interact with Pbx1 and Pbx2 and does not alter their levels in *Prep1*$^{i/i}$ cells.

In mammalian cells, overexpression of *Prep1* increases the stability of Pbx1 and

Pbx2 by preventing their proteasomal degradation [76]. Moreover in mouse embryo, *Prep1* deficiency decreases the protein level of Pbx1 and Pbx2 [171], both of which can interact with Prep1. To explain the inability of Prep1ΔHR1+2 to inhibit *Meis1*-induced tumor formation, I checked the effect of each *Prep1* mutant overexpression on the Pbx1 and Pbx2 protein levels and their ability to interact with Pbx proteins. Pbx1 and Pbx2 protein levels were assessed by western blotting in *Prep1*$^{i/i}$ MEFs infected with FLAG-tagged versions of *Prep1*, *Prep1ΔHR1+2*, *Prep1ΔHD* or *Prep1ΔC* retroviruses (figure 2.8A). As shown in the graph, the Prep1ΔHR1+2 mutant is the only mutant unable to increase Pbx1 and Pbx2 protein levels. The interaction of each mutant with Pbx1 and Pbx2 proteins was checked by immunoprecipitation (IP) with anti-FLAG antibody followed by immunoblotting with specific antibodies. Also in this case, Prep1ΔHR1+2 was the only mutant unable to interact with these proteins, as expected [75]. The defect of this mutant in interacting with Pbx proteins may explain its inability to inhibit *Meis1*-induced tumorigenicity. The other mutants showed no defect both in the increase of, and in the interaction with Pbx1 and Pbx2 proteins.

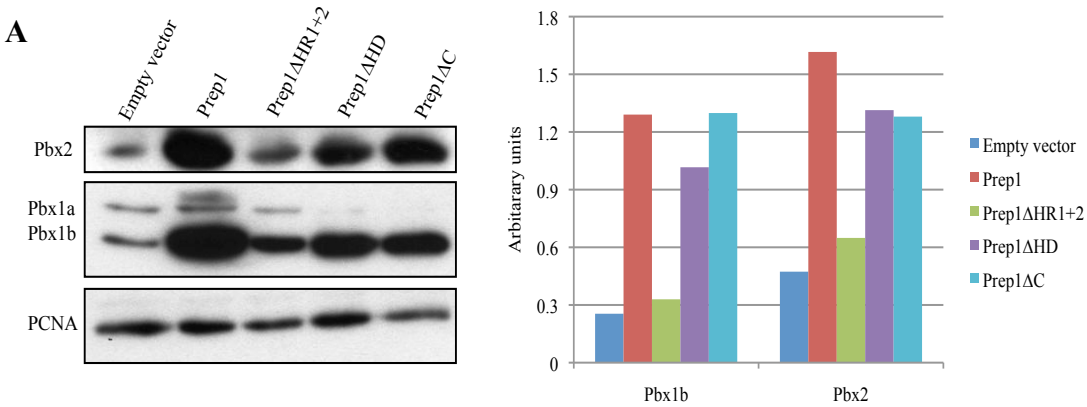

B

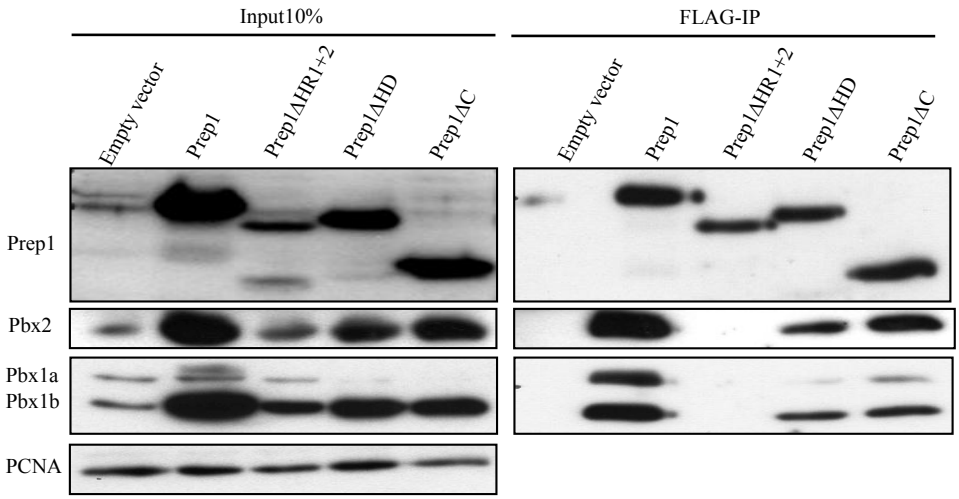

Figure 2.8. The HR1+2 domain is required for interaction with Pbx proteins and their subsequent stabilization. (A) Immunoblot performed on the nuclear lysates prepared from infected cells and tested for Pbx1 and Pbx2 using appropriate antibodies. PCNA was used as loading control. The densitometric analysis was performed using ImageJ (normalized to the level of PCNA). (B) 300 μg of the nuclear extracts of the *Prep1*$^{i/i}$ MEFs infected with FLAG-tagged Prep1 and Prep1 deletion mutants or with empty vector were immunoprecipitated with M2 anti-FLAG antibody and immunoblotted with the anti Prep1, Pbx1 and Pbx2 specific antibodies. 1/10 of the lysate used for immunoprecipitation was loaded as inputs.

2.9. Purification and identification of Meis1a interacting proteins by TAP and mass spectrometry respectively.

In order to gain further insights into the molecular mechanisms underlying Meis1a oncogenic activity and its interruption by *Prep1* re-expression, I purified Meis1a interactors in the *Meis1a* overexpressing WT, *Prep1* deficient and *Prep1* deficient cells re-expressing *Prep1,* using Tandem Affinity Purification (TAP) (Figure 2.9A). For this, I generated a TAP-tagged *Meis1a* retroviral construct and retrovirally infected immortalized *Prep1*$^{i/i}$ and *Prep1*^{wt} MEFs. *Prep1*$^{i/i}$ cells overexpressing *Meis1a*-TAP were also secondarily infected with *Prep1*-coding retroviruses. Before performing TAP, I checked the functionality of Meis1a-TAP protein by subcutaneous transplantation of the

cells overexpressing Meis1a-TAP. As expected, only *Prep1*$^{i/i}$ cells overexpressing *Meis1a*-TAP and not WT cells formed tumor in the transplanted nude mice (Data not shown). TAP was performed on the nuclear extracts of *Prep1*$^{i/i}$ and *Prep1*^{wt} MEFs and also on the nuclear extracts of *Prep1*$^{i/i}$ cells re-expressing *Prep1*. Purified proteins were run on SDS-PAGE (Figure 2.9B) and were identified by mass spectrometry analysis This analysis revealed that Meis1a is associated with the other member of TALE family proteins Pbx1, as previously reported in *MLL*-induced leukemia [149] (Table 2.1). It also interacts with the other member of this family, Pbx2. Moreover, Meis1a is associated with p160 myb-binding protein, which has been also shown to interact with Prep1 through the HR1 domain [72,223]. However, no peptides of Prep1 were found in the MS analysis, indicating that Meis1a and Prep1 do not form a complex. In addition, we identified a series of novel non-homeodomain proteins that co-purified with Meis1a only in *Prep1*$^{i/i}$ and not in WT cells nor in *Prep1*$^{i/i}$ cells re-expressing *Prep1* (Table 2.1). Of these proteins, two ATP-dependent RNA helicases known as Ddx5 and Ddx3x co-purified with Meis1a only in the absence of Prep1. The complete list of the Meis1a interacting proteins along with the information about mascot score and emPAI index of each interactor are shown in Table 2.1. Some of these interactions were further validated by immunoblotting of the TAP purification product with appropriate antibodies (Figure 2.9C). The recruitment of the Ddx5 and Ddx3x RNA helicases by Meis1 only in *Prep1*$^{i/i}$ and not in WT cells or *Prep1*$^{i/i}$ cells overexpressing *Prep1* suggests that these proteins play a role in the *Prep1* inhibition of *Meis1* tumorigenicity. For example, they might play a role in promoting active transcription from promoters bound by Meis1a in the absence of Prep1. Therefore I assessed the biological relevance of Meis1 interaction with Pbx1, Ddx3x and Ddx5 proteins in the context of tumor formation.

A

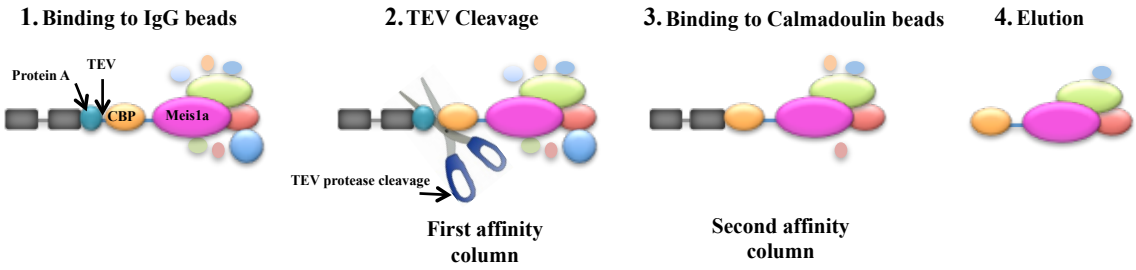
1. Binding to IgG beads
2. TEV Cleavage
3. Binding to Calmadoulin beads
4. Elution
Protein A
TEV
CBP
Meis1a
TEV protease cleavage
First affinity column
Second affinity column

B

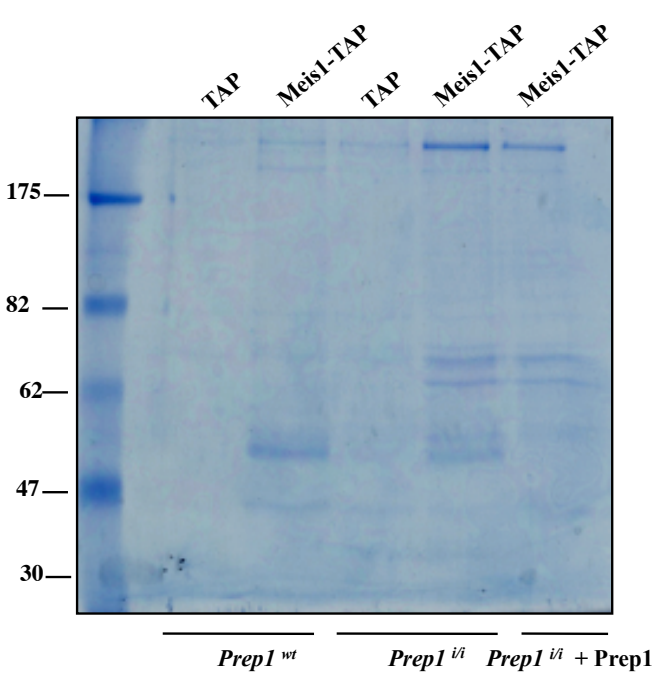
TAP
Meis1-TAP
TAP
Meis1-TAP
Meis1-TAP
175
82
62
47
30
Prep1 wt
Prep1 i/i
Prep1 i/i + Prep1

C

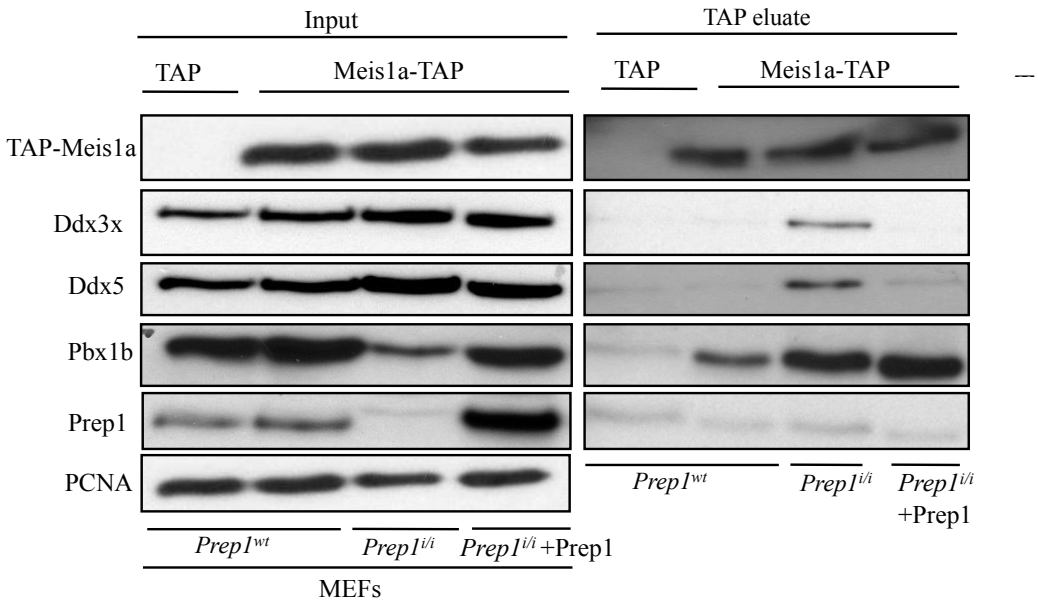
Input
TAP eluate
TAP
Meis1a-TAP
TAP
Meis1a-TAP
TAP-Meis1a
Ddx3x
Ddx5
Pbx1b
Prep1
PCNA
Prep1wt
Prep1i/i
Prep1i/i +Prep1
Prep1wt
Prep1i/i
Prep1i/i +Prep1
MEFs

Figure 2.9. Protein composition of TAP-purified Meis1a. (A) Schematic representation of the tandem affinity purification (TAP) protocol. TAP tag is composed of three different components: Protein A as an immunoglobulin G (IgG)-binding domain, a tobacco etch virus (TEV) protease cleavage site and a calmodulin-binding domain. TAP-tagged Meis1 was expressed in *Prep1*^{wt}, *Prep1*$^{i/i}$ and *Prep1*$^{i/i}$ MEFs re-expressing Prep1 and purified using rabbit (IgG) agarose beads. Then the purified complexes were eluted by TEV protease cleavage (first affinity column). The remaining complex after TEV cleavage was purified using calmodulin beads (second affinity column) and eluted by boiling in SDS sample buffer. **(B)** The final TAP eluate was separated on a 10% SDS-PAGE and stained by colloidal coomassie blue. The entire lane was cut out from the gel and divided into different zones. Protein complex compositions of each zone were identified by LC-MSMS and are listed in table 2.1. Exponentially modified protein abundance index (emPAI) is indicated as measure of relative quantitation of proteins in each sample. A purification from cells infected with TAP empty vector is presented as negative control (TAP). **(C)** Immunoblots of TAP purified proteins from the TAP eluate of nuclear extracts of the indicated cells, using specific antibodies.

2.10. Ddx3x and Ddx5 proteins co-precipitate only with Meis1a and not Prep1. Prep1 protein level restoration in *Prep1*$^{i/i}$ cells impairs the interaction.

Among the novel Meis1a interactors, I focused on Ddx3x and Ddx5 RNA helicases, because they copurified with Meis1a only in the absence of Prep1 protein. Indeed Meis1a induces transformation of *Prep1*-deficient but not WT MEFs, and *Prep1* re-expression partially inhibits tumor formation. Thus these RNA helicases might be novel Meis1a interactors, which associate with Meis1a and promote cellular transformation only in the absence of Prep1. Indeed, these genes have been shown to be involved in the cancer (see introduction) [191,207]. To confirm Meis1a interaction with Ddx3x and Ddx5, I retrovirally infected *Prep1*$^{i/i}$ and *Prep1*$^{i/i}$ MEFs re-expressing *Prep1* with FLAG-tagged Meis1a and empty vector as negative control. FLAG-tagged Meis1a overexpression did not alter the nuclear level of Ddx3x and Ddx5 proteins (figure 2.10A Input panel). FLAG-tagged Meis1a was immunoprecipitated with an M2 anti-FLAG affinity resin from nuclear lysates of the infected cells and immunoblotted using specific Ddx3x, Ddx5, Pbx1, Pbx2 and anti FLAG anibodies (Figure 2.10A IP panel). Overall, these experiments

revealed that Meis1a, Ddx3x and Ddx5 can form a stable complex in vivo in the absence of Prep1. However, Pbx1 and Pbx2 form complexes with Meis1a both in the absence and in the presence of Prep1.

Furthermore, I performed co-immunoprecipitation to investigate whether Meis1a interaction with Ddx3x and Ddx5 RNA helicases is specific to the oncogenic member of the TALE family or it also extends to the tumor suppressive member of the family, Prep1 [19]. I retrovirally infected *Prep1*$^{i/i}$ MEFs with FLAG-tagged Prep1, Prep1 deletion mutants and empty vector as negative control. Prep1 deletion mutants have been described in section 2.6. The overexpression of different Prep1 mutants did not affect the nuclear level of Ddx3x and Ddx5 proteins (Figure 2.10B Input panel). Nuclear lysates of the cells infected with Prep1 deletion mutants' retroviruses were immunoprecipitated with an M2 anti-FLAG affinity resin and immunoblotted using specific Ddx3x, Ddx5, Meis1 and Prep1 antibodies (Figure 2.10B). The results show that neither full-length Prep1 nor any of the Prep1 deletion mutants forms a complex with these proteins. Although Pbx1 and Pbx2 co-immunoprecipitation with Prep1 showed that the co-IP worked (see figure 2.8B). Therefore the Ddx3x and Ddx5 interaction is specific to the oncogenic Meis1. Moreover, Meis1 also does not immunoprecipitate with Prep1, as expected.

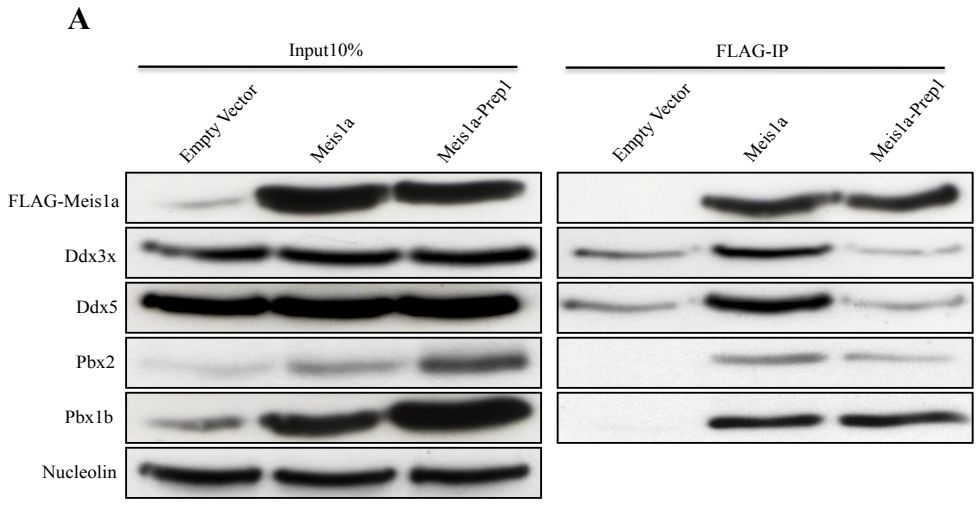

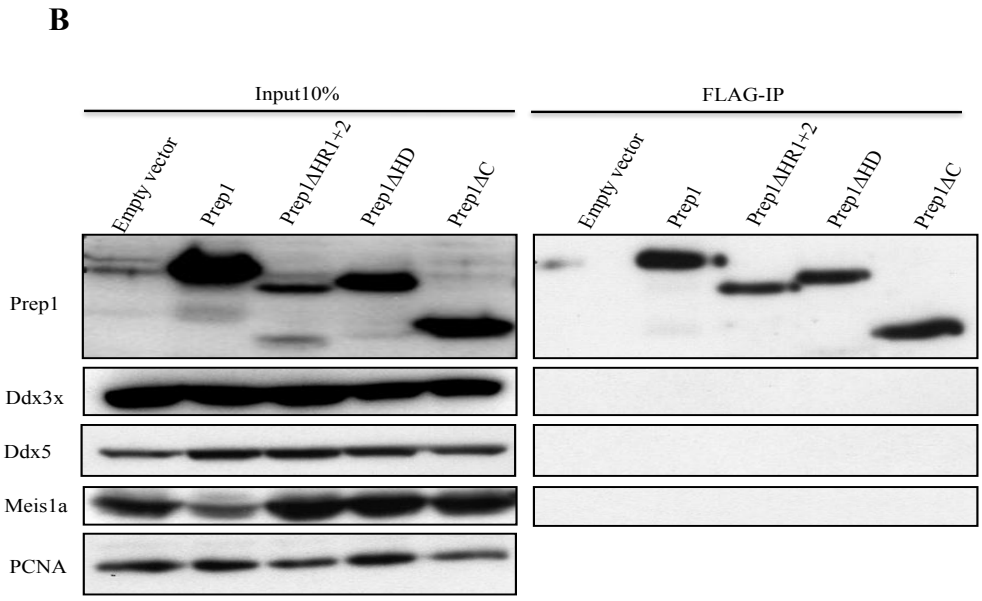

Figure 2.10. Ddx3x and Ddx5 interact specifically with Meis1 and not Prep1. **(A)** 300 μg of the nuclear extracts of the *Prep1*$^{i/i}$ MEFs infected either with FLAG-tagged Meis1a alone, along with Prep1 or empty vector was immunoprecipitated with M2 anti-FLAG antibody and immunoblotted with the anti FLAG, Ddx3x, Ddx5, Pbx1 and Pbx2 specific antibodies. 1/10 of the lysate used for immunoprecipitation was loaded as input. **(B)** FLAG-tagged Prep1 and FLAG-tagged Prep1 mutants were immunoprecipitated from 300 μg of nuclear extracts of the cells infected with these mutants using M2 anti-FLAG antibody. Lysate from cells infected with empty vector was used as negative control. The Prep1, Prep1 mutants, Pbx1 and Pbx2 in the input and precipitated samples were identified by western blotting using appropriate antibodies.

2.11. Ddx3x interacts with the homeodomain and Ddx5 interacts with both the homeodomain and the C-terminus of Meis1a.

To map the Meis1a domains required for the interaction with Ddx3x and Ddx5, I generated the following GST-Meis1a deletion mutants (Figure 2.11A): a) Deletion of the DNA binding homeodomain and C-terminus of Meis1a (Meis1aΔHD+Cter, deleted residues: 267-390); b) Deletion of the N-terminus and Pbx interacting domain of Meis1a DNA (Meis1aHD+Cter, deleted residues: 1-266); c) Deletion of both N- and C-terminal sequences, generating Meis1a DNA binding homeodomain (Meis1aHD, residues: 267-338); d) Deletion of the whole N-terminus plus homeodomain, generating Meis1a C-terminal domain (Meis1aCter, residues: 339-390). I performed a pull-down assay with the

nuclear lysate of the *Prep1*$^{i/i}$ MEFs overexpressing Meis1a. GST was used as a negative control to check the specificity of the interactions. Figure 2.11B (Bottom panel) shows the Coomassie staining of the GST and GST-Meis1a mutants' preparations. Figure 2.11B (upper panel) shows the specific interaction of both Ddx3x and Ddx5 with the Meis1aHD and in the case of Ddx5 also with the C-terminal part of Meis1a. No interaction was observed with a construct containing the N-terminus and the Pbx interacting domain only. Even if Ddx3x interacts specifically with the HD of Meis1a, there is 50% reduction of Ddx3x binding efficiency to the HD compared to the full-length Meis1a (Figure 2.11C upper graph). Apparently, Ddx3x does not interact with the C-terminus of Meis1a, while Ddx5 interacts with HD+Cter almost as efficiently as with the full-length Meis1a. Ddx5 interaction with either HD or C-terminus of Meis1a is 2.5-fold less efficient than with the HD+Cter construct (Figure 2.11C lower graph). This suggests that Ddx5 interaction requires both the HD and the C-terminus of Meis1a. Neither Ddx3x nor Ddx5 interact with the N-terminus and Pbx-interacting domains (HR1+2) of Meis1a (Figure 2.11C).

A

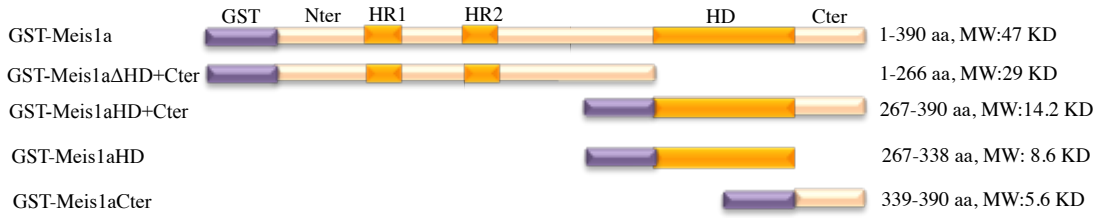

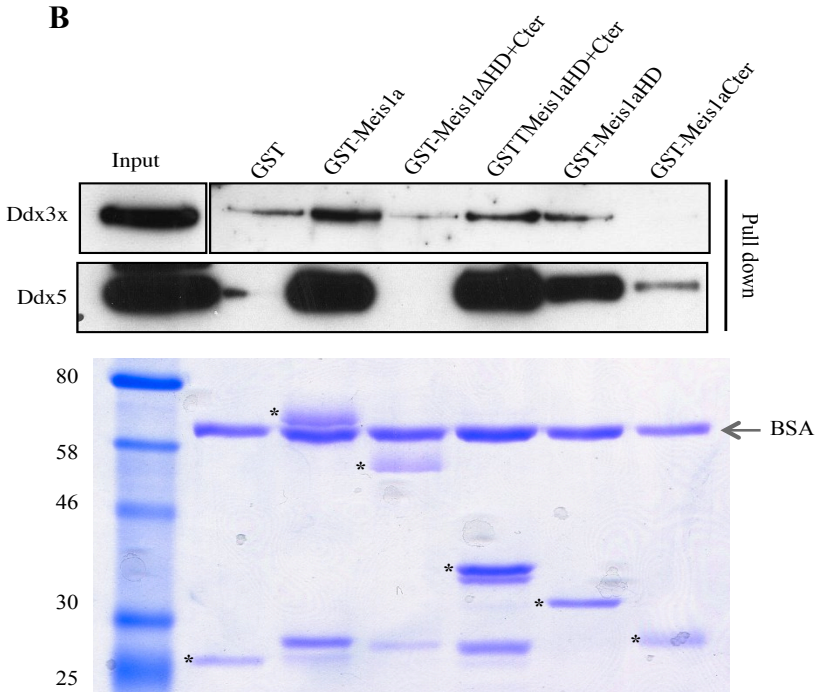
B
Input
GST
GST-Meis1a
GST-Meis1aΔHD+Cter
GSTTMeis1aHD+Cter
GST-Meis1aHD
GST-Meis1aCter
Ddx3x
Ddx5
Pull down
80
58
46
30
25
BSA

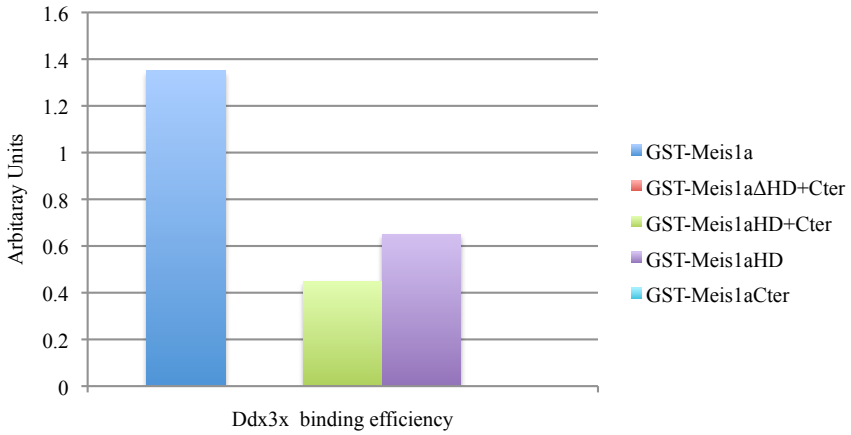
1.6
1.4
1.2
1
0.8
0.6
0.4
0.2
0
Arbitaray Units
Ddx3x binding efficiency
GST-Meis1a
GST-Meis1aΔHD+Cter
GST-Meis1aHD+Cter
GST-Meis1aHD
GST-Meis1aCter

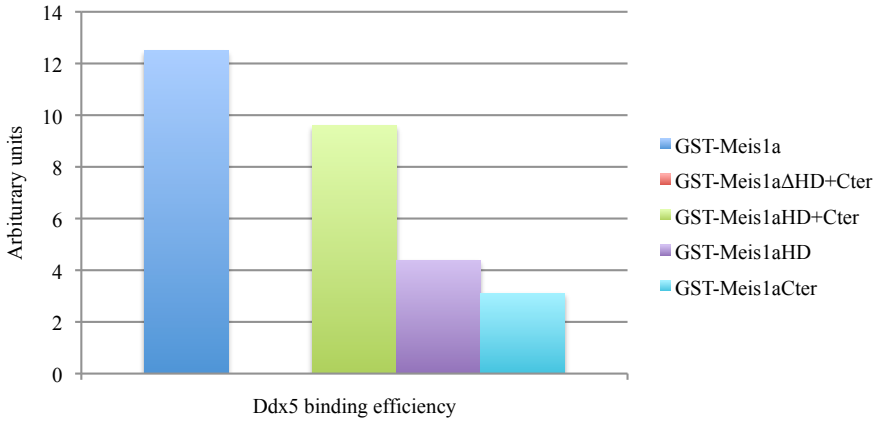
14
12
10
8
6
4
2
0
Arbitrary units
Ddx5 binding efficiency
GST-Meis1a
GST-Meis1aΔHD+Cter
GST-Meis1aHD+Cter
GST-Meis1aHD
GST-Meis1aCter

Figure 2.11. Identification of the Meis1a domains required for Ddx3x and Ddx5 interactions. (A) Schematic representation of GST-Meis1a deletion mutants. Pbx interacting domains (HR1 and HR2) and DNA binding domain (HD) are indicated. **(B)** After coupling of GST-constructs to the beads, GST and GST-Meis1a deletion mutant beads were blocked with BSA to prevent non-specific bindings. GST beads were incubated with 300 μg of the nuclear lysates from Meis1a overexpressing *Prep1*$^{i/i}$ cells. Western blot with Ddx3x and Ddx5 specific antibodies was performed to reveal interaction with Meis1a domains (upper panel). The position of each GST-construct is shown by an asterisk (bottom panel). **(C)** Immunoblots were normalized on the bands of the each GST-constructs obtained from Coomassie stained gel using ImageJ and were plotted as binding efficiency of either Ddx3x or Ddx5 compared to each GST-constructs.

2.12. *Meis1*-mediated transformation and *Prep1*-inhibition of *Meis1* tumorigenesis require the homeodomain protein Pbx1.

Analysis of the Meis1 interactome by mass spectrometry confirmed the interaction between Meis1 and TALE homeodomain proteins Pbx1 and Pbx2 (Section 2.9). On the other hand also Prep1 interacts with Pbx1 and Pbx2, using the same interaction surface (HR1+HR2) [75]. *Prep1,* however partially inhibits *Meis1* tumorigenicity. To assess the biological relevance of Pbx1 in *Meis1*-induced tumorigenicity and its inhibition by Prep1, *Prep1*$^{i/i}$ MEFs overexpressing *Meis1a* or *Meis1a* and *Prep1* were depleted of Pbx1 by specific shRNAs. This resulted in 80 - 90% reduction of Pbx1 protein level (Figure 2.12A upper panel). Pbx1 depletion did not have any major effect on the level and subcellular localization of overexpressed Meis1a and Prep1 (Figure 2.12A lower panel). Importantly, Prep1 overexpression reduced the Meis1a protein level by 2.6-fold (also see figure 2.6C). However, Pbx1 knockdown resulted in almost 2-fold and 3-fold increase of Pbx2 in Meis1a and Meis1a/Prep1 overexpressing cells, respectively (Figure 2.12A lower panel). The consequences of Pbx1 depletion on the proliferation and tumorigenic potential of these cells were studied. The effect of Pbx1 downregulation on the cell proliferation was assessed by growth curve assay and cell cycle analysis by FACS. Pbx1-depleted *Meis1a* overexpressing cells proliferated almost as efficiently as the scrambled shRNA control cells (Figure 2.12B) and FACS analysis did not reveal a significant difference in the

proportion of S/G2/M-phase cells (Figure 2.12C). Likewise, no effect was observed in *Meis1*-transduced *Prep1* overexpressing cells (data not shown). I conclude that Pbx1 downregulation does not affect cell proliferation in this system.

To study the tumorigenic potential of Pbx1 knockdown ($Pbx1^{kd}$) cells, soft agar assays and allograft studies in nude mice were performed. The colony formation potential of $Pbx1^{kd}$ *Meis1*-transformed cells was substantially decreased (>69%) when compared with *Meis1*-transformed cells transduced with a scrambled shRNA vector (Figure 2.12D). The effect of Pbx1 knockdown was not observed in cells also overexpressing Prep1, whose tumorigenic activity is already lower in the presence of a scrambled vector (Figure 2.12D). In addition, mice transplanted with $Pbx1^{kd}$ *Meis1*-transformed cells yielded smaller tumors compared to the control group (Figure 2.12E upper graph). Whereas Pbx1 knockdown had essentially no effect on *Meis1*-transformed $Pbx1^{kd}$ cells overexpressing Prep1 (Figure 2.12E lower graph). For clarity the effect of Pbx1 downregulation on *Meis1* tumorigenicity and *Prep1* tumor suppressive function has been reported in two separate graphs. However, the experiment was performed at the same time.

The fact that *Meis1* did not transform the Pbx1 downregulated cells as efficiently as control, indicates that *Meis1*-mediated transformation is dependent on the presence of Pbx1 protein and further supports the idea that not only in *MLL*-induced leukemia but also in MEFs transformation, *Meis1* functions in complex with Pbx proteins [149]. The minor effect of Prep1 on $Pbx1^{kd}$ *Meis1*-transformed cells shows that also *Prep1*-inhibition of *Meis1* tumorigenicity requires Pbx1. Thus in $Prep1^{i/i}$ cells, overexpression of Meis1 induces strong tumorigenicity which is decreased by Pbx1 kock-down. Likewise, the inhibition of tumorigenicity by Prep1 is only slightly stimulated by Pbx1 kock-down. All this suggests that Meis1 and Prep1 compete for Pbx1 and hence that Pbx1 cooperates with an oncogene (*Meis1*) as well as with a tumorsuppressor (*Prep1*), confirming the previous data with Prep1ΔHR1+2 (Figure 2.6 D and E).

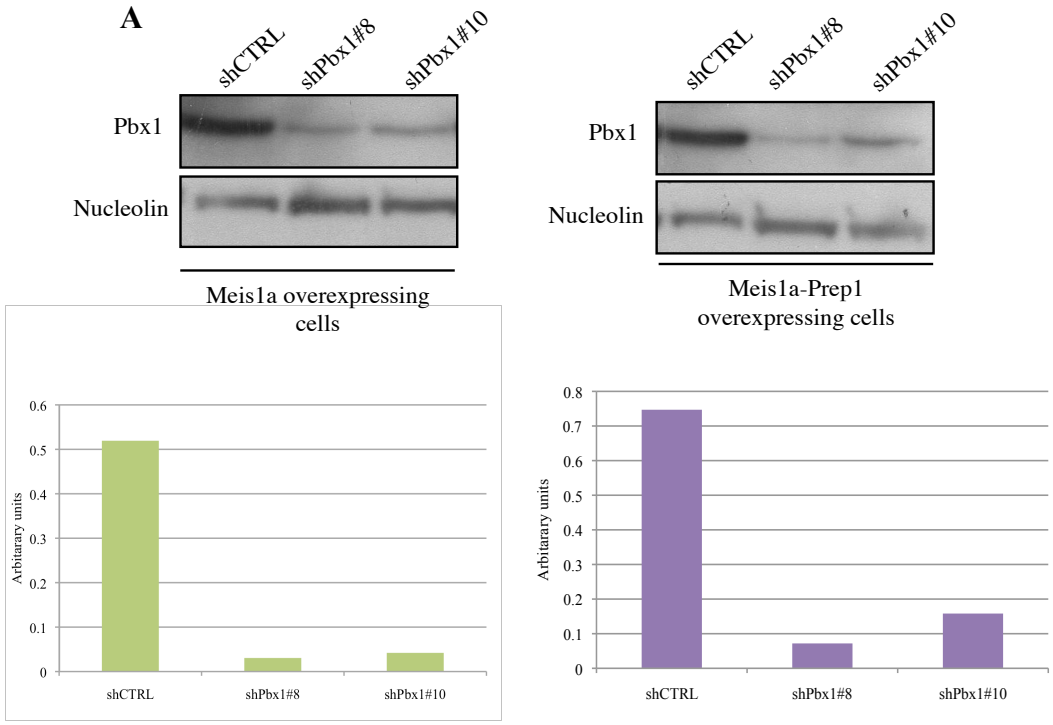
A
shCTRL
shPbx1#8
shPbx1#10
Pbx1
Nucleolin
Meis1a overexpressing cells
Arbitrary units
0.6
0.5
0.4
0.3
0.2
0.1
0
shCTRL
shPbx1#8
shPbx1#10
shCTRL
shPbx1#8
shPbx1#10
Pbx1
Nucleolin
Meis1a-Prep1 overexpressing cells
Arbitrary units
0.8
0.7
0.6
0.5
0.4
0.3
0.2
0.1
0
shCTRL
shPbx1#8
shPbx1#10

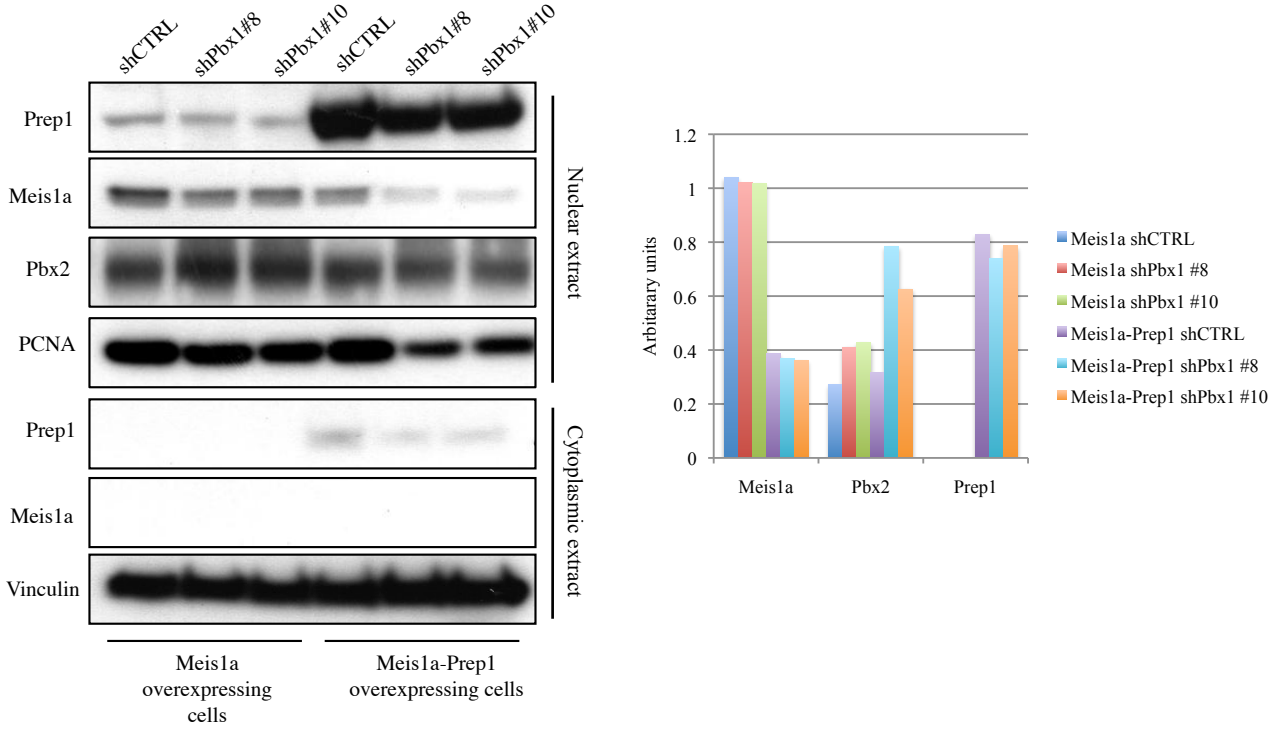
shCTRL
shPbx1#8
shPbx1#10
shCTRL
shPbx1#8
shPbx1#10
Prep1
Meis1a
Pbx2
PCNA
Nuclear extract
Prep1
Meis1a
Vinculin
Cytoplasmic extract
Meis1a overexpressing cells
Meis1a-Prep1 overexpressing cells
Arbitrary units
1.2
1
0.8
0.6
0.4
0.2
0
Meis1a
Pbx2
Prep1
Meis1a shCTRL
Meis1a shPbx1 #8
Meis1a shPbx1 #10
Meis1a-Prep1 shCTRL
Meis1a-Prep1 shPbx1 #8
Meis1a-Prep1 shPbx1 #10

B

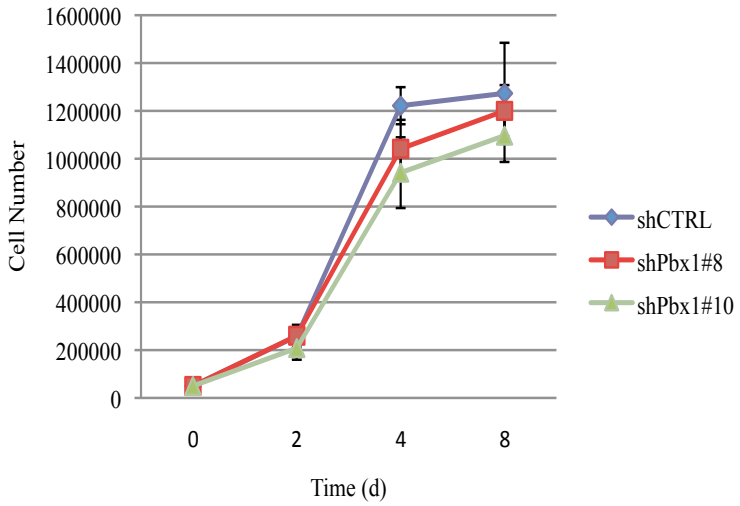
1600000
1400000
1200000
1000000
800000
600000
400000
200000
0
Cell Number
0
2
4
8
Time (d)
shCTRL
shPbx1#8
shPbx1#10

C

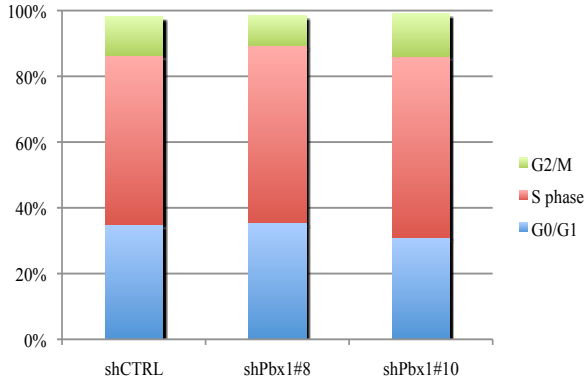
100%
80%
60%
40%
20%
0%
shCTRL
shPbx1#8
shPbx1#10
G2/M
S phase
G0/G1

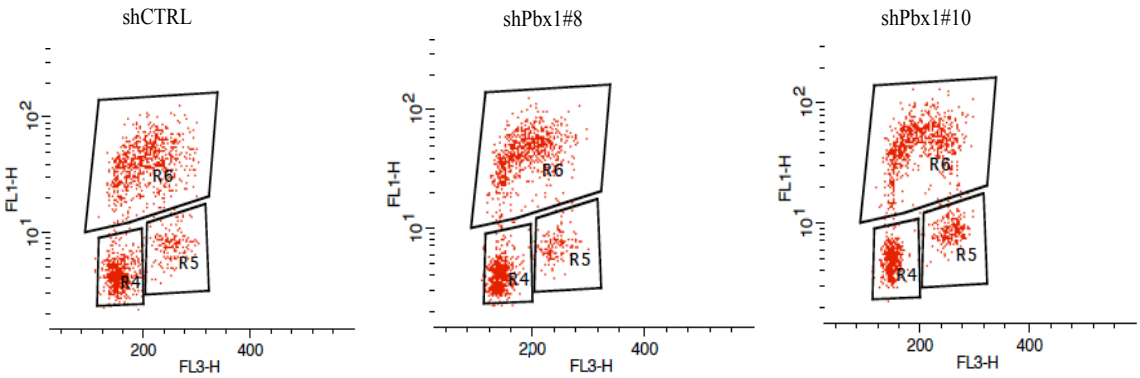
shCTRL
shPbx1#8
shPbx1#10
FL1-H
FL3-H
R4
R5
R6
200
400

D

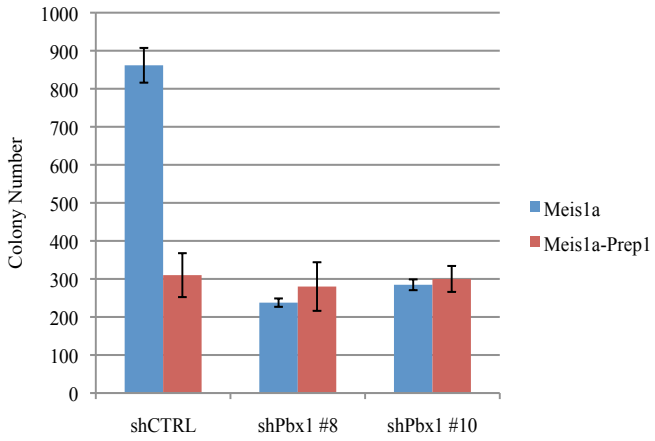
1000
900
800
700
600
500
400
300
200
100
0
Colony Number
shCTRL
shPbx1 #8
shPbx1 #10
Meis1a
Meis1a-Prep1

E

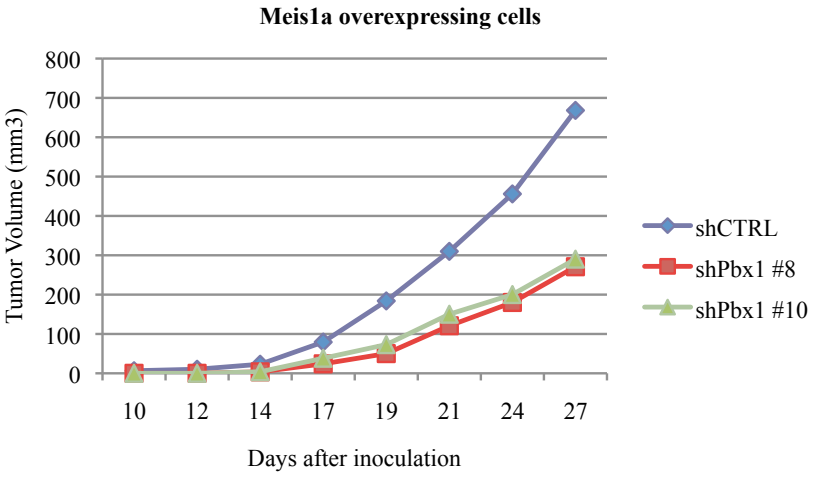
Meis1a overexpressing cells
800
700
600
500
400
300
200
100
0
Tumor Volume (mm3)
10
12
14
17
19
21
24
27
Days after inoculation
shCTRL
shPbx1 #8
shPbx1 #10

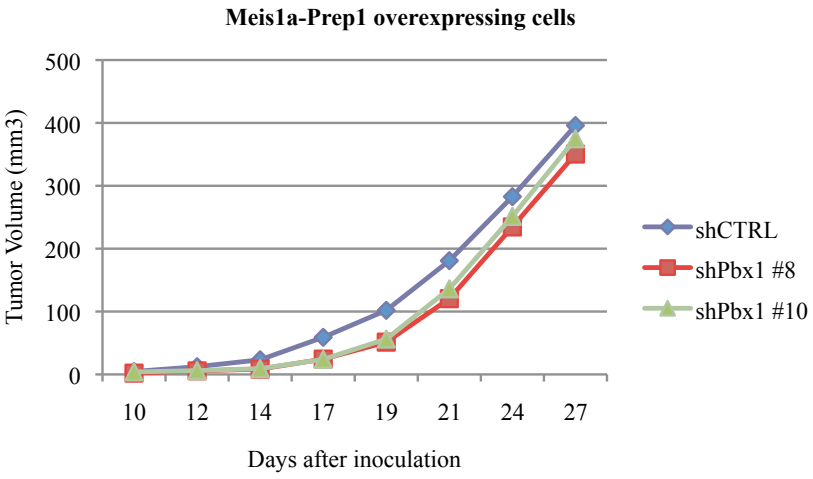
Meis1a-Prep1 overexpressing cells
500
400
300
200
100
0
Tumor Volume (mm3)
10
12
14
17
19
21
24
27
Days after inoculation
shCTRL
shPbx1 #8
shPbx1 #10

Figure 2.12. Pbx1 is required for *Meis1*-mediated transformation and *Prep1*-inhibition of *Meis1* tumorigenicity. (A, upper panel) Immunoblot represents the Pbx1 downregulation efficiency in the nuclear lysate of Meis1a or Meis1a plus Prep1 overexpressing *Prep*1$^{i/i}$ MEFs. Two different shRNA were used against Pbx1, namely shPbx1 #8 and Pbx1 #10. Nucleolin was used for protein loading control. Quantification of the bands was done by densitometric analysis. **(A, lower panel)** Immunoblots show the protein level of Meis1a, and Prep1 in the nuclear and cytoplasmic extracts of the Pbx1-depleted cells compared to the control. Pbx2 protein level was only checked in the nuclear lysates. PCNA and vinculin were used as loading controls of nuclear and cytoplasmic lysates, respectively. Quantification was done by densitometry on nuclear lysates only. **(B)** 5×10^4 Pbx1^{kd} *Prep*1$^{i/i}$ cells overexpressing Meis1a were plated in 6-well plates and were counted at the indicated time points. The experiment was performed in triplicate. Error bars indicate standard deviation. **(C)** DNA content analysis was determined by FACS analysis of Pbx1^{kd} *Prep*1$^{i/i}$ cells overexpressing Meis1a after BrdU /PI staining. Asynchronously growing cells were pulse-labeled with BrdU for 45 min before harvesting. After fixation, cells were stained with FITC-coupled anti-BrdU antibody and analyzed by flow cytometry to determine BrdU incorporation and cell cycle distribution. Cells were stained with PI for DNA content. 1×10^6 cells were used for FACS analysis. The graph shows the percentage of the cells in the different phases of the cell cycle. Representative scatter plots with the log FITC anti-BrdU staining (FL1-H) versus PI staining (FL3-H) are shown. Cell cycle distribution of cells was calculated using the gates shown in the scatter plots: R4, G1 phase; R6, S phase; R5, G2/M phase. **(D)** Soft agar colony formation of Pbx1^{kd} cells overexpressing Meis1a or Meis1a along with Prep1 is shown relative to cells transduced with scrambled lentiviral vector. 1×10^5 cells per plate was used for each experimental points and the experiment was performed in triplicate. Error bars indicate standard deviations of two independent experiments. **(E)** Pbx1^{kd} cells overexpressing Meis1a (upper panel) or coexpressing Meis1a and Prep1 (lower panel) were subcutaneously transplanted in nude mice (1×10^6 cell per animal) and the tumor volume was monitored over time. Lines represent the average of five animals per group. For clarity SD is not shown. $P < 0.05$.

2.13. Ddx3x and Ddx5 depletion impair cell proliferation and colony formation in soft agar.

To investigate the functional relation between Ddx3x or Ddx5 and Meis1a, we assessed the role of Ddx3x or Ddx5 on *Meis1*-induced tumor formation in the *Prep1*$^{i/i}$ MEFs. Ddx3x or Ddx5 protein levels were respectively depleted by ~50% and ~70% in these cells with two independent shRNAs targeting each genes (Figure 2.13A). Ddx downregulation did not affect protein level of Meis1a and its partner Pbx1 (Data not shown). Ddx3x^{kd} and Ddx5^{kd} cells changed their morphology compared to the control cells. They became abnormally flat looking like serum-starved cells and round bodies

appeared that may correspond to cell carcasses (Figure 2.13B). Therefore as expected [194,224], Ddx downregulation severely compromised the proliferation ability of Meis1a transduced *Prep1*$^{i/i}$ cells (Figure 2.13C). Furthermore I studied the impact of Ddx depletion on Meis1 induced transformation. To this end, I measured the anchorage independent growth in semi-solid medium. As shown in figure 2.13D, Ddx^{kd} cells showed a strong reduction in the number of colonies when plated in soft agar. Overall, these results indicate that both *Ddx3x* and *Ddx5* have important roles in cell proliferation and their downregulation inhibits *Meis1*-induced transformation *in vitro*.

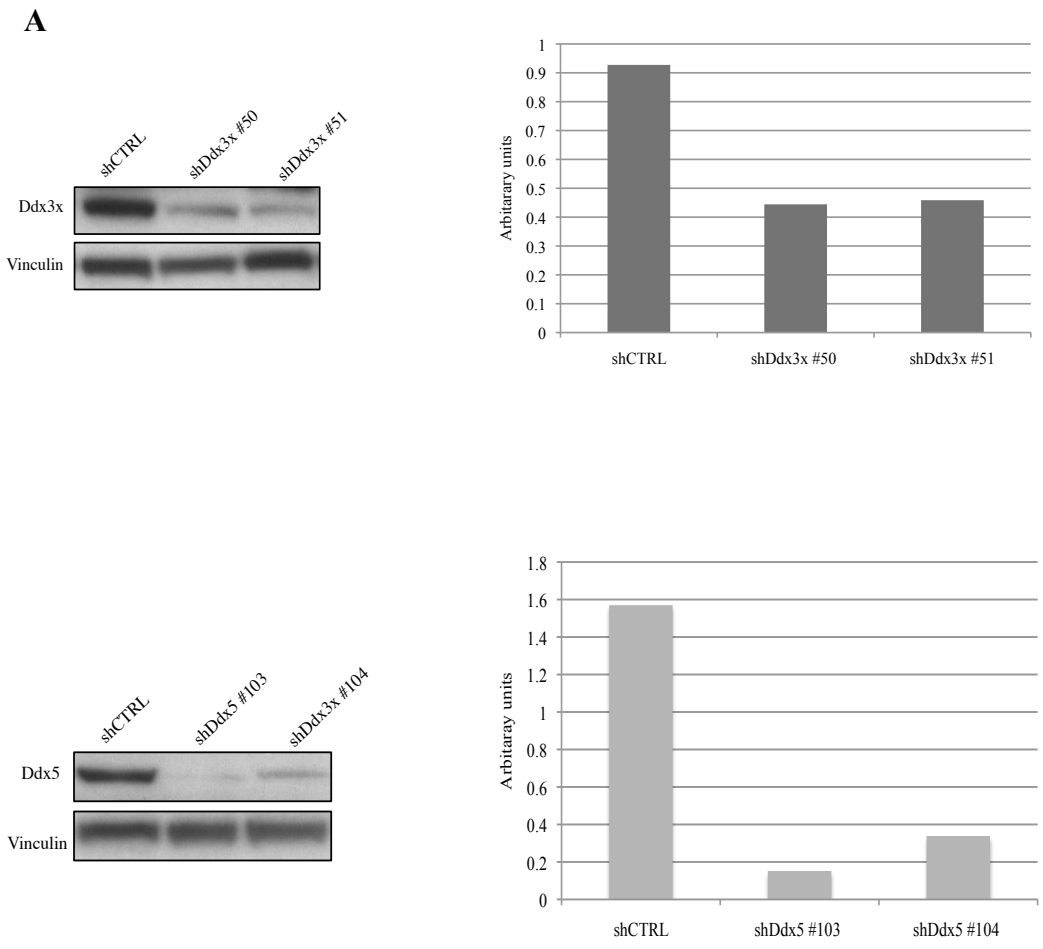

B

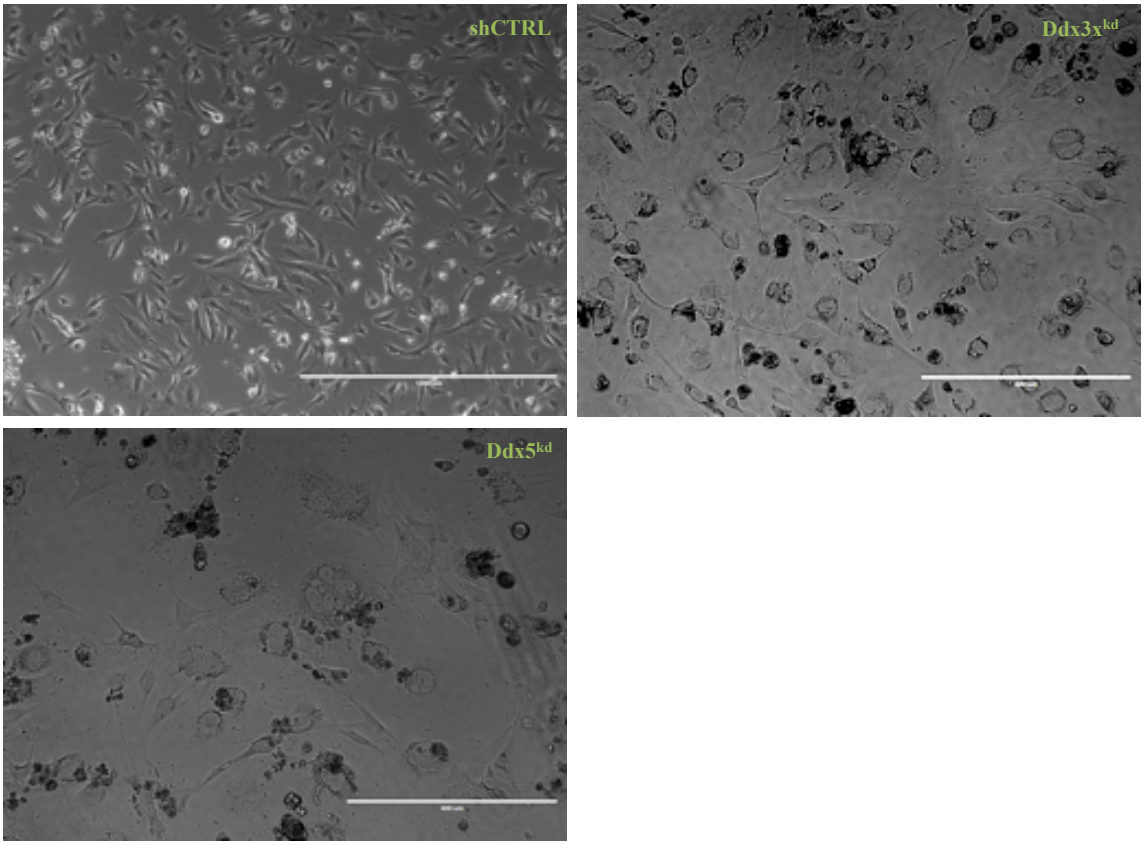
shCTRL
Ddx3x^{kd}
Ddx5^{kd}

C

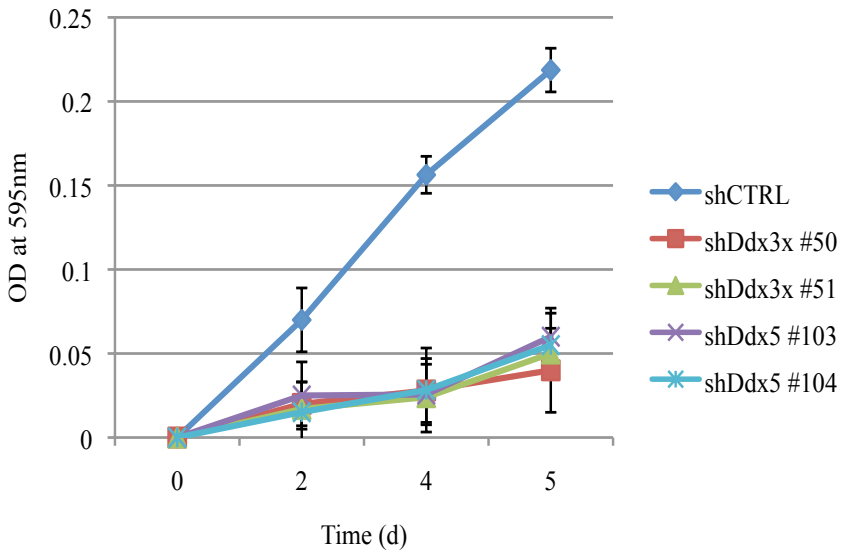
0.25
0.2
0.15
0.1
0.05
0
OD at 595nm
0
2
4
5
Time (d)
shCTRL
shDdx3x #50
shDdx3x #51
shDdx5 #103
shDdx5 #104

D

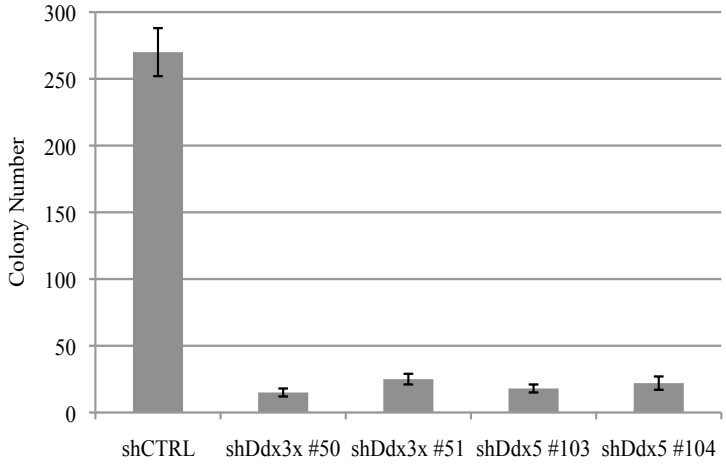

Figure 2.13. Impaired proliferation and transformation activity of Ddx3x or Ddx5 depleted cells. (A) *Prep1*$^{i/i}$ cells overexpression Meis1a were treated with Ddx3x, Ddx5 and scrambled shRNA retroviruses resulting in efficient downregulation of protein level of these genes as shown by western blotting. Vinculin was used as a loading control. Quantification of the bands was done by densitometric analysis. **(B)** Ddx3x^{kd} and Ddx5^{kd} cells were photographed one weeks after infection. Cells induced with scrambled shRNA were used as control. **(C)** 5×10^4 Ddx^{kd} cells were plated in 6-well plates, fixed at the indicated time points, stained with 0.1% crystal violet solution and the OD 595 nm determined. The experiment was performed in triplicate. Error bars indicate standard deviation. **(D)** Soft agar colony formation of Ddx3x^{kd} and Ddx5^{kd} cells overexpressing Meis1a is shown relative to cells transduced with scrambled lentiviral vector. 1×10^5 cells per plate were used for each experimental points and the experiment was performed in triplicate. Error bars indicate standard deviations of two independent experiments.

Chapter 3: *Discussion*

Accumulating evidence implicates several members of the TALE protein in a growing number of diseases including cancer: *Pbx1* in B-cell ALL [79,101], *Meis1* as a *Hoxa9* collaborating oncogene in AML induction [41,43] and *Prep1* as a tumor suppressor in man and mouse [19]. In this thesis, I studied the oncogenic role of Meis1 in MEFs and its possible interaction with *Prep1* to better understand the pathways affected by these proteins.

3.1. *Meis1* is a bona-fide oncogene in MEFs.

The effect of *Meis1* on proliferation and tumorigenesis had been studied in the context of leukemia. Although genetic signature studies of cancer have revealed the overexpression of *Meis1* in a number of so called expression modules activated in tumors of lung, neural, liver, breast and prostate origin [225], so far only very few studies have shown the involvement of *Meis1* in solid tumors [157,158]. Therefore, the effect of *Meis1* expression in non-hematological malignancies is largely unexplored. In this regard, I took advantage of MEFs to study the oncogenic impact of the *Meis1* in non-hematic cells. Moreover, MEFs provide an easy model system to dissect the molecular pathways underlying *Meis1* oncogenicity and its interactions with the tumor suppressor member of the TALE transcription factors, *Prep1*.

I have shown that *Meis1* induces cell proliferation in primary $p53^{ko}$ and late-passage $Prep1^{i/i}$ MEFs. In rodent fibroblasts, absence of either p53 or p16 is sufficient to inhibit oncogene-induced proliferation arrest. In fact, Serrano et al. [226] have shown that oncogenic *Ras* alone efficiently transforms either p53 or p16 knockout primary MEFs but needs a cooperating oncogene such as *Myc* to transform wild-type cells. Consistent with these observations, I show that transformation of MEFs by *Meis1* requires either a cooperating oncogene such as *Hoxa9*, *Ras* or *Myc* or the inactivation of a tumor

suppressor such as *p53* in primary cells or *Prep1* in late-passage cells. These results indicate that *p53* and *Prep1* are essential to inhibit *Meis1*-induced proliferation and subsequent transformation and that the inactivation of either *p53* in primary cells or *Prep1* in late passage MEFs alone is sufficient for the transformation.

Longobardi et al. [19] demonstrated that *Prep1* deficiency leads to spontaneous tumors in mice and that its haploinsufficiency accelerates lymphomagenesis in the *EμMyc* mice model. Consistent with these data, $Prep1^{i/i}$ MEFs are easily transformed by *Meis1* alone as studied by soft-agar assays and tumor formation in mice. Indeed, *Meis1* alone transforms $Prep1^{i/i}$ cells as efficiently as when co-expressed with *Hoxa9*. Colony formation in soft-agar indicates loss of contact inhibition and a transformed phenotype. $Prep1^{i/i}$ cells transduced with *Meis1* formed colonies in soft-agar and tumors in nude mice. However in wild type cells, *Meis1* requires the oncogene *Hoxa9* to transform cells. Interestingly, *Hoxa9* alone transforms primary bone marrow cells and *Meis1* coexpression only accelerates leukemogenesis [41]. This shows that the oncogenic activity of oncogenes such as *Meis1* and *Hoxa9* is context and cell type dependent. Thus *Meis1* is a bona-fide oncogene in MEFs but *Hoxa9* is not. These results also show a major difference between *Meis1* and *Prep1*. The former must act by stimulating the signaling pathways leading to cancer; whereas *Prep1* acts in the opposite direction inducing cell changes that prevent the activity of an oncogene like *Meis1*.

3.2. Why does *Meis1* transform MEFs in the absence of *Prep1*?

It appears that *Prep1* mainly exerts its tumor suppressor function by maintaining genomic stability [179]. In early embryogenesis, *Prep1* protects epiblast cells from accumulating DNA damage that induce apoptosis. The absence of *Prep1* results in *p53*-

dependent apoptosis of epiblast cells, which do not reach gastrulation and differentiation [168]. The role of *Prep1* in maintaining genomic stability is not only limited to embryogenesis and epiblast cells but is also exerted in the other cell types. In MEFs and in the human fibroblast cell line, BJ, *Prep1*-deficiency leads to genetic instability shown by increased DNA damage response, aneuploidy and chromosomal aberrations [179]. The genomic instability is one of the common characteristics of cancer [27], and actually, mutations in genes involved in processes like DNA repair, checkpoint control, chromosomal segregation, and centrosome duplication have oncogenic effects [227]. Many tumor suppressor genes are acting by controlling these processes. The genomic lesions emerged in the absence of *Prep1* makes cells susceptible to oncogene-induced transformation.

Since *Meis1* alone is not able to transform primary $Prep1^{i/i}$ MEFs and since $Prep1^{i/i}$ mice which escape embryonic lethality develop tumors only later in life, my conclusion is that regardless of the cellular context, *Prep1*-deficiency over time causes the accumulation of genetic alterations which favor tumorigenicity. This is probably why *Meis1* transforms late-passage and not primary $Prep1^{i/i}$ cells.

Furthermore, I addressed the effect of *Prep1* restoration level on *Meis1*-induced tumor formation and found that *Meis1*-tumorigenicity is partially rescued by *Prep1* re-expression both *in vitro* by growth in soft-agar and *in vivo* by tumor formation in nude mice. This suggests that *Prep1* is capable of an at least partial reversal of the tumorigenicity. The effect of Prep1 re-expression might be important for future therapeutic developments since many human tumors [19] express very low levels of *Prep1*.

Why can Prep1 level restoration not fully rescue *Meis1*-tumorigenic effect? Since genomic lesions are irreversible, *Prep1* re-expression can not reverse those lesions.

However, the partial rescue may identify some tumorigenic pathways not caused by mutations but by changes of gene expression. These maybe studied as a prosecution of this work as they would present tumor suppressive pathways.

3.3. Meis1 and Prep1 compete for Pbx1 in the context of tumorigenecity.

The first attempt to better understand the tumor suppressive function of *Prep1* was to find the domains responsible for its tumor suppressor function. Molecular dissection of *Prep1* revealed that the HR1+2 (Pbx-interacting) domain of *Prep1* is indispensable for its tumor suppressive function. Indeed, the deletion of the HR1+2 domain blocked *Prep1* inhibition of anchorage-independent cell growth and tumor formation induced by *Meis1*. However, the fact that HR1+2 domain on its own is endowed with the tumor-inhibition activity needs to be further studied. To do so, I have generated a construct carrying only the HR1+2 domain of Prep1, which will be tested in the inhibition of *Meis1*-induced tumorigenicity. Both Meis1 and Prep1 interact with Pbx homeoproteins through the HR1+2 domain [75]. In fact, Prep1ΔHR1+2 mutant is not able to interact with Pbx1, as I have shown by IP, and hence cannot stabilize Pbx1 proteins. In fact, Prep1 dimerization with Pbx is important to prevent Pbx protesomal degradation [76]. Accordingly, the interaction with Pbx1 is unaffected in cells overexpressing the other domains of Prep1, Prep1ΔHD and Prep1ΔC mutants. These mutants interact with Pbx1 and elevate its protein level as shown by IP and western blotting.

Prep1 does not have an NLS and to date it is believed that it needs to dimerize with Pbx1 to be translocated to the nucleus [75]. Thus, to exclude the possibility that the impaired tumor suppressor function of Prep1ΔHR1+2 mutant was not due to the lack of functional Pbx1 interaction but to its inability to translocate to the nucleus, where *Meis1* exerts its oncogenic activity, I performed IF and western blotting on the $Prep1^{i/i}$ cells

overexpressing Prep1ΔHR1+2 as well as other Prep1 mutants. Although Prep1ΔHR1+2 cannot interact with Pbx1, it still can be detected in both nucleus and cytoplasm of the infected cells. The other mutants showed mainly nuclear localization, as expected. This indicates that Prep1 nuclear translocation is not necessarily limited to the interaction with Pbx1 but that also other proteins or mechanisms may be involved in this translocation.

Several studies have shown the involvement of Meis-Pbx and Hox-Pbx interactions in carcinogenesis [42,228]. The ability of Meis1 to interact with Pbx proteins is essential for the induction and maintenance of *MLL*-mediated myeloid transformation. Both the deletion of the HR1+2 domain of Meis1 [42] or depletion of Pbx [149] abolish *Meis1* oncogenic activity. Thus *MLL*-mediated transformation requires *Meis1* as well as Pbx proteins [42,149]. Moreover the oncogenic potential of Hoxa1 relies on the interaction with Pbx1 through the hexapeptide motif and the mutated hexapeptide motif loses the interaction with Pbx1 and is not able to confer oncogenic potential to Hoxa1 [228]. Likewise, the mutated HOXB4 hexapeptide impairs *HoxB4*-induced transformation [229]. Similarly, Fernandez et al. [230] showed that a dominant negative mutant of PBX, unable to bind to DNA but capable of binding Prep1, reduces the oncogenic activity of HoxB7. Thus the integrity of the Pbx-interacting domains of Meis1 and Hox proteins is important for their oncogenic activity.

Consistent with the importance of the Meis1-Pbx interaction in *MLL*-mediated myeloid transformation [42,149], I have shown that also in MEFs *Meis1* requires *Pbx* for oncogenic transformation. Indeed, Pbx1 depletion in *Prep1*$^{i/i}$ cells overexpressing Meis1 attenuated the tumorigenic potential of these cells. The number of colonies formed in soft-agar and the size of the tumors in transplanted mice decreased in Pbx1-depleted cells. Moreover, also Prep1 was unable to rescue the residual *Meis1*-induced tumorigenicity in the Pbx1 down-regulated cells. In fact, cells co-expressing *Meis1* and *Prep1* showed the

same tumorigenic potential in Pbx1 depleted and control cells both *in vitro* and *in vivo*. Thus also *Prep1* suppressive function requires *Pbx1*. Meis1 and Prep1 proteins share 60% sequence identity in their Pbx interacting domain and both can recruit Pbx for their biological functions [43,51,76]. Based on the observations that both Meis1 and Prep1 need to interact with Pbx proteins to exert their oncogenic and oncosuppressive activities, respectively, I suggest that Meis1 and Prep1 compete for Pbx1 in the context of tumorigenesis.

In addition to competing for Pbx1, *Prep1* re-expression significantly decreases the endogenous and exogenous Meis1 protein level. This might well explain the smaller tumor size. Therefore, *Prep1* can prevent *Meis1* oncogenic activity by both competing for Pbx1 and decreasing *Meis1*.

3.4. Meis1 interacts with Ddx3x and Ddx5 RNA helicases only in the absence of Prep1.

The fact that Meis1 only transforms *Prep1*$^{i/i}$ and not wild type cells not only depends on the ability of Prep1 to compete for the common partner, Pbx1, but also relies on the loss of other interactions of Meis1. Competition for Pbx1 would be only one of the possible explanations for *Meis1* and *Prep1* opposite functions in tumorigenicity, since mass spectrometry analysis showed that the presence of Prep1 alters the composition of the Meis1 protein complex.

In fact, I have shown that Meis1 interacts with ATP-dependent RNA helicases Ddx3x and Ddx5 proteins only in *Prep1*$^{i/i}$ cells. Ddx3x and Ddx5 are known to have oncogenic properties [191,196]. In addition, restoration of Prep1 level perturbs this interaction. The interaction with Ddx3x and Ddx5 is specific for Meis1, since Prep1 does

not interact with these proteins. IP experiments performed on the nuclear lysate of *Prep1*$^{i/i}$ and *Prep1*$^{i/i}$ cells re-expressing Prep1, showed that in the presence of Prep1 the interaction of Meis1 with Ddx3x and Ddx5 was lost.

By molecular dissection of Meis1, I show that Ddx3x mainly binds to the homeodomain (DNA-binding) of Meis1 while Ddx5 interacts with both the homeodomain and the C-terminal domain (CTD) of Meis1. Several studies have shown that the homeodomain and the CTD of Meis1 contribute to its pro-tumorigenic activities [42,135,136,137,231]. For instance, Meis1 CTD is sufficient to transform non-oncogenic Prep1 into a *Hoxa9* cooperating oncoprotein [137]. The CTD of Meis1 has transactivating properties which are missing or different in Prep1. Meis1 and a chimeric Meis1-Prep1 regulate an overlapping set of genes implicated in control of cellular proliferation and division, showing that the leukemogenic potential of *Meis1* relies on its ability to deregulate multiple pathways [137]. Thus the interaction of Meis1 with Ddx3x and Ddx5 might have an important impact on *Meis1*-induced oncogenicity.

Overall, my data on one hand show that *Meis1*-induced tumor formation is much more complex than a simple Meis1-Pbx interaction and on the other hand demonstrate that *Prep1* may employ a broad range of ways to suppress *Meis1* oncogenicity; at least competition for Pbx, interaction with the RNA helicases and control of Meis1 gene expression.

3.4.1. What is the role of Ddx RNA-helicases in *Meis1*-induced transformation?

DEAD-box proteins are the largest RNA helicase family, with 38 members in man that are associated with almost all processes involving RNA, including ribosome

biogenesis, transcription, pre-mRNA splicing, RNA maturation, RNA export, translation and RNA decay [181,182]. Multiple studies have shown overexpression of some members of the DEAD-box family in tumor cell lines and tumor tissues. Some of them are also known to be implicated in DNA repair and cell growth control. Thus, DEAD-box proteins have potentially important roles in cancer development [203].

DDX3X (*DDX3* or *DBX*) is a member of the human DEAD-box family of RNA helicases, first identified in 1997 as one of the five genes on the X-chromosome which have homologs in the non-recombining region of the Y-chromosome (*DDX3Y* or *DBY*). It escapes X-inactivation and is ubiquitously expressed in a broad range of tissues [232]. As depicted in Figure 3.1, *DDX3X* has been involved in all processes regulating gene expression, including transcription, pre-mRNA splicing, RNA export and translation. Furthermore, it has also been implicated in cell cycle control and apoptosis regulation. Interestingly, a great deal of research has focused on *DDX3X* because of its role in the replication of HCV, HIV and poxviruses [195,232]. Ddx5 is one of the prototypic members of the DEAD-Box family of RNA helicases. Like DDX3X, it functions in the entire process of gene expression and RNA metabolism [203].

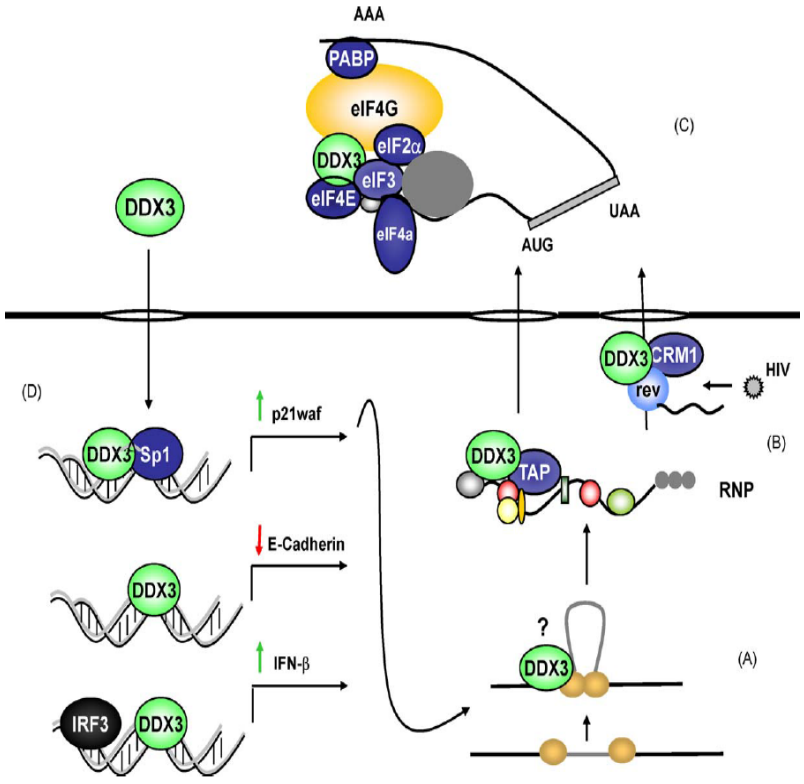

Figure 3.1. DDX3 involvement at different stage of gene expression regulation. (A) DDX3 interacts with splicing factors and Ribonucleoproteins (RNPs). **(B)** CRM1 and TAP export shuttle export DDX3 from the nucleolus. **(C)** DDX3 is involved in the regulation of translation. **(D)** DDX3 is implicated in the transcriptional regulation of different genes (see the text for more information) [232].

Thus one of the common and at the same time interesting functions of these two proteins is their involvement in transcription and cell cycle regulation. They interact with different transcription factors and act as transcriptional coactivators/corepressors. DDX3X is recruited to specific promoters. It binds to Sp1 transcription factor and increases the expression of p21WAF. It also has been shown to bind to the E-Cadherin and IFNβ promoters, to upregulate IFNβ and downregulate E-Cadherin expression (Figure 3.1) [232]. How DDX3 is recruited to the promoters is still unknown. DDX3 was first suggested to have a leucine-zipper motif but there is no evidence that it can bind to specific DNA sequences. Thus, more likely DDX3 recruitment to specific promoters

takes place through interaction with promoter-specific transcription factors or other coactivators as shown for the p21waf promoter [232]. DDX5 can act both as a transcriptional coactivator interacting with CBP, p300, SRC1 and RNA polymerase II, as well as a transcriptional corepressor by interacting with HDAC1 [203]. It would be interesting to identify Ddx3x and Ddx5 target genes by ChIPseq, an experiment that might be done in the near future.

Consistent with the above data, Meis1 might recruit Ddx3x and Ddx5 to the regulatory regions of its target genes or sequester them preventing the interaction with other genes. In fact, DDX5 can bridge transcription factors, coactivators and RNA polymerase II [203]. In turn, these proteins might bridge Meis1 to other transcriptional regulators and control *Meis1*-dependent gene expression acting like bona fide transcription activators or repressors. Likewise, their absence from specific regulatory sites may have important transcriptional consequences. The impairment of Meis1 interaction with Ddx proteins suggests their importance for *Meis1*-dependent gene expression. However, the impact of the *Ddx3x* and *Ddx5* on *Meis1* transcriptional activity still requires to be assessed.

The involvement of Ddx5 and its close homologue Ddx17 in the regulation of oncogenes such as *c-Myc*, *Cyclin D1*, *Fra-1*, and *c-jun* suggests that they could have an impact on cell proliferation [207]. In the developing zebrafish eye, *Meis1* controls the proliferation of multipotent cells by regulating *Cyclin D1* and *c-Myc* expression [233] and in leukemogenesis cyclin D3 is a direct downstream target of Meis1 [135]. These data provide a link between Ddx proteins and Meis1 in proliferation and cell cycle control in both development and tumorigenesis.

I tried to downregulate either *Ddx3x* or *Ddx5* in *Prep1*$^{i/i}$ cells overexpressing *Meis1*. However, this procedure severely impaired cells proliferation (Figure 2.13C). The cells

lost their anchorage independent-growth capacity, as also shown by Shin et al. [207] in colon cancer cells. This has so far prevented me from examining the direct responsibility of Ddx proteins in *Meis1* tumorigenesis. *Ddx5* and *Ddx17* are overexpressed in colon cancer and their downregulation in colon strongly compromises the ability of the cells to proliferate and form tumors in mice [207]. Overexpression of these proteins correlates with the progression of the disease from polyp to adenoma to adenocarcinoma [207]. However, in the present study, Ddx3x and Ddx5 protein level did not change in the *Meis1* overexpressing cells. However, it is known that Ddx5 stability might be posttranslationally modified in cancer cells by tyrosine phosphorylation or ubiquitylation [213,214]. At this stage the hypothesis can be made that Meis1 complexes with Ddx3x and Ddx5 transform cells by activating the expression of genes involved in cell proliferation. As a result, impairment of this complex (for example by Prep1), reduces Meis1 ability to activate cell proliferation, suppressing *Meis1*-induced tumorigenesis. This hypothesis can be experimentally verified.

3.5. Final Remarks

The TALE family of transcription factors is a very complex family within the homeodomain transcription factors superfamily. *PBC* and *MEIS* subfamilies are both structurally and functionally related with a wide range of common targets and/or functions not only in development but also in diseases including cancer. However the mechanisms underlying their functions are mainly unknown. The facts that two closely related members of the *MEIS* subfamily, *Meis1* and *Prep1*, exert opposite roles in carcinogenesis, indicates that their cross-modulation can affect multiple cellular pathways. The data presented in the present thesis will be helpful to understand the role of

TALE proteins in cancer; however a great deal of further research is required to elucidate the affected pathway and how they are misregulated.

Chapter 4: *Materials and Methods*

4.1. Buffers and Solutions

4.1.1. Phosphate-Buffered Saline (PBS)

NaCl	137 mM
KCl	2.7 mM
KH_2PO_4	1.47 mM
$Na_2HPO_4 \times 7H_2O$	8.0 mM

To prepare 1 liter of 10X PBS 80 g of Nacl, 2 g of KCl, 21.6 g of $Na_2HPO_4 \times 7H_2O$ and 2g of KH_2PO_4 were solved in 800 mL of distilled water. The pH was adjusted to 7.4 with HCl.

4.1.2 Tris-Buffered Saline (TBS)

NaCl	150 mM
KCl	2.7 mM
Tris HCl pH 8.0	25 mM

To prepare 1 liter of 10X TBS, 80 g of NaCl, 30 g of Tris base and 2 g of KCl was dissolved in 800 mL of distilled H_2O and the pH was adjusted to 8.0 with HCl.

4.1.3. TBST

TBS	1X
Tween 20	0.1% (v/v)

4.1.4. Tris-Acetate-EDTA (TAE) 50X

Tris base	2 M
Glacial acetic acid	1 M
EDTA, pH 8	10 mM

To prepare 1 liter of 50X TAE, 242 g of Tris base, 57.1 mL of Glacial acetic acid and 20 mL of EDTA (0.5 M, pH 8.0) were dissolved in 800 mL of distilled H_2O and pH was adjusted to 8.3 with Glacial acetic acid.

4.1.5. Tris EDTA (TE) 10X

Tris	100 mM
EDTA	10 mM

The pH was adjusted to 7.5 with HCl. To prepare 1 liter of 10X TE, 12.1 g of Tris, 20 mL of EDTA and 4.2 mL of HCl were used.

4.1.6. Tris-HCl 1M

121.1 g of Tris-base is dissolved in 800 mL of distilled H_2O. The pH is adjusted either to 7.4, 7.6 or 8.0 with HCl. The volume was adjusted to 1 liter by adding distilled H_2O.

4.1.7. HBS 2X

Hepes	50 mM
KCl	10 mM
Dextrose	12 mM
NaCl	280 mM
$Na_2HPO_4 \times 7H_2O$	1.5 mM

The pH was adjusted to 7.05 and solution was passed through 0.22 μm filter and stored at -20 °C.

4.1.8. SDS-PAGE Running Buffer 10X

Tris	250 mM
Glycine	192 mM
SDS	1% (w/v)

To prepare 1 liter of 10X running buffer, 30 g of Tris base, 144 g of Glycine and 50 mL of 20% SDS were used.

4.1.9. Western Transfer Buffer 10X

Tris HCl pH 8.3	250 mM
Glycine	192 mM

To prepare 1X transfer buffer, the 10X stock is diluted 1 to 10 with distilled H_2O and Methanol or Ethanol was added up to 20% (v/v).

4.1.10. Laemmli Buffer 4X

Tris HCl pH 6.8	200 mM
SDS	8% (v/v)
Glycerol	40% (v/v)
Bromophenol Blue	0.01% (w/v)

4.1.11. Ponceau Solution

Ponceau	0.1% (w/v)
Glacial acetic acid	5% (v/v)

4.1.12. Coomassie Brilliant Blue Stain

Coomassie brilliant blue R-250	0.2% (w/v)
Glacial acetic acid	10% (v/v)
Ethanol	30% (v/v)

4.1.13. Coomassie De-Staining Solution

Glacial acetic acid	10% (v/v)
Ethanol	30% (v/v)

4.1.14. Proteinase K Lysis Buffer (PKLB)

Tris-HCl pH 8.5	100 mM
EDTA	5 mM

SDS	0.2% (v/v)
NaCl	200 mM
Proteinase K	100 µg/mL

4.2. Reagents

4.2.1. Primary Antibodies

Antibody	Type	Product Code	Dilution	Use
Prep1 CH12.2	Mouse-monoclonal	Home made	1 µg/mL	WB
Prep1	Rabbit-polyclonal	Santa Cruz sc-6245	1 µg/mL	WB/IF
Meis1 K845	Rabbit-polyclonal	Provided by Miguel Torres	1 µg/mL	WB
Pbx1	Rabbit-polyclonal	Santa Cruz sc-889X	1 µg/mL	WB
Pbx1b	Mouse-monoclonal	Provided by Micheal Cleary	2 µg/mL	WB
Pbx2	Rabbit-polyclonal	Santa Cruz sc-890	1 µg/mL	WB
Ddx5	Goat-polyclonal	Abcam ab10261	1:2000	WB
Ddx3X	Rabbit-polyclonal	Millipore NG1895575	1:1000	WB
FLAG Clone M2	Mouse-monoclonal	Sigma F3165-5MG	1:5000	WB
Nucleolin	Rabbit-polyclonal	Novus Biologicals NB600-241A1	1:4000	WB
Vinculin	Mouse-monoclonal	Sigma V9B1-o.5ML	1:10000	WB
Hoxa9	Rabbit-polyclonal	Upstate 07-178	2 µg/mL	WB

PCNA	Mouse-monoclonal	Abcam ab29-100	1:1000	WB
Ras	Mouse-monoclonal	BD Transduction labratories™ 610002	1:500	WB
c-Myc	Rabbit-polyclonal	Santa Cruz sc-764	1:200	WB

4.2.2. Secondary Antibodies

Antibody	**Product Code**	**Dilution**	**Use**
Goat polyclonal anti-Mouse IgG-HRP (H+L)	Biorad (170-6516)	1:10000	WB
Goat polyclonal anti-Rabbit IgG-HRP (H+L)	Biorad (170-6515)	1:10000	WB
Rabbit polyclonal anti-Goat IgG-HRP (H+L)	Dako (P044902)	1:3500	WB
Alexa Fluor® 647 Donkey anti-rabbit IgG (H+L)	Invitrogen (A31373)	1:100 of 2 mg/mL stock	IF

4.2.3. shRNA Lentiviral Vectors

Sequence-verified MISSION® shRNA lentiviral plasmids (pLKO.1-puro) were purchased from Sigma to downregulate *Ddx3x*, *Ddx5* and Pbx1 genes expression.

Target gene	**TRC number**	**shRNA sequence**
Ddx5 (NM_007840)	TRCN0000071103	CCGGCGGGAAGCTAATCAAGCAATTCTCGAGAATTGCTTGATTAGCTTCCCGTTTTTG
Ddx5 (NM_007840)	TRCN0000071104	CCGGGCGAATGTCATGGATGTGATTCTCGAGAATCACATCCATGACATTCGCTTTTTG

Ddx3x (NM_010028)	TRCN0000103750	CCGGGCTGTGATTCTCCACTGAAATCTCGAGATTTCAGTGGAGAATCACAGCTTTTTG
Ddx3x (NM_010028)	TRCN0000103751	CCGGCCGTGATTTCTTAGATGAGTACTCGAGTACTCATCTAAGAAATCACGGTTTTTG
Pbx1 #8 (NM_008783)	TRCN0000012575	CCGGGCCTGCCTTGTTTAATGTGTTCTCGAGAACACATTAAACAAGGCAGGCTTTTT
Pbx1 #10 (NM_008783)	TRCN0000012577	CCGGCTCACAGATCAGACAAATCTACTCGAGTAGATTTGTCTGATCTGTGAGTTTTT
SHC002 Mission non-Target shRNA control vector	TRC1/1.5	CCGGCAACAAGATGAAGAGCACCAACTCGAGTTGGTGCTCTTCATCTTGTTGTTTTT

4.3. Cloning Techniques and Plasmids

4.3.1. Agarose Gel Electrophoresis

DNA samples (either PCR products or digested DNA fragments) were loaded onto 0.8% - 2% agarose gel prepared in 1X TAE buffer containing 1X Gel Red (from Biotium). Electrophoresis was carried out at 80 V. The DNA bands were visualized under UV light exposure. 1 kb or 100 bp DNA ladders (from promega) were used as molecular size standard.

4.3.2. Bacterial Transformation and Plasmid Mini-Preparation

One Shot® TOP10 chemically competent *E.coli* (Invitrogen™ Cat No. C4040-06) was used for transformation. For each reaction 1 vial of competent bacteria was thawed on ice. 1 to 5 µL of plasmid DNA (10 pg to 100 ng) was gently mixed with bacteria and incubated on ice for 30 min. Cells were heat-shocked for 40 sec at 42 °C and placed on ice for 2 min. 250 µL of pre-warmed S.O.C. Medium was added to each vial aseptically

and shake horizontally at 37°C for 1 hour at 225 rpm in a shaking incubator. 20 - 200 μL from each transformation was spread on a pre-warmed LB agar plates supplemented with 100 μg/mL ampicillin and incubated overnight at 37 °C. Single bacterial colonies were picked and cultured in overnight 10 mL LB supplemented with 100 μg/mL ampicillin. Plasmid DNA was extracted from the bacterial pellet of overnight culture using Wizard® *Plus* SV Minipreps DNA Purification System (Promega Cat.No. A1465). The accuracy of the cloned fragments was check by sequencing.

4.3.3. Plasmid Maxi-Preparation

Plasmid DNA was isolated from 250 mL of overnight bacterial culture in LB broth supplemented with 100 μg/mL ampicillin using QIAGEN Plasmid Maxi Kit (QIAGEN Cat.No. 12163).

4.3.4. Retroviral Expression Vectors

Prep1 deletion mutants have been described [73]. They carry the following modifications: a) deletion of the Pbx interacting domain (*Prep1ΔHR1+2*, deleted residues: 58-137); b) deletion of the DNA binding homeodomain (*Prep1ΔHD*, deleted residues: 259-318). The mutants were amplified from the original vector using primers listed in the following table and were cloned in pMSCV-hygro vector along with FALG-tag.

Primers set	**Sequences (5′→3′)**
*Prep1-**XhoI***-FLAG-Fwd	cgc***CTCGAG***ATGGACTACAAGGACGACGATGACAAG ATGATGGCTACACAGACATTAAG
*Prep1-**XhoI***-Rev	cgc***CTCGAG***CTACTGCAGGGAGTCACTGTTC

Prep1ΔC construct was generated by deletion the C-terminal domain of the protein (residues: 318-436). cDNA pool from MEFs was used as template for the PCR reaction. Phusion® high fidelity DNA polymerase (FINNZYMES Cat.No. F530S) was used in PCR reactions to amplify Prep1ΔC fragment. This fragment was cloned in pMSCV-hygro vector along with FALG-tag. The primers used for this cloning are listed below.

Primers set	**Sequences (5′→3′)**
*Prep1-**XhoI***-Flag-Fwd	cgc***CTCGAG***ATGGACTACAAGGACGACGATGACAAGAT GATGGCTACACAGACATTAAG
*Prep1-**XhoI***-Rev	cgc***CTCGAG***TTACATTGGCTGAAGAATTGGTC

Other retroviral vectors used in this study are listed in the table below:

Vector	**Tag**	**Insert**	**Species**	**Cloning site**	**Selection markers**
pMSCV	FLAG	*Meis1*	Mouse	BglII/XhoI	Puromycin
MigRI	FLAG	*Prep1*	Human	XhoI	GFP
pBabe		*Myc*	Mouse		Hygromycin
pBabe		*Prep1*	Human	SnaBI/SalI	Puromycin
pBabe		*H-Ras^{v12}*	Human		Hygromycin
pBabe		*H-Ras^{v12}*	Human		Puromycin

4.3.5. TAP-*Meis1a* Construct

To construct *Meis1a*-TAP vector, seamless gene fusion technique by overlap PCR was used [234]. TAP cassette which contains a calmodulin binding peptide (CBP), a TEV cleavage sequence, and two protein A (ProtA) modules, was amplified using pBabe–*Prep1*-TAP vector as template [223]. The *Meis1a* and TAP cassette fragments are PCR products amplified individually so that the end of *Meis1a* reverse primer has 15 bases complementary to the TAP cassette forward primer. cDNA pool from MEFs was used to amplify *Meis1a* cDNA. The PCR products were then used as templates for a second PCR amplification with *Meis1a* forward and TAP cassette reverse primers. To facilitate efficient PCR amplification, a similar melting temperature (Tm) used for all primers in the range of 57 °C to 61 °C. Gel purified *Meis1a*-TAP fusion fragments were digested with XhoI-HpaI restriction enzymes and cloned in pMSCV-puro retroviral vector. Some positive clones were sequenced to verify the sequence of the fusion fragment. The sets of primers used for this cloning are listed below.

Primers sets	**Sequences (5′→3′)**
Meis1a Forward Primer	ATGGCGCAAAGGTACGACGAC
Meis1a Reverse Primer + TAP overlap sequence	CTTCTCTTTTCCATTTGCATGTAGTGCC ACTGC
TAP cassette Forward Primer	ATGGAAAAGAGAAGATGGAAAAAGAA TTTC
TAP cassette Reverse Primer	TCAGGTTGACTTCCCCGCG

4.3.6. Plasmids Used in Pull-Down Assay

4.3.6.1. pGEX-*Meis1a* Mutant Constructs

Meis1a, Meis1a-Nter (residues: 1-266), *Meis1a-HD+Cter* (residues: 267-390), *Meis1a-HD* (residues: 267-338) and Meis1a-Cter (residues: 339-390) fragments were

amplified using primers listed below and cDNA pool prepared from MEFs as template. The amplified fragments were digested by EcoRI-XhoI double digestion and gel purified. The digested fragments were cloned in frame with the glutathione S-transferase (GST) of pGEX-6p-1 vector (from GE Healthcare). The ligation products were transformed in One Shot® TOP10 competent *E.coli* bacteria (Invitrogen™ Cat No. C4040-06) and positive clones were verified by sequencing.

Primers sets	**Forward Primers (5′→3′)**	**Reverse Primers (5′→3′)**
Meis1a	ATGGCGCAAAGGTACGACGAC	TTACATGTAGTGCCACTGCC
Meis1a-Nter	ATGGCGCAAAGGTACGACGAC	AGGGTCATCATCGTCACCTGTG
Meis1a-HD+Cter	GATAAGGACAAAAAGCGTCAC	TTACATGTAGTGCCACTGCC
Meis1a-HD	GATAAGGACAAAAAGCGTCAC	GGACTGGTCTATCATGGGC
Meis1a-Cter	AACCGAGCAGTCAGCCAAG	TTACATGTAGTGCCACTGCC

4.4. Cell Culture

4.4.1. Isolation and Culturing of Primary MEFs

To obtain primary Mouse Embryonic Fibroblasts (MEFs), either *Prep1*$^{+/i}$ [171] or *p53*$^{+/-}$ (Jackson Labs, Bar Harbor, ME, USA) animals were mated. Mice were sacrificed by carbon monoxide inhalation at 14.5 d.p.c. and embryos were collected in 50 mL falcon tubes containing ice cold PBS. Under the dissecting microscope, embryos were dissected from the yolk sac. Head and liver were removed. Yolk sac and head were used for

genotyping as described in section 4.4.2. Embryos were carefully minced with a sterile scalpel blade. 6 mL of DMEM medium supplemented with 10% fetal bovine serum North American (TET system approved from PAA laboratories), 0.1 mg/mL gentamicin (GIBCO™ Gentamicin Reagent Solution (50 mg/mL) liquid from Invitrogen Cat.No. 15750060), 100 units/mL penicillin (Euroclone), 100 g/mL stereptomycin (Euroclone), 2 mM L-glutamin (Euroclone); were added to the 6 cm Petri dish containing minced embryo. The tissue/medium was passed through the 2 mL syringe with 22 g needle several times and maintained at 37 °C, in a humidified incubator with 3% O_2 and 5% CO_2. The medium was changed every day. MEF p0 cells were split (1:3) when the cells were 80% confluent and some cells were frozen in freezing medium containing FBS+10% dimethylsulfoxyde (DMSO). MEFs in culture were split every 2-3 days and were used for experiments between passages 2 and 5.

4.4.2. Genotyping of *Prep1*$^{i/i}$ and *p53*^{ko} Mice

Tail and yolk sac of the dissected embryos were lysed in 500 µL of PKLB at 55 °C for 3 hours. Proteinase K was inactivated by incubating at 95 °C for 5 minutes. 5 µL of the digestion product was used for genotyping with primers as previously described for *Prep1*$^{i/i}$ mice genotyping [171]. For *Prep1*$^{i/i}$ genotyping, the PCR was performed in 50 µL reaction composed of 5 µL of 5X PCR buffer (GoTaq® Felxi DNA polymerase, Promega), 3 mM $MgCl_2$, 0.1 mM dNTPs, 0.25 µM of each primer and 0.025 units Taq Polymerase. PCR was carried out on GeneAmp PCR System 2400 (Perkin Elmer), using a pre-PCR step of 10 min at 94 °C, followed by 35 cycles of 15 sec at 94 °C, 15 sec at 55 °C and 30 sec at 72 °C. Followed with the final extension for 10 minutes at 72 °C. Primers set used to genotype *Prep1*$^{i/i}$ embryos are listed in the table below.

Primers sets	**Sequences (5´→3´)**
Prep1F1	CCAAGGGCAGTAAGAGAAGCTCTGGAG
Prep1R1	GGAGTGCCAACCATGTTAAGAAGTCCC
LTR2	AAAATGGCGTTACTTAAGCTAGCTTGC

To genotype *p53*^{ko} mice, the PCR was performed in 50 µL reaction composed of 5 µL of 5X PCR buffer (GoTaq® Felxi DNA polymerase, Promega), 3 mM $MgCl_2$, 0.1 mM dNTPs, 2 µL of primer trimix and 0.04 units Taq Polymerase. Primer trimix for p53 is made of 16 µL of 53/93 (25 µM), 16 µL of WT92 (25 µM) and 32 µL of KO94 (25 µM) primers in a final volume of 200 µL in water. The final concentration of the primers in the trimix is 2 µM except for KO94 that is 4 µM. The cycling was carried out with 1 cycle of 10 minutes at 94 °C; 35 cycles of 30 sec at 94 °C, 30 sec at 55 °C and 1 minute at 72 °C. A final extension step was performed for 5 minutes at 72 °C.

Primers sets	**Sequences (5´→3´)**
P53/93	GGATGGTGGTATACTCAGAGC
P53WT92	AGCGTGGTGGTACCTTATGAGC
P53KO94	GCTATCAGGACATAGCGTTGG

4.4.3. Immortalization of MEFs Using 3T3 Protocol

To immortalize MEFs, 3T3 protocol was used. For serial 3T3 cultivation, WT and *Prep1*$^{i/i}$ primary MEFs were maintained on a defined 3 day schedule by plating 3×10^5 cells in 60-mm Petri dishes. Cells were kept under low oxygen tension (3%) during the entire immortalization steps. Immortalized subclones were expanded and were used for the experiments.

4.4.4. Calcium Phosphate Transfection

48 hours prior to the transfection, ecotropic Phoenix packaging cells were plated at density of 1.8×10^6 cells per 10 cm plates filled with DMEM medium supplemented with 10% FBS-NA and 1% Glutamine. Cells were 70-80% confluent at the time of transfection. To perform transfection:

- 10 μg of plasmid DNA
- 61 μL of 2M $CaCl_2$
- ddH_2O up to 500 μL

were mixed thoroughly and added to 500 μL of 2X HBS (Hepes Buffered Saline) in a dropwise manner and kept for 10 minutes at room temperature to allow the formation of fine precipitates between calcium ions and DNA phosphate groups. Cells were treated with Cloroquine at a final concentration of 20 μM for 10 minutes. The prepared transfection solution was gently added to the plates and incubated at 37 °C. 8 hours post transfection the medium was replaced with 10 mL of fresh supplemented DMEM. The day after, medium was replaced with 5.5 mL of fresh supplemented DMEM in order to concentrate viral supernatant.

4.4.5. Retroviral Infection

MEFs target cells were plated 24 hour prior to the infection to reach 50% confluence by the time of infection. The viral supernatant were collected from Pheonix packaging cells and filtered with 0.45 μm filter and added to the target cells in the presence of 8 μg/mL polybrene (Hexadimethrine bromide Sigma). After 3 to 4 hours of incubation, a second run of infection was performed with the fresh viral supernatant for the next 3 to 4 hours. The day after, cells were further infected with 3rd and 4th runs of

infection. 48 hours after 1st run of infection, cells were either sorted for GFP expression or selected for puromycin dehydrochloride (2 μg/mL, PAA laboratories) or hygromycin B (100 μg/mL, invitrogen) antibiotics resistance for 4 and 8 days, respectively.

4.4.6. Lentiviral Infection

5×10^6 HEK-293T helper cells per 10 cm Petri dish were plated at the day of transfection. Cells were transfected with 10 μg of the shRNA constructs together with the plasmids required for the production of viral capsid proteins following the calcium phosphate transfection method (section 4.4.4):

- ENV (VSV-G) 2.8 μg
- PRE (gag & pol) 5 μg
- REV 2.5 μg

48 hours after transfection, supernatant was collected and filtered with 0.45 μm filter. Polybrene (8 μg/mL) was added to the supernatant and cells were incubated with the viral supernatant for 3 hours. 2nd run of infection was performed with the fresh viral supernatant overnight. 48 hours post infection, cells were selected with puromycin (2 μg/mL) for 4 days.

4.5. Cell Lysis and Western Blotting

4.5.1. Total Protein Extraction

Culture medium was removed and cells were washed with ice cold PBS. Cells were scraped and collected in a falcon tube. RIPA buffer (Tris HCL pH8 50mM, Nacl 150mM, SDS 0.1%, Na.Deoxycholate 0.5%, Triton X-100 or NP40 1% and protease inhibitor

cocktail 1x (from Roche)) was added to the pellet of the cells. 300 μL of RIPA buffer was used to lyse around 3 to 4 × 10^6 cells. Cells in RIPA buffer were kept on ice for 5 min, pipeting up and down occasionally. Lysates were centrifuged at 13000 rpm for 15 min at 4°C to pellet the cell debris. Supernatants were transferred to a new microtube and protein concentration was measured by Bradford assay (Biorad), following manufacture instructions. 60 μg of total extracts were used for western blotting analysis.

4.5.2. Nuclear and Cytoplasmic Protein Extraction

Cells were lysed to obtain nuclear and cytoplasmic fractions [235]. 100 μL or 300 μL of buffer A (10 mM HEPES KOH pH 7.9, 1.5 mM $MgCl_2$, 10 mM KCl, 0.5 mM DTT plus a cocktail of protease inhibitors) were used to suspend cells collected from 6 cm or 10 cm Petri dishes respectively and incubated on ice for 10 min. 1/30 of the volume of 10% Triton X-100 were added to the cell extract and were vortex for 30 seconds. Then cell extracts were centrifuged for 1 min at 11000 rpm. The resulting nuclear pellet was treated with 1/5 of the volume of buffer C (20 mM HEPES pH 7.8, 25% glycerol, 420 mM NaCl, 1.5 mM $MgCl_2$, 0.2 mM EDTA plus protease inhibitors) for 30 min at 4°C and centrifuged at 13000 rpm for 15 min. The supernatant was the nuclear fraction. The cytoplasmic fraction was treated with 0.11 volume of buffer B (0.3 M HEPES, pH 7.9, 1.4 M KCl, 30 mM $MgCl_2$), rotated for 30 min at 4°C and centrifuged for 15 min at 13000 rpm. 30 μg of Nuclear and 60 μg of cytoplasmic extracts were used for western blotting analysis.

4.5.3. SDS-Polyacrylamide Gel Electrophoresis (SDS-PAGE)

Proteins were resolved on polyacrylamide gels prepared from 30% of stock solutions with a ratio Acrylamide/Bisacrylamide of 29:1 (EuroClone, EMR069250). 10% ammonium persulphate (APS) and TEMED (EuroClone, EMR228100) were used as polymerization catalysts. Indicated amount of proteins were mixed with 4X sample buffer prior to the use and boiled at 95°C for 5 minutes. Samples loaded onto 1-1.5mm thick SDS-PAGE gels were run in running buffer at 25-35 mA (Biorad).

Separating gel components	**Gel %**				
	6%	7.5%	8%	10%	12%
ddH_2O (mL)	5.3	4.9	4.6	4	3.3
30% acrylamide mix (mL)	2	2.7	2.7	3.3	4
1.5 M Tris HCl pH8.8 (mL)	2.5	2.5	2.5	2.5	2.5
10% SDS (mL)	0.1	0.1	0.1	0.1	0.1
10% APS (mL)	0.1	0.1	0.1	0.1	0.1
TEMED (mL)	0.008	0.007	0.006	0.004	0.004
Total (mL)	10	10	10	10	10

Stacking gel components	**5% gel**
ddH_2O (mL)	6.8
30% acrylamide mix (mL)	1.7
1.5 M Tris HCl pH6.8 (mL)	1.25
10% SDS (mL)	0.1
10% APS (mL)	0.1
TEMED (mL)	0.01
Total (mL)	10

4.5.4. Western Blotting

Proteins were transferred to the nitrocellulose transfer membranes (PORTRAN®, pore size 0.45 μm) in western transfer tanks (Biorad) filled with 1X transfer buffer at 300 mA for 90 minutes or at 30 mA overnight at 4°C. At the end of the transfer, membranes were stained with Ponceau solution to get rough estimation of the amount of the transferred proteins on the membranes and quality of the transferring procedure. Membranes were briefly washed in TBS + 0.1% Tween (TBS-T) and blocked in 5% dry milk in TBST for 1 hour at room temperature. Membranes then were incubated with primary antibodies, diluted in TBS-T 5% dry milk overnight at 4°C, followed by three washes of 10 minutes each with TBST-T. Membranes were then incubated with the appropriate horseradish peroxidase conjugated secondary antibody diluted in 5% dry milk in TBS-T for 1 hour at room temperature. The membranes were washed as already indicated and peroxidase activity was measured using the ECL methods (Amersham). In case of need to re-blot the membranes, they were stripped using Scientific Restore Stripping Buffer (Thermo Scientific Cat.No.21059) according to the manufactures instructions and after blocking with 5% dry milk in TBST, immunoblotted with desired antibodies. All densitometric analysis was performed using ImageJ software.

4.6. Co-Immunoprecipitation

Cells were subjected to nuclear/cytoplasmic protein extraction protocol according to the standard protocol (see section 4.5.2). 500 μg of nuclear lysate were used for each single immunoprecipitation reaction. The ANTI-FLAG® M2 Magnetic Beads (Sigma Cat.No. M8823) were used for co-immunoprecipitations. 40 μL of the 50% bead suspension (~ 20 μL of packed gel volume) was used per reaction. The packed gel was

washed twice with 10 packed gel volumes of TBS buffer. Indicated amount of nuclear lysate was added to the washed resin beads. The final volume was adjusted to 1 mL by adding IgG binding buffer (IBB buffer: 10 mM Tris-HCl pH 8, 0.2% NP-40, 150 mM NaCl). As a negative control, lysate from not infected cells were used. All samples were gently rotated overnight at 4 °C. The tubes were placed in the appropriate magnetic separator and supernatant was removed. The resins were washed 3 times with 1 mL TBS each time, rotating at 4 °C for the total of 45 minutes. FLAG fusion proteins were eluted from the beads with either one of methods mentioned below:

- Protein elution under native condition by competition with FLAG® peptide (Sigma Cat.No. F3290). 50 µL of a working concentration of 100 µg/mL of FLAG peptide was used for elution.
- Elution under acidic conditions with 0.1 M glycine HCl, pH 3.0. 50 µL of 0.1 M glycine HCl, pH 3.0 was added to each sample and control resin and incubated for 5 minutes at room temperature. Tubes were placed in the appropriate magnetic separator and supernatants were transferred to fresh tubes containing 10 µL of 0.5 M Tris HCl, pH 7.4 with 1.5 M NaCl. The IP eluates along with 50 µg of input lysate/each sample were loaded on an 8% SDS-PAGE and proceed to immunoblotting using appropriate antibodies.

4.7. Tandem Affinity Purification (TAP) of Meis1a Interactome

4.7.1. TAP protocol

TAP is a two-step affinity purification protocol to isolate TAP-tagged proteins together with associated proteins. To isolate Meis1a interacting proteins, cell pellet collected from 15 × 15 cm Petri dishes were subjected to nuclear/cytoplasmic protein extraction. Nuclear fractions were adjusted to the IgG binding conditions (IBB buffer: 10

mM Tris-HCl pH 8, 0.2% NP-40, 150 mM NaCl), incubated in batch with 100 µL of IgG sepharose 6 fast low beads (GE Healthcare, Cat.No. 17-0969-01) and rotated overnight at 4°C. After washing three times with 10 mL of IBB buffer and once with 10 mL of TEV Cleavage Buffer (TCB: 10 mM Tris-HCl pH 8, 150 mM NaCl, 0.2% NP-40, 0.5 mM EDTA, 0.5 mM DTT), TEV cleavage was performed by incubation with 1 mL of TCB and 1.5 µL of TEV protease (5.75 mg/ mL) (Antibody and protein facility, IFOM-IEO campus), for 1 h at room temperature, rotating. For each milliliter of TEV eluate, 4 µL of 1 M $CaCl_2$ and three volumes of calmodulin-binding buffer CBB (50 mM Tris-HCl pH 8, 150 mM NaCl, 1 mM Mg-acetate, 1 mM imidazole, 4 mM $CaCl_2$, 0.2% NP-40, 10 mM β-mercaptoethanol) were added and mixed with 100 µL of MS-Grade calmodulin beads (Stratagene 240106) for 4 h at 4°C. Calmodulin beads were washed three times with 10 mL of CBB and boiled for 3 min with 100 µL of 3X sample buffer.

4.8. Mass-Spectrometry analysis

4.8.1. Gel Separation of Proteins, In-Gel Digestion and LC-MS/MS Analysis

The TAP eluates were resolved on one-dimensional 10% SDS-PAGE gel of 1-mm thickness. The gel was fixed in 50% methanol + 10% acetic acid and stained overnight with Colloidal Blue staining kit (Invitrogen LC6025). Different regions were cut out from the gel and trypsinized as previously described [236] Peptides were desalted [237] dried in a Speed-Vac and resuspended in 7 µL of 0.1% TFA (Trifluoroacetic acid). LC-ESI-MS/MS of 5µL of each sample was performed on a Fourier transformed-LTQ mass spectrometer (FT-LTQ) (Thermo Electron, San Jose, CA). Peptides separation was

performed on a linear gradient from 100% solvent A (5 % ACN (acetonitrile), 0.1% formic acid) to 20% solvent B (ACN, 0.1% formic acid) over 20 minutes and from 20% to 80% solvent B in 5 minutes at a constant flow rate of 0.3 µL/min on Agilent chromatographic separation system 1100 (Agilent Technologies, Waldbronn, Germany) where the LC system was connected to a 10.5 cm fused-silica emitter of 100 µm inner diameter (New Objective, Inc. Woburn, MA USA), packed in-house with ReproSil-Pur C18-AQ 3 µm beads (Dr. Maisch Gmbh, Ammerbuch, Germany) using a high-pressure bomb loader (Proxeon, Odense, Denmark).

Data acquisition mode was set to obtain one MS scan followed by five MS/MS scans of the five most intense ions in each MS scan. MS/MS spectra were limited to one scans per precursor ion followed by 1 minute of exclusion. MGF file were extracted using DTASuperCharge (v.1.19, www.cebi.sdu.dk) while Database search was performed using Mascot Daemon already set up with the following parameters: Database NCBInr, Taxonomy Mouse (Mus musculuus), enzyme Trypsin, Max missing cleavage 2, fixed modification carbamidomethyl (C), variable modification oxidation (M), peptide tolerance 10 ppm, MS/MS tolerance 0.5 Da, Instrument ESI-TRAP. The mass spectrometry analysis was performed by the Mass spectrometry Unit at IFOM-IEO campus.

4.9. Pull-down Assay Using GST Fusion Protein

4.9.1. GST-Fusion Protein Production and Purification

Meis1a-GST and *Prep1*-GST mutant [72] constructs were transformed in BL21(DE3)pLysS competent cells (promega, Cat.No. L1191). A single clone was inoculated in 10 mL LB medium + Ampicillin sodium salt (100 µg/mL, Sigma Cat.No.

A0166-25G) overnight at 37 °C in agitation. The bacterial culture was poured in 100 mL of LB medium + Ampicillin sodium salt and grown to OD ≈ 0.8. IPTG was added to the final concentration of 0.1 mM to induce GST-fusion proteins induction, for 3 hours at 37 °C agitating. The bacterial pellet was suspended in 10 mL of ice cold PBS + protease inhibitor cocktail (Roche) and was sonicated on ice at power 2,8 for a total of 5 minutes with 10 sec intervals. 20% Triton X-100 was added to a final concentration of 1% and rotated at 4 ºC for 30 minutes. The lysate was centrifuge at 1300 rpm at 4ºC for 15 minutes and either used to cross-link to glutatione beads or aliquoted and stored at -80 °C for later use.

4.9.2. Cross-Linking GST Fusion Proteins to Glutathione Beads

40 µL of the 50% Glutathione-Sepharose™ 4B bead suspension (~ 20 µL of packed gel volume) (GE Health care, Cat.No. 17-0756-05) were washed 3 times with PBS prior to the use and incubated roughly with 60 µg of the bacterial lysate in 500 µL PBS-T 1% (plus protease inhibitors) for 1 hour at 4ºC rotating. The GST-fusion proteins were eluted from the beads by boiling for 5 minutes in 20 µL of 2X sample buffer and run on the 10% SDS-PAGE gel along with 1 µg, 3 µg, 5 µg, 7 µg and 10 µg of BSA as an internal reference. Proteins were visualized by Coomassie brilliant blue staining for 15 minutes at room temperature shaking. The staining was followed by de-staning in Coomassie de-stain solution for 1-2 hours. Finally, the concentration of the induced GST-fusion proteins was estimated based on the BSA concentrations.

4.9.3. GST-Pull Down Protocol

60 μg of each GST-fusion protein was bound to 40 μL of the 50% Glutathione-Sepharose™ 4B bead as previously described. 300 μg of the nuclear lysate was mixed with GST-fusion protein, which adsorbed to Glutathione-Sepharose beads. The binding reaction was carried out for 1 hour at 4ºC in 1 mL IBB buffer (section 4.6). After thoroughly washing, 20 μL of 2X sample buffer was added to each sample and boiled for 5 minutes. 30 μg of the lysate (as input) along with specifically bound proteins to the GST-fusion protein were subjected to 10% SDS–PAGE followed by western blotting analysis.

4.10. Cell Proliferation Assay

Cells were counted using trypan blue dye and 70000 cells/well were seeded in a 6-well culture plates. All experiments were performed in triplicate. The day of plating was referred as T0 (12 hours post plating). Depending on the experiment, cells were either tripsinized and counted on the indicated time points or fixed with 4% paraformaldehyde for 10 minutes at room temperature and stained with crystal violet solution (0.1% crystal violet in PBS). The plates were air-dried and to solubilize crystal violet, cells were treated with a solution of 1% SDS in H_2O and 100 μL of each sample was transferred to a 96-well plate. Absorbance was read at 595 nm on a Victor^3™ 1420 multilabel plate counter (PerkinElmer). In the last method, the growth was expressed as the value of absorbance at a given time point subtracted by the level of absorbance at T0.

4.11. Cell Cycle Analysis by FACS

3×10^6 cells were pulsed in medium containing 33 μM BrdU for 45 minutes. Cells were harvested and washed well in PBS. The pellet of cells was resuspended in 750 μL

PBS and fixed by adding 2250 μL pure ethanol dropwise while vortexing and kept on ice for 30 minutes. Cells were then washed in 1 mL PBS + 1% BSA and resuspended in 1 mL denaturating solution (2N HCl) and incubated at room temperature for 25 minutes. To neutralize HCl, 3 mL of 0.1 M Sodium Borate ($Na_2B_4O_7$ pH 8.5) were added and incubated for 2 minutes at room temperature. Cells were washed in 1 mL PBS + 1% BSA twice. Pellet of cells was resuspended in 100 μL pure mouse anti-BrdU (BD Biosciences) (diluted 1 to 5 in PBS + 1% BSA) and incubated for 1 hour at room temperature light protected. Cells were washed in 1 mL PBS + 1% BSA and resuspended in 100 μL FITC-conjugated anti-mouse IgG (1:50 in PBS +1% BSA). Cells were incubated for 1 hour at room temperature, light protected. Cells were washed in 1 mL PBS + 1% BSA and resuspended in 1 mL Propidium Iodide (PI) (2.5 μg/mL) + RNase (250 μg/mL) and incubated at 4 ºC overnight rotating. The proportion of BrdU-incorporating cells was determined with FACSCalibur (BD Biosciences).

4.12. Transformation Assay

4.12.1. Focus Formation Assay

5×10^3 cells were plated in 10 cm cell culture dish. The medium was changed every three days. After two weeks, the medium was removed and cells were washed once with PBS. Colonies were fixed with 4% paraformaldehyde for 10 minutes at room temperature and stained with crystal violet solution (0.1% crystal violet, 20% ethanol) for 5 minutes. Plates were rinsed twice with dH_2O and dried inverted. The visible foci were scored.

4.12.2. Soft-Agar Colony Formation Assay (anchorage independent growth assay)

To prepare soft agar dishes, 5% low melting agarose (Gellyphor Euroclone, Cat.No. EMR911100) in PBS was autoclaved prior to the use. 36 mL of the complete DMEM medium was mixed with 4 mL of 5% low melting agarose. 3 mL of the resulting 0.5% agarose/medium mix was poured in each 6 cm dishes to serve as bottom layer. After solidifying, cells were counted using tryphan blue dye and 3×10^5 viable cells were suspended in 3 mL of complete DMEM medium and added to the 9 mL of 0.4% agarose/medium mix. To perform the experiment in triplicate, 12 mL cell suspension was poured on the top of the three solidified bottom layer agarose plates (4 mL each). Colonies were scored and counted after one week of the incubation.

4.12.3. Allograft Studies in Mice

7 weeks old Hsd:Athymic Nude-*Foxn1nu* (Harlan) females were subcutaneously inoculated with 1×10^6 infected MEFs, suspended in 100 µL of PBS. Primary tumor growth was monitored every 2 to 3 days by caliper. Tumor volume was calculated using the following formula: volume = length × width^2 × 0.526. Mice were euthanized when the tumors were 1.5 cm^3 and allografts were recovered for analysis. 5 mice were used for each experimental group. Mice were maintained in “Specific Pathogen Free” (SPF) units. All experiments were performed according to the guidelines for care and use of laboratory animals approved by the institutional ethical animal care committee (Institutional Animal Care and Use Committee Project 110/11).

4.13. Immunofluorescence and Localization Studies

40000 cells were plated on poly-D-lysine-coated coverslips in 24 well plates. The day after, culturing medium was removed and cells were washed twice with PBS. Cells were fixed with in 4% Paraformaldehyde (in PBS) for 10 minutes at room temperature followed by 2 washes in PBS each for 10 minutes. Cells were permabilized in 0.5 % Triton X-100 (in PBS) for 5 minutes at room temperature. And then washed 3 times in PBS each for 5 minutes. To prevent non-specific binding of the antibodies, cells were blocked in 2% BSA in PBS (Filtered with 0.45 μm filter) for 1 hour at room temperature. Cells were incubated with primary antibody diluted in blocking buffer (anti-Prep1 rabbit polyclonal 1:50 Santa Cruz) over night at 4 °C. Cells were washed 3 times, 5 minutes each and then incubated with Donkey anti-rabbit Cy5-conjugated secondary antibody (Alexa Fluor® 647) for 90 minutes at room temperature (light protected). After 3 washes with PBS 5 minutes each, DAPI staining was performed (1:5000 of 1 mg/mL stock concentration, Sigma) for 5 minutes at room temperature. Coverslips were washed 3 times with PBS and mounted with Mowiol medium. Images were acquired either with a wide field BX61 (Olympus) motorized fluorescence microscope or a confocal laser microscopy (Leica TCS SP2). Images were analyzed with ImageJ software developed by American National Institute of Health (NIH).

4.14. Total RNA Extraction and cDNA Synthesis

RNeasy mini kit (Qiagen) was used to perform all RNA extractions, following the manufacture's instructions. Total RNA was quantified by spectrophotometer (Nanodrop). 1 μg of total RNA of each sample was retro-transcribed using Supercript ™ III First-Strand Synthesis System for RT-PCR Kit (Invitrogen), using random primers. Each reaction mix was composed of:

Component	**Amount**
- Total RNA	1 µg
- 10mM dNTPmix	1 µL
- Random hexamers	50-250 ng/µL
- RNase-free water	Up to 13 µL

RNA/primer mixture was incubated at 65 °C for 5 minutes and then placed on ice for at least 1 minute. In a separate tube the following 2X reaction mix was prepared.

Component	**Amount for 1 reaction**
5X First-Strand buffer	4 µL
0.1 M DTT	2 µL
0.2 M RNaseOUT™ (40U/µL)	1 µL

7 µL of the 2X reaction mix was added to each RNA/primer mixture. 1 µL of Superscript ™ III RT was added to each sample. For minus RT controls 1 µL of RNase-free water was added. The reactions have been performed in 3 steps: 5 minutes at 25 °C, 50 minutes at 50 °C and 15 minutes at 70 °C.

4.15. Semiquantitative PCR

1 µL of cDNA was used as template to perform semiquantitative PCR using primers listed below in a reaction volume of 50 µL composed of:

Component	**Amount**
5X Green GoTaq® Reaction buffer	2.5 µL
10 mM dNTP mix	0.5 µL
10 µM Forward primer	0.6 µL
10 µM Reverse primer	0.6 µL
25 mM $MgCl_2$	1.5 µL

GoTaq® DNA Polymerase (5 U/ µl)	0.125 µL
Template	1 µL
H_2O	Up to 25 µL

PCR was carried out either on EPENDORF mastercycler gradient or GeneAmp PCR system a700 using a pre-PCR step of 2 minutes at 97°C, followed by 28 cycles of 30 sec at 97 °C, 30 sec at X °C, 30 sec at 72 °C and final extension 10 minutes at 72 °C. For Prep1 mutants (Δ proteins) the extension was performed for 1 minute at 72 °C. 10 µL of the PCR product was mixed with 6X loading dye and run on a 1 % agarose gel in TAE running buffer.

Primers sets	**Tm °C**	**Sequences (5′→3′)**
Prep1 Forward Primer	62.5	ATGATGGCTACACAGACATTAAG
Prep1 Reverse Primer		CTACTGCAGGGAGTCACTGTTC
Prep1ΔHR12 Forward Primer	62.5	ATGATGGCTACACAGACATTAAG
Prep1ΔHR12 Reverse Primer		CTACTGCAGGGAGTCACTGTTC
Prep1ΔHD Forward Primer	62.5	ATGATGGCTACACAGACATTAAG
Prep1ΔHD Reverse Primer		CTACTGCAGGGAGTCACTGTTC
Prep1ΔC Forward Primer	62.5	ATGATGGCTACACAGACATTAAG
Prep1ΔC Reverse Primer		TTACATTGGCTGAAGAATTGGTC
Prep1 Forward Primer	60	ACAGACGCTAAGTATAGACAG
Prep1 Reverse Primer		AATCTGCTGGGATTGCACA
Meis1 Forward Primer	65	GTAATGGACGGTCAGCAGCAC
Meis1 Reverse Primer		GTGCACTCATTGTCGGGTCTC
Pbx1a/b Forward Primer	55	CAGAGCCACCAATGTGTC
Pbx1a/b Reverse Primer		TCCGTCACTGTATCCTCC
Pbx2 Forward Primer	62	GCCACAGCCGCACCAGCTCT
Pbx2 Reverse Primer		GGACACCCCACTCTCCCTG
Gapdh Forward Primer	58	GTCTACATGTTCCAGTATGACTCC
Gapdh Reverse Primer		AGTGAGTTGTCATATTTCTCGTGGT

Tables

Table 2.1. The list of co-purified proteins with *Mesi1a*-TAP, analyzed by mass-spectrometry

Prep1^{wt} MEFs	emPAI	Mascot Score	Prep1^{tri} MEFs	emPAI	Mascot Score	Prep1^{tri} MEFs re-expressing Prep	emPAI	Mascot Score
Meis1	0.28	254	Meis1	0.28	221	Meis1	0.13	153
Pbx1	0.37	270	Pbx1	0.46	303	Pbx1	0.37	260
Pbx2	0.28	232	Pbx2	0.23	176	Pbx2	0.28	242
			Ddx3x	4.04	2430			
			Ddx5	2.72	1603			
fibronectin precursor	0.7	3056	fibronectin precursor	0.62	2803	fibronectin precursor	0.66	29500
plectin 1	0.01	110	plectin 1	0.03	241	plectin 1	0.18	1386
p160 myb-binding protein	0.04	149	p160 myb-binding protein	0.04	144	p160 myb-binding protein	0.16	444
			Ras GTPase-activating-like protein	0.04	144	Ras GTPase-activating-like protein	0.29	970
			RNA-binding protein FUS	0.72	532	RNA-binding protein FUS	0.44	377
Cux homeodomain protein	0.05	166						
SNW domain-containing protein	0.17	183	SNW domain-containing protein	0.37	358			
						Cald1 protein	9.8	749
Gamma-actin	1.72	907				Gamma-actin	7.64	1679
			nucleolar RNA helicase II/Gu	0.11	137	nucleolar RNA helicase II/Gu	0.43	642

5. References

1. Alberts Bruce JA, Lewis Julian, Raff Martin, Roberts Keith, Walter Peter (2002) Molecular biology of the cell. New York: Garland science.
2. Hanahan D, Weinberg RA (2000) The hallmarks of cancer. Cell 100: 57-70.
3. Pietras K, Ostman A Hallmarks of cancer: interactions with the tumor stroma. Exp Cell Res 316: 1324-1331.
4. Futreal PA, Kasprzyk A, Birney E, Mullikin JC, Wooster R, et al. (2001) Cancer and genomics. Nature 409: 850-852.
5. Stratton MR, Campbell PJ, Futreal PA (2009) The cancer genome. Nature 458: 719-724.
6. Berdasco M, Esteller M (2010) Aberrant epigenetic landscape in cancer: how cellular identity goes awry. Dev Cell 19: 698-711.
7. Holland-Frei (2003) Cancer medicine: BC Decker.
8. Duesberg PH, Vogt PK (1970) Differences between the ribonucleic acids of transforming and nontransforming avian tumor viruses. Proc Natl Acad Sci U S A 67: 1673-1680.
9. Martin GS (1970) Rous sarcoma virus: a function required for the maintenance of the transformed state. Nature 227: 1021-1023.
10. Croce CM (2008) Oncogenes and cancer. N Engl J Med 358: 502-511.
11. Bishop JM (1991) Molecular themes in oncogenesis. Cell 64: 235-248.
12. Rodenhuis S (1992) ras and human tumors. Semin Cancer Biol 3: 241-247.
13. Keung YK, Cobos E, Morgan D, Whitehead RP, Tonk V (1997) Double minute chromosomes and myelodysplastic syndrome: a case report and literature review. Cancer Genet Cytogenet 97: 94-96.
14. Schwab M (1998) Amplification of oncogenes in human cancer cells. Bioessays 20: 473-479.
15. Siebert R, Matthiesen P, Harder S, Zhang Y, Borowski A, et al. (1998) Application of interphase cytogenetics for the detection of t(11;14)(q13;q32) in mantle cell lymphomas. Ann Oncol 9: 519-526.
16. Aspland SE, Bendall HH, Murre C (2001) The role of E2A-PBX1 in leukemogenesis. Oncogene 20: 5708-5717.
17. Stanbridge EJ (1976) Suppression of malignancy in human cells. Nature 260: 17-20.
18. Knudson AG, Jr. (1971) Mutation and cancer: statistical study of retinoblastoma. Proc Natl Acad Sci U S A 68: 820-823.
19. Longobardi E, Iotti G, Di Rosa P, Mejetta S, Bianchi F, et al. (2010) Prep1 (pKnox1)-deficiency leads to spontaneous tumor development in mice and accelerates EmuMyc lymphomagenesis: a tumor suppressor role for Prep1. Mol Oncol 4: 126-134.
20. Quon KC, Berns A (2001) Haplo-insufficiency? Let me count the ways. Genes Dev 15: 2917-2921.
21. Balmain A, Gray J, Ponder B (2003) The genetics and genomics of cancer. Nat Genet 33 Suppl: 238-244.
22. Fabbro M, Henderson BR (2003) Regulation of tumor suppressors by nuclear-cytoplasmic shuttling. Exp Cell Res 282: 59-69.
23. Sherr CJ (2004) Principles of tumor suppression. Cell 116: 235-246.
24. Macleod K (2000) Tumor suppressor genes. Curr Opin Genet Dev 10: 81-93.
25. Kinzler KW, Vogelstein B (1997) Cancer-susceptibility genes. Gatekeepers and caretakers. Nature 386: 761, 763.

26. Kinzler KW, Vogelstein B (1998) Landscaping the cancer terrain. Science 280: 1036-1037.
27. Hanahan D, Weinberg RA (2011) Hallmarks of cancer: the next generation. Cell 144: 646-674.
28. Cheng N, Chytil A, Shyr Y, Joly A, Moses HL (2008) Transforming growth factor-beta signaling-deficient fibroblasts enhance hepatocyte growth factor signaling in mammary carcinoma cells to promote scattering and invasion. Mol Cancer Res 6: 1521-1533.
29. Slamon DJ, Clark GM, Wong SG, Levin WJ, Ullrich A, et al. (1987) Human breast cancer: correlation of relapse and survival with amplification of the HER-2/neu oncogene. Science 235: 177-182.
30. Medema RH, Bos JL (1993) The role of p21ras in receptor tyrosine kinase signaling. Crit Rev Oncog 4: 615-661.
31. Burkhart DL, Sage J (2008) Cellular mechanisms of tumour suppression by the retinoblastoma gene. Nat Rev Cancer 8: 671-682.
32. Lane DP (1992) Cancer. p53, guardian of the genome. Nature 358: 15-16.
33. Sherr CJ, McCormick F (2002) The RB and p53 pathways in cancer. Cancer Cell 2: 103-112.
34. Adams JM, Cory S (2007) The Bcl-2 apoptotic switch in cancer development and therapy. Oncogene 26: 1324-1337.
35. Wright WE, Pereira-Smith OM, Shay JW (1989) Reversible cellular senescence: implications for immortalization of normal human diploid fibroblasts. Mol Cell Biol 9: 3088-3092.
36. Mitchell PJ, Tjian R (1989) Transcriptional regulation in mammalian cells by sequence-specific DNA binding proteins. Science 245: 371-378.
37. Babu MM, Luscombe NM, Aravind L, Gerstein M, Teichmann SA (2004) Structure and evolution of transcriptional regulatory networks. Curr Opin Struct Biol 14: 283-291.
38. Levine M, Tjian R (2003) Transcription regulation and animal diversity. Nature 424: 147-151.
39. Pabo CO, Sauer RT (1992) Transcription factors: structural families and principles of DNA recognition. Annu Rev Biochem 61: 1053-1095.
40. Darnell JE, Jr. (2002) Transcription factors as targets for cancer therapy. Nat Rev Cancer 2: 740-749.
41. Kroon E, Krosl J, Thorsteinsdottir U, Baban S, Buchberg AM, et al. (1998) Hoxa9 transforms primary bone marrow cells through specific collaboration with Meis1a but not Pbx1b. EMBO J 17: 3714-3725.
42. Mamo A, Krosl J, Kroon E, Bijl J, Thompson A, et al. (2006) Molecular dissection of Meis1 reveals 2 domains required for leukemia induction and a key role for Hoxa gene activation. Blood 108: 622-629.
43. Thorsteinsdottir U, Kroon E, Jerome L, Blasi F, Sauvageau G (2001) Defining roles for HOX and MEIS1 genes in induction of acute myeloid leukemia. Mol Cell Biol 21: 224-234.
44. McGinnis W, Garber RL, Wirz J, Kuroiwa A, Gehring WJ (1984) A homologous protein-coding sequence in Drosophila homeotic genes and its conservation in other metazoans. Cell 37: 403-408.
45. Scott MP, Weiner AJ (1984) Structural relationships among genes that control development: sequence homology between the Antennapedia, Ultrabithorax, and fushi tarazu loci of Drosophila. Proc Natl Acad Sci U S A 81: 4115-4119.

46. Gehring WJ, Affolter M, Burglin T (1994) Homeodomain proteins. Annu Rev Biochem 63: 487-526.
47. Gehring WJ, Qian YQ, Billeter M, Furukubo-Tokunaga K, Schier AF, et al. (1994) Homeodomain-DNA recognition. Cell 78: 211-223.
48. Pearson JC, Lemons D, McGinnis W (2005) Modulating Hox gene functions during animal body patterning. Nat Rev Genet 6: 893-904.
49. Abate-Shen C (2002) Deregulated homeobox gene expression in cancer: cause or consequence? Nat Rev Cancer 2: 777-785.
50. Holland PW, Booth HA, Bruford EA (2007) Classification and nomenclature of all human homeobox genes. BMC Biol 5: 47.
51. Moens CB, Selleri L (2006) Hox cofactors in vertebrate development. Dev Biol 291: 193-206.
52. Shah N, Sukumar S (2010) The Hox genes and their roles in oncogenesis. Nat Rev Cancer 10: 361-371.
53. Grier DG, Thompson A, Kwasniewska A, McGonigle GJ, Halliday HL, et al. (2005) The pathophysiology of HOX genes and their role in cancer. J Pathol 205: 154-171.
54. Takahashi O, Hamada J, Abe M, Hata S, Asano T, et al. (2007) Dysregulated expression of HOX and ParaHOX genes in human esophageal squamous cell carcinoma. Oncol Rep 17: 753-760.
55. Golub TR, Slonim DK, Tamayo P, Huard C, Gaasenbeek M, et al. (1999) Molecular classification of cancer: class discovery and class prediction by gene expression monitoring. Science 286: 531-537.
56. Ghannam G, Takeda A, Camarata T, Moore MA, Viale A, et al. (2004) The oncogene Nup98-HOXA9 induces gene transcription in myeloid cells. J Biol Chem 279: 866-875.
57. Calvo KR, Sykes DB, Pasillas MP, Kamps MP (2002) Nup98-HoxA9 immortalizes myeloid progenitors, enforces expression of Hoxa9, Hoxa7 and Meis1, and alters cytokine-specific responses in a manner similar to that induced by retroviral co-expression of Hoxa9 and Meis1. Oncogene 21: 4247-4256.
58. Nakamura T, Yamazaki Y, Hatano Y, Miura I (1999) NUP98 is fused to PMX1 homeobox gene in human acute myelogenous leukemia with chromosome translocation t(1;11)(q23;p15). Blood 94: 741-747.
59. Waltregny D, Alami Y, Clausse N, de Leval J, Castronovo V (2002) Overexpression of the homeobox gene HOXC8 in human prostate cancer correlates with loss of tumor differentiation. Prostate 50: 162-169.
60. Kikugawa T, Kinugasa Y, Shiraishi K, Nanba D, Nakashiro K, et al. (2006) PLZF regulates Pbx1 transcription and Pbx1-HoxC8 complex leads to androgen-independent prostate cancer proliferation. Prostate 66: 1092-1099.
61. Raman V, Martensen SA, Reisman D, Evron E, Odenwald WF, et al. (2000) Compromised HOXA5 function can limit p53 expression in human breast tumours. Nature 405: 974-978.
62. Chu MC, Selam FB, Taylor HS (2004) HOXA10 regulates p53 expression and matrigel invasion in human breast cancer cells. Cancer Biol Ther 3: 568-572.
63. Miao J, Wang Z, Provencher H, Muir B, Dahiya S, et al. (2007) HOXB13 promotes ovarian cancer progression. Proc Natl Acad Sci U S A 104: 17093-17098.
64. Mukherjee K, Burglin TR (2007) Comprehensive analysis of animal TALE homeobox genes: new conserved motifs and cases of accelerated evolution. J Mol Evol 65: 137-153.

65. Burglin TR (1997) Analysis of TALE superclass homeobox genes (MEIS, PBC, KNOX, Iroquois, TGIF) reveals a novel domain conserved between plants and animals. Nucleic Acids Res 25: 4173-4180.
66. Burglin TR (1998) The PBC domain contains a MEINOX domain: coevolution of Hox and TALE homeobox genes? Dev Genes Evol 208: 113-116.
67. Berthelsen J, Zappavigna V, Mavilio F, Blasi F (1998) Prep1, a novel functional partner of Pbx proteins. EMBO J 17: 1423-1433.
68. Stevens KE, Mann RS (2007) A balance between two nuclear localization sequences and a nuclear export sequence governs extradenticle subcellular localization. Genetics 175: 1625-1636.
69. Laurent A, Bihan R, Omilli F, Deschamps S, Pellerin I (2008) PBX proteins: much more than Hox cofactors. Int J Dev Biol 52: 9-20.
70. Chang CP, Jacobs Y, Nakamura T, Jenkins NA, Copeland NG, et al. (1997) Meis proteins are major in vivo DNA binding partners for wild-type but not chimeric Pbx proteins. Mol Cell Biol 17: 5679-5687.
71. Knoepfler PS, Calvo KR, Chen H, Antonarakis SE, Kamps MP (1997) Meis1 and pKnox1 bind DNA cooperatively with Pbx1 utilizing an interaction surface disrupted in oncoprotein E2a-Pbx1. Proc Natl Acad Sci U S A 94: 14553-14558.
72. Diaz VM, Mori S, Longobardi E, Menendez G, Ferrai C, et al. (2007) p160 Myb-binding protein interacts with Prep1 and inhibits its transcriptional activity. Mol Cell Biol 27: 7981-7990.
73. Berthelsen J, Zappavigna V, Ferretti E, Mavilio F, Blasi F (1998) The novel homeoprotein Prep1 modulates Pbx-Hox protein cooperativity. EMBO J 17: 1434-1445.
74. Jaw TJ, You LR, Knoepfler PS, Yao LC, Pai CY, et al. (2000) Direct interaction of two homeoproteins, homothorax and extradenticle, is essential for EXD nuclear localization and function. Mech Dev 91: 279-291.
75. Berthelsen J, Kilstrup-Nielsen C, Blasi F, Mavilio F, Zappavigna V (1999) The subcellular localization of PBX1 and EXD proteins depends on nuclear import and export signals and is modulated by association with PREP1 and HTH. Genes Dev 13: 946-953.
76. Longobardi E, Blasi F (2003) Overexpression of PREP-1 in F9 teratocarcinoma cells leads to a functionally relevant increase of PBX-2 by preventing its degradation. J Biol Chem 278: 39235-39241.
77. Saleh M, Huang H, Green NC, Featherstone MS (2000) A conformational change in PBX1A is necessary for its nuclear localization. Exp Cell Res 260: 105-115.
78. Kilstrup-Nielsen C, Alessio M, Zappavigna V (2003) PBX1 nuclear export is regulated independently of PBX-MEINOX interaction by PKA phosphorylation of the PBC-B domain. EMBO J 22: 89-99.
79. Kamps MP, Look AT, Baltimore D (1991) The human t(1;19) translocation in pre-B ALL produces multiple nuclear E2A-Pbx1 fusion proteins with differing transforming potentials. Genes Dev 5: 358-368.
80. Nourse J, Mellentin JD, Galili N, Wilkinson J, Stanbridge E, et al. (1990) Chromosomal translocation t(1;19) results in synthesis of a homeobox fusion mRNA that codes for a potential chimeric transcription factor. Cell 60: 535-545.
81. Monica K, Galili N, Nourse J, Saltman D, Cleary ML (1991) PBX2 and PBX3, new homeobox genes with extensive homology to the human proto-oncogene PBX1. Mol Cell Biol 11: 6149-6157.

82. Wagner K, Mincheva A, Korn B, Lichter P, Popperl H (2001) Pbx4, a new Pbx family member on mouse chromosome 8, is expressed during spermatogenesis. Mech Dev 103: 127-131.
83. Popperl H, Rikhof H, Chang H, Haffter P, Kimmel CB, et al. (2000) lazarus is a novel pbx gene that globally mediates hox gene function in zebrafish. Mol Cell 6: 255-267.
84. Chang CP, Shen WF, Rozenfeld S, Lawrence HJ, Largman C, et al. (1995) Pbx proteins display hexapeptide-dependent cooperative DNA binding with a subset of Hox proteins. Genes Dev 9: 663-674.
85. Magnani L, Ballantyne EB, Zhang X, Lupien M (2011) PBX1 genomic pioneer function drives ERalpha signaling underlying progression in breast cancer. PLoS Genet 7: e1002368.
86. Selleri L, Depew MJ, Jacobs Y, Chanda SK, Tsang KY, et al. (2001) Requirement for Pbx1 in skeletal patterning and programming chondrocyte proliferation and differentiation. Development 128: 3543-3557.
87. Kim SK, Selleri L, Lee JS, Zhang AY, Gu X, et al. (2002) Pbx1 inactivation disrupts pancreas development and in Ipf1-deficient mice promotes diabetes mellitus. Nat Genet 30: 430-435.
88. Chang CP, Brocchieri L, Shen WF, Largman C, Cleary ML (1996) Pbx modulation of Hox homeodomain amino-terminal arms establishes different DNA-binding specificities across the Hox locus. Mol Cell Biol 16: 1734-1745.
89. Piper DE, Batchelor AH, Chang CP, Cleary ML, Wolberger C (1999) Structure of a HoxB1-Pbx1 heterodimer bound to DNA: role of the hexapeptide and a fourth homeodomain helix in complex formation. Cell 96: 587-597.
90. Ferretti E, Marshall H, Popperl H, Maconochie M, Krumlauf R, et al. (2000) Segmental expression of Hoxb2 in r4 requires two separate sites that integrate cooperative interactions between Prep1, Pbx and Hox proteins. Development 127: 155-166.
91. Samad OA, Geisen MJ, Caronia G, Varlet I, Zappavigna V, et al. (2004) Integration of anteroposterior and dorsoventral regulation of Phox2b transcription in cranial motoneuron progenitors by homeodomain proteins. Development 131: 4071-4083.
92. DiMartino JF, Selleri L, Traver D, Firpo MT, Rhee J, et al. (2001) The Hox cofactor and proto-oncogene Pbx1 is required for maintenance of definitive hematopoiesis in the fetal liver. Blood 98: 618-626.
93. Lawrence HJ, Helgason CD, Sauvageau G, Fong S, Izon DJ, et al. (1997) Mice bearing a targeted interruption of the homeobox gene HOXA9 have defects in myeloid, erythroid, and lymphoid hematopoiesis. Blood 89: 1922-1930.
94. Condie BG, Capecchi MR (1994) Mice with targeted disruptions in the paralogous genes hoxa-3 and hoxd-3 reveal synergistic interactions. Nature 370: 304-307.
95. Rhee JW, Arata A, Selleri L, Jacobs Y, Arata S, et al. (2004) Pbx3 deficiency results in central hypoventilation. Am J Pathol 165: 1343-1350.
96. Selleri L, DiMartino J, van Deursen J, Brendolan A, Sanyal M, et al. (2004) The TALE homeodomain protein Pbx2 is not essential for development and long-term survival. Mol Cell Biol 24: 5324-5331.
97. Cooper KL, Leisenring WM, Moens CB (2003) Autonomous and nonautonomous functions for Hox/Pbx in branchiomotor neuron development. Dev Biol 253: 200-213.
98. Berkes CA, Bergstrom DA, Penn BH, Seaver KJ, Knoepfler PS, et al. (2004) Pbx marks genes for activation by MyoD indicating a role for a homeodomain protein in establishing myogenic potential. Mol Cell 14: 465-477.

99. Bailey JS, Rave-Harel N, McGillivray SM, Coss D, Mellon PL (2004) Activin regulation of the follicle-stimulating hormone beta-subunit gene involves Smads and the TALE homeodomain proteins Pbx1 and Prep1. Mol Endocrinol 18: 1158-1170.
100. Park JT, Shih Ie M, Wang TL (2008) Identification of Pbx1, a potential oncogene, as a Notch3 target gene in ovarian cancer. Cancer Res 68: 8852-8860.
101. Carroll AJ, Crist WM, Parmley RT, Roper M, Cooper MD, et al. (1984) Pre-B cell leukemia associated with chromosome translocation 1;19. Blood 63: 721-724.
102. Bain G, Maandag EC, Izon DJ, Amsen D, Kruisbeek AM, et al. (1994) E2A proteins are required for proper B cell development and initiation of immunoglobulin gene rearrangements. Cell 79: 885-892.
103. Goldfarb AN, Flores JP, Lewandowska K (1996) Involvement of the E2A basic helix-loop-helix protein in immunoglobulin heavy chain class switching. Mol Immunol 33: 947-956.
104. Rivera RR, Johns CP, Quan J, Johnson RS, Murre C (2000) Thymocyte selection is regulated by the helix-loop-helix inhibitor protein, Id3. Immunity 12: 17-26.
105. Monica K, LeBrun DP, Dedera DA, Brown R, Cleary ML (1994) Transformation properties of the E2a-Pbx1 chimeric oncoprotein: fusion with E2a is essential, but the Pbx1 homeodomain is dispensable. Mol Cell Biol 14: 8304-8314.
106. Thorsteinsdottir U, Krosl J, Kroon E, Haman A, Hoang T, et al. (1999) The oncoprotein E2A-Pbx1a collaborates with Hoxa9 to acutely transform primary bone marrow cells. Mol Cell Biol 19: 6355-6366.
107. LeBrun DP, Matthews BP, Feldman BJ, Cleary ML (1997) The chimeric oncoproteins E2A-PBX1 and E2A-HLF are concentrated within spherical nuclear domains. Oncogene 15: 2059-2067.
108. Feldman BJ, Hampton T, Cleary ML (2000) A carboxy-terminal deletion mutant of Notch1 accelerates lymphoid oncogenesis in E2A-PBX1 transgenic mice. Blood 96: 1906-1913.
109. Yeh HY, Cheng SW, Lin YC, Yeh CY, Lin SF, et al. (2009) Identifying significant genetic regulatory networks in the prostate cancer from microarray data based on transcription factor analysis and conditional independency. BMC Med Genomics 2: 70.
110. Morgan R, Plowright L, Harrington KJ, Michael A, Pandha HS (2010) Targeting HOX and PBX transcription factors in ovarian cancer. BMC Cancer 10: 89.
111. Thiaville MM, Stoeck A, Chen L, Wu RC, Magnani L, et al. (2012) Identification of PBX1 target genes in cancer cells by global mapping of PBX1 binding sites. PLoS One 7: e36054.
112. Qiu Y, Wang ZL, Jin SQ, Pu YF, Toyosawa S, et al. (2012) Expression level of pre-B-cell leukemia transcription factor 2 (PBX2) as a prognostic marker for gingival squamous cell carcinoma. J Zhejiang Univ Sci B 13: 168-175.
113. Ramberg H, Alshbib A, Berge V, Svindland A, Tasken KA (2011) Regulation of PBX3 expression by androgen and Let-7d in prostate cancer. Mol Cancer 10: 50.
114. Moskow JJ, Bullrich F, Huebner K, Daar IO, Buchberg AM (1995) Meis1, a PBX1-related homeobox gene involved in myeloid leukemia in BXH-2 mice. Mol Cell Biol 15: 5434-5443.
115. Nakamura T, Largaespada DA, Shaughnessy JD, Jr., Jenkins NA, Copeland NG (1996) Cooperative activation of Hoxa and Pbx1-related genes in murine myeloid leukaemias. Nat Genet 12: 149-153.
116. Nakamura T, Jenkins NA, Copeland NG (1996) Identification of a new family of Pbx-related homeobox genes. Oncogene 13: 2235-2242.

117. Fognani C, Kilstrup-Nielsen C, Berthelsen J, Ferretti E, Zappavigna V, et al. (2002) Characterization of PREP2, a paralog of PREP1, which defines a novel sub-family of the MEINOX TALE homeodomain transcription factors. Nucleic Acids Res 30: 2043-2051.
118. Haller K, Rambaldi I, Kovacs EN, Daniels E, Featherstone M (2002) Prep2: cloning and expression of a new prep family member. Dev Dyn 225: 358-364.
119. Hisa T, Spence SE, Rachel RA, Fujita M, Nakamura T, et al. (2004) Hematopoietic, angiogenic and eye defects in Meis1 mutant animals. EMBO J 23: 450-459.
120. Jacobs Y, Schnabel CA, Cleary ML (1999) Trimeric association of Hox and TALE homeodomain proteins mediates Hoxb2 hindbrain enhancer activity. Mol Cell Biol 19: 5134-5142.
121. Ferretti E, Cambronero F, Tumpel S, Longobardi E, Wiedemann LM, et al. (2005) Hoxb1 enhancer and control of rhombomere 4 expression: complex interplay between PREP1-PBX1-HOXB1 binding sites. Mol Cell Biol 25: 8541-8552.
122. Cecconi F, Proetzel G, Alvarez-Bolado G, Jay D, Gruss P (1997) Expression of Meis2, a Knotted-related murine homeobox gene, indicates a role in the differentiation of the forebrain and the somitic mesoderm. Dev Dyn 210: 184-190.
123. Azcoitia V, Aracil M, Martinez AC, Torres M (2005) The homeodomain protein Meis1 is essential for definitive hematopoiesis and vascular patterning in the mouse embryo. Dev Biol 280: 307-320.
124. Capdevila J, Tsukui T, Rodriquez Esteban C, Zappavigna V, Izpisua Belmonte JC (1999) Control of vertebrate limb outgrowth by the proximal factor Meis2 and distal antagonism of BMPs by Gremlin. Mol Cell 4: 839-849.
125. Mercader N, Tanaka EM, Torres M (2005) Proximodistal identity during vertebrate limb regeneration is regulated by Meis homeodomain proteins. Development 132: 4131-4142.
126. Toresson H, Parmar M, Campbell K (2000) Expression of Meis and Pbx genes and their protein products in the developing telencephalon: implications for regional differentiation. Mech Dev 94: 183-187.
127. Zhang X, Friedman A, Heaney S, Purcell P, Maas RL (2002) Meis homeoproteins directly regulate Pax6 during vertebrate lens morphogenesis. Genes Dev 16: 2097-2107.
128. Choe SK, Vlachakis N, Sagerstrom CG (2002) Meis family proteins are required for hindbrain development in the zebrafish. Development 129: 585-595.
129. Dibner C, Elias S, Frank D (2001) XMeis3 protein activity is required for proper hindbrain patterning in Xenopus laevis embryos. Development 128: 3415-3426.
130. Crijns AP, de Graeff P, Geerts D, Ten Hoor KA, Hollema H, et al. (2007) MEIS and PBX homeobox proteins in ovarian cancer. Eur J Cancer 43: 2495-2505.
131. WWW.proteinatlas.org.
132. Wermuth PJ, Buchberg AM (2005) Meis1-mediated apoptosis is caspase dependent and can be suppressed by coexpression of HoxA9 in murine and human cell lines. Blood 105: 1222-1230.
133. Kawagoe H, Humphries RK, Blair A, Sutherland HJ, Hogge DE (1999) Expression of HOX genes, HOX cofactors, and MLL in phenotypically and functionally defined subpopulations of leukemic and normal human hematopoietic cells. Leukemia 13: 687-698.
134. Serrano E, Lasa A, Perea G, Carnicer MJ, Brunet S, et al. (2006) Acute myeloid leukemia subgroups identified by pathway-restricted gene expression signatures. Acta Haematol 116: 77-89.

135. Argiropoulos B, Yung E, Xiang P, Lo CY, Kuchenbauer F, et al. (2010) Linkage of the potent leukemogenic activity of Meis1 to cell-cycle entry and transcriptional regulation of cyclin D3. Blood 115: 4071-4082.
136. Wang GG, Pasillas MP, Kamps MP (2005) Meis1 programs transcription of FLT3 and cancer stem cell character, using a mechanism that requires interaction with Pbx and a novel function of the Meis1 C-terminus. Blood 106: 254-264.
137. Bisaillon R, Wilhelm BT, Krosl J, Sauvageau G (2011) C-terminal domain of MEIS1 converts PKNOX1 (PREP1) into a HOXA9-collaborating oncoprotein. Blood 118: 4682-4689.
138. Wang GG, Pasillas MP, Kamps MP (2006) Persistent transactivation by meis1 replaces hox function in myeloid leukemogenesis models: evidence for co-occupancy of meis1-pbx and hox-pbx complexes on promoters of leukemia-associated genes. Mol Cell Biol 26: 3902-3916.
139. Calvo KR, Knoepfler PS, Sykes DB, Pasillas MP, Kamps MP (2001) Meis1a suppresses differentiation by G-CSF and promotes proliferation by SCF: potential mechanisms of cooperativity with Hoxa9 in myeloid leukemia. Proc Natl Acad Sci U S A 98: 13120-13125.
140. Sitwala KV, Dandekar MN, Hess JL (2008) HOX proteins and leukemia. Int J Clin Exp Pathol 1: 461-474.
141. Mackarehtschian K, Hardin JD, Moore KA, Boast S, Goff SP, et al. (1995) Targeted disruption of the flk2/flt3 gene leads to deficiencies in primitive hematopoietic progenitors. Immunity 3: 147-161.
142. Morgado E, Albouhair S, Lavau C (2007) Flt3 is dispensable to the Hoxa9/Meis1 leukemogenic cooperation. Blood 109: 4020-4022.
143. Jin G, Yamazaki Y, Takuwa M, Takahara T, Kaneko K, et al. (2007) Trib1 and Evi1 cooperate with Hoxa and Meis1 in myeloid leukemogenesis. Blood 109: 3998-4005.
144. Hess JL, Bittner CB, Zeisig DT, Bach C, Fuchs U, et al. (2006) c-Myb is an essential downstream target for homeobox-mediated transformation of hematopoietic cells. Blood 108: 297-304.
145. Dasse E, Volpe G, Walton DS, Wilson N, Del Pozzo W, et al. (2012) Distinct regulation of c-myb gene expression by HoxA9, Meis1 and Pbx proteins in normal hematopoietic progenitors and transformed myeloid cells. Blood Cancer J 2: e76.
146. Imamura T, Morimoto A, Takanashi M, Hibi S, Sugimoto T, et al. (2002) Frequent co-expression of HoxA9 and Meis1 genes in infant acute lymphoblastic leukaemia with MLL rearrangement. Br J Haematol 119: 119-121.
147. Zeisig BB, Milne T, Garcia-Cuellar MP, Schreiner S, Martin ME, et al. (2004) Hoxa9 and Meis1 are key targets for MLL-ENL-mediated cellular immortalization. Mol Cell Biol 24: 617-628.
148. Ayton PM, Cleary ML (2003) Transformation of myeloid progenitors by MLL oncoproteins is dependent on Hoxa7 and Hoxa9. Genes Dev 17: 2298-2307.
149. Wong P, Iwasaki M, Somervaille TC, So CW, Cleary ML (2007) Meis1 is an essential and rate-limiting regulator of MLL leukemia stem cell potential. Genes Dev 21: 2762-2774.
150. Nguyen AT, Taranova O, He J, Zhang Y (2011) DOT1L, the H3K79 methyltransferase, is required for MLL-AF9-mediated leukemogenesis. Blood 117: 6912-6922.
151. Kumar AR, Li Q, Hudson WA, Chen W, Sam T, et al. (2009) A role for MEIS1 in MLL-fusion gene leukemia. Blood 113: 1756-1758.

152. Orlovsky K, Kalinkovich A, Rozovskaia T, Shezen E, Itkin T, et al. (2011) Down-regulation of homeobox genes MEIS1 and HOXA in MLL-rearranged acute leukemia impairs engraftment and reduces proliferation. Proc Natl Acad Sci U S A 108: 7956-7961.
153. Wang Z, Iwasaki M, Ficara F, Lin C, Matheny C, et al. (2010) GSK-3 promotes conditional association of CREB and its coactivators with MEIS1 to facilitate HOX-mediated transcription and oncogenesis. Cancer Cell 17: 597-608.
154. Cho EC, Mitton B, Sakamoto KM (2011) CREB and leukemogenesis. Crit Rev Oncog 16: 37-46.
155. Esparza SD, Chang J, Shankar DB, Zhang B, Nelson SF, et al. (2008) CREB regulates Meis1 expression in normal and malignant hematopoietic cells. Leukemia 22: 665-667.
156. Liu J, Wang Y, Birnbaum MJ, Stoffers DA (2010) Three-amino-acid-loop-extension homeodomain factor Meis3 regulates cell survival via PDK1. Proc Natl Acad Sci U S A 107: 20494-20499.
157. Spieker N, van Sluis P, Beitsma M, Boon K, van Schaik BD, et al. (2001) The MEIS1 oncogene is highly expressed in neuroblastoma and amplified in cell line IMR32. Genomics 71: 214-221.
158. Geerts D, Schilderink N, Jorritsma G, Versteeg R (2003) The role of the MEIS homeobox genes in neuroblastoma. Cancer Lett 197: 87-92.
159. Baird K, Davis S, Antonescu CR, Harper UL, Walker RL, et al. (2005) Gene expression profiling of human sarcomas: insights into sarcoma biology. Cancer Res 65: 9226-9235.
160. Tommasi S, Karm DL, Wu X, Yen Y, Pfeifer GP (2009) Methylation of homeobox genes is a frequent and early epigenetic event in breast cancer. Breast Cancer Res 11: R14.
161. Pfeifer GP, Rauch TA (2009) DNA methylation patterns in lung carcinomas. Semin Cancer Biol 19: 181-187.
162. Sabates-Bellver J, Van der Flier LG, de Palo M, Cattaneo E, Maake C, et al. (2007) Transcriptome profile of human colorectal adenomas. Mol Cancer Res 5: 1263-1275.
163. Rohrbeck A, Muller VS, Borlak J (2009) Molecular characterization of lung dysplasia induced by c-Raf-1. PLoS One 4: e5637.
164. Chen H, Rossier C, Nakamura Y, Lynn A, Chakravarti A, et al. (1997) Cloning of a novel homeobox-containing gene, PKNOX1, and mapping to human chromosome 21q22.3. Genomics 41: 193-200.
165. Berthelsen J, Vandekerkhove J, Blasi F (1996) Purification and characterization of UEF3, a novel factor involved in the regulation of the urokinase and other AP-1 controlled promoters. J Biol Chem 271: 3822-3830.
166. De Cesare D, Palazzolo M, Blasi F (1996) Functional characterization of COM, a DNA region required for cooperation between AP-1 sites in urokinase gene transcription. Oncogene 13: 2551-2562.
167. Ferretti E, Schulz H, Talarico D, Blasi F, Berthelsen J (1999) The PBX-regulating protein PREP1 is present in different PBX-complexed forms in mouse. Mech Dev 83: 53-64.
168. Fernandez-Diaz LC, Laurent A, Girasoli S, Turco M, Longobardi E, et al. (2010) The absence of Prep1 causes p53-dependent apoptosis of mouse pluripotent epiblast cells. Development 137: 3393-3403.

169. Deflorian G, Tiso N, Ferretti E, Meyer D, Blasi F, et al. (2004) Prep1.1 has essential genetic functions in hindbrain development and cranial neural crest cell differentiation. Development 131: 613-627.
170. Zambrowicz BP, Abuin A, Ramirez-Solis R, Richter LJ, Piggott J, et al. (2003) Wnk1 kinase deficiency lowers blood pressure in mice: a gene-trap screen to identify potential targets for therapeutic intervention. Proc Natl Acad Sci U S A 100: 14109-14114.
171. Ferretti E, Villaescusa JC, Di Rosa P, Fernandez-Diaz LC, Longobardi E, et al. (2006) Hypomorphic mutation of the TALE gene Prep1 (pKnox1) causes a major reduction of Pbx and Meis proteins and a pleiotropic embryonic phenotype. Mol Cell Biol 26: 5650-5662.
172. Di Rosa P, Villaescusa JC, Longobardi E, Iotti G, Ferretti E, et al. (2007) The homeodomain transcription factor Prep1 (pKnox1) is required for hematopoietic stem and progenitor cell activity. Dev Biol 311: 324-334.
173. Penkov D, Di Rosa P, Fernandez Diaz L, Basso V, Ferretti E, et al. (2005) Involvement of Prep1 in the alphabeta T-cell receptor T-lymphocytic potential of hematopoietic precursors. Mol Cell Biol 25: 10768-10781.
174. Smith KS, Jacobs Y, Chang CP, Cleary ML (1997) Chimeric oncoprotein E2a-Pbx1 induces apoptosis of hematopoietic cells by a p53-independent mechanism that is suppressed by Bcl-2. Oncogene 14: 2917-2926.
175. Micali N, Ferrai C, Fernandez-Diaz LC, Blasi F, Crippa MP (2009) Prep1 directly regulates the intrinsic apoptotic pathway by controlling Bcl-XL levels. Mol Cell Biol 29: 1143-1151.
176. Micali N, Longobardi E, Iotti G, Ferrai C, Castagnaro L, et al. (2010) Down syndrome fibroblasts and mouse Prep1-overexpressing cells display increased sensitivity to genotoxic stress. Nucleic Acids Res 38: 3595-3604.
177. Ohgaki K, Iida A, Kasumi F, Sakamoto G, Akimoto M, et al. (1998) Mapping of a new target region of allelic loss to a 6-cM interval at 21q21 in primary breast cancers. Genes Chromosomes Cancer 23: 244-247.
178. Park WS, Oh RR, Park JY, Yoo NJ, Lee SH, et al. (2000) Mapping of a new target region of allelic loss at 21q22 in primary gastric cancers. Cancer Lett 159: 15-21.
179. Iotti G, Longobardi E, Masella S, Dardaei L, De Santis F, et al. (2011) Homeodomain transcription factor and tumor suppressor Prep1 is required to maintain genomic stability. Proc Natl Acad Sci U S A 108: E314-322.
180. Umate P, Tuteja N, Tuteja R (2011) Genome-wide comprehensive analysis of human helicases. Commun Integr Biol 4: 118-137.
181. Parsyan A, Svitkin Y, Shahbazian D, Gkogkas C, Lasko P, et al. (2011) mRNA helicases: the tacticians of translational control. Nat Rev Mol Cell Biol 12: 235-245.
182. Cordin O, Banroques J, Tanner NK, Linder P (2006) The DEAD-box protein family of RNA helicases. Gene 367: 17-37.
183. You LR, Chen CM, Yeh TS, Tsai TY, Mai RT, et al. (1999) Hepatitis C virus core protein interacts with cellular putative RNA helicase. J Virol 73: 2841-2853.
184. Kim YS, Lee SG, Park SH, Song K (2001) Gene structure of the human DDX3 and chromosome mapping of its related sequences. Mol Cells 12: 209-214.
185. Lardone MC, Parodi DA, Valdevenito R, Ebensperger M, Piottante A, et al. (2007) Quantification of DDX3Y, RBMY1, DAZ and TSPY mRNAs in testes of patients with severe impairment of spermatogenesis. Mol Hum Reprod 13: 705-712.

186. Yedavalli VS, Neuveut C, Chi YH, Kleiman L, Jeang KT (2004) Requirement of DDX3 DEAD box RNA helicase for HIV-1 Rev-RRE export function. Cell 119: 381-392.
187. Sun C, Pager CT, Luo G, Sarnow P, Cate JH (2011) Hepatitis C virus core-derived peptides inhibit genotype 1b viral genome replication via interaction with DDX3X. PLoS One 5.
188. Ariumi Y, Kuroki M, Abe K, Dansako H, Ikeda M, et al. (2007) DDX3 DEAD-box RNA helicase is required for hepatitis C virus RNA replication. J Virol 81: 13922-13926.
189. Huang JS, Chao CC, Su TL, Yeh SH, Chen DS, et al. (2004) Diverse cellular transformation capability of overexpressed genes in human hepatocellular carcinoma. Biochem Biophys Res Commun 315: 950-958.
190. Chang PC, Chi CW, Chau GY, Li FY, Tsai YH, et al. (2006) DDX3, a DEAD box RNA helicase, is deregulated in hepatitis virus-associated hepatocellular carcinoma and is involved in cell growth control. Oncogene 25: 1991-2003.
191. Botlagunta M, Vesuna F, Mironchik Y, Raman A, Lisok A, et al. (2008) Oncogenic role of DDX3 in breast cancer biogenesis. Oncogene 27: 3912-3922.
192. Sun M, Song L, Zhou T, Gillespie GY, Jope RS (2011) The role of DDX3 in regulating Snail. Biochim Biophys Acta 1813: 438-447.
193. Sun M, Song L, Li Y, Zhou T, Jope RS (2008) Identification of an antiapoptotic protein complex at death receptors. Cell Death Differ 15: 1887-1900.
194. Lai MC, Chang WC, Shieh SY, Tarn WY (2010) DDX3 regulates cell growth through translational control of cyclin E1. Mol Cell Biol 30: 5444-5453.
195. Botlagunta M, Krishnamachary B, Vesuna F, Winnard PT, Jr., Bol GM, et al. (2010) Expression of DDX3 is directly modulated by hypoxia inducible factor-1 alpha in breast epithelial cells. PLoS One 6: e17563.
196. Janknecht R (2010) Multi-talented DEAD-box proteins and potential tumor promoters: p68 RNA helicase (DDX5) and its paralog, p72 RNA helicase (DDX17). Am J Transl Res 2: 223-234.
197. Fukuda T, Yamagata K, Fujiyama S, Matsumoto T, Koshida I, et al. (2007) DEAD-box RNA helicase subunits of the Drosha complex are required for processing of rRNA and a subset of microRNAs. Nat Cell Biol 9: 604-611.
198. Guil S, Gattoni R, Carrascal M, Abian J, Stevenin J, et al. (2003) Roles of hnRNP A1, SR proteins, and p68 helicase in c-H-ras alternative splicing regulation. Mol Cell Biol 23: 2927-2941.
199. Lin C, Yang L, Yang JJ, Huang Y, Liu ZR (2005) ATPase/helicase activities of p68 RNA helicase are required for pre-mRNA splicing but not for assembly of the spliceosome. Mol Cell Biol 25: 7484-7493.
200. Rossler OG, Straka A, Stahl H (2001) Rearrangement of structured RNA via branch migration structures catalysed by the highly related DEAD-box proteins p68 and p72. Nucleic Acids Res 29: 2088-2096.
201. Bond AT, Mangus DA, He F, Jacobson A (2001) Absence of Dbp2p alters both nonsense-mediated mRNA decay and rRNA processing. Mol Cell Biol 21: 7366-7379.
202. Ishizuka A, Siomi MC, Siomi H (2002) A Drosophila fragile X protein interacts with components of RNAi and ribosomal proteins. Genes Dev 16: 2497-2508.
203. Fuller-Pace FV (2006) DExD/H box RNA helicases: multifunctional proteins with important roles in transcriptional regulation. Nucleic Acids Res 34: 4206-4215.

204. Caretti G, Schiltz RL, Dilworth FJ, Di Padova M, Zhao P, et al. (2006) The RNA helicases p68/p72 and the noncoding RNA SRA are coregulators of MyoD and skeletal muscle differentiation. Dev Cell 11: 547-560.
205. Bates GJ, Nicol SM, Wilson BJ, Jacobs AM, Bourdon JC, et al. (2005) The DEAD box protein p68: a novel transcriptional coactivator of the p53 tumour suppressor. EMBO J 24: 543-553.
206. Clark EL, Coulson A, Dalgliesh C, Rajan P, Nicol SM, et al. (2008) The RNA helicase p68 is a novel androgen receptor coactivator involved in splicing and is overexpressed in prostate cancer. Cancer Res 68: 7938-7946.
207. Shin S, Rossow KL, Grande JP, Janknecht R (2007) Involvement of RNA helicases p68 and p72 in colon cancer. Cancer Res 67: 7572-7578.
208. Jensen ED, Niu L, Caretti G, Nicol SM, Teplyuk N, et al. (2008) p68 (Ddx5) interacts with Runx2 and regulates osteoblast differentiation. J Cell Biochem 103: 1438-1451.
209. Rossow KL, Janknecht R (2003) Synergism between p68 RNA helicase and the transcriptional coactivators CBP and p300. Oncogene 22: 151-156.
210. Stevenson RJ, Hamilton SJ, MacCallum DE, Hall PA, Fuller-Pace FV (1998) Expression of the 'dead box' RNA helicase p68 is developmentally and growth regulated and correlates with organ differentiation/maturation in the fetus. J Pathol 184: 351-359.
211. Kahlina K, Goren I, Pfeilschifter J, Frank S (2004) p68 DEAD box RNA helicase expression in keratinocytes. Regulation, nucleolar localization, and functional connection to proliferation and vascular endothelial growth factor gene expression. J Biol Chem 279: 44872-44882.
212. Nicol SM, Causevic M, Prescott AR, Fuller-Pace FV (2000) The nuclear DEAD box RNA helicase p68 interacts with the nucleolar protein fibrillarin and colocalizes specifically in nascent nucleoli during telophase. Exp Cell Res 257: 272-280.
213. Causevic M, Hislop RG, Kernohan NM, Carey FA, Kay RA, et al. (2001) Overexpression and poly-ubiquitylation of the DEAD-box RNA helicase p68 in colorectal tumours. Oncogene 20: 7734-7743.
214. Yang L, Lin C, Liu ZR (2005) Phosphorylations of DEAD box p68 RNA helicase are associated with cancer development and cell proliferation. Mol Cancer Res 3: 355-363.
215. Wortham NC, Ahamed E, Nicol SM, Thomas RS, Periyasamy M, et al. (2009) The DEAD-box protein p72 regulates ERalpha-/oestrogen-dependent transcription and cell growth, and is associated with improved survival in ERalpha-positive breast cancer. Oncogene 28: 4053-4064.
216. Wei Y, Hu MH (2001) [The study of P68 RNA helicase on cell transformation]. Yi Chuan Xue Bao 28: 991-996.
217. Yang L, Lin C, Liu ZR (2006) P68 RNA helicase mediates PDGF-induced epithelial mesenchymal transition by displacing Axin from beta-catenin. Cell 127: 139-155.
218. Mooney SM, Grande JP, Salisbury JL, Janknecht R (2009) Sumoylation of p68 and p72 RNA helicases affects protein stability and transactivation potential. Biochemistry 49: 1-10.
219. Newbold RF, Overell RW (1983) Fibroblast immortality is a prerequisite for transformation by EJ c-Ha-ras oncogene. Nature 304: 648-651.
220. Land H, Parada LF, Weinberg RA (1983) Tumorigenic conversion of primary embryo fibroblasts requires at least two cooperating oncogenes. Nature 304: 596-602.

221. Macpherson I, Montagnier L (1964) Agar Suspension Culture for the Selective Assay of Cells Transformed by Polyoma Virus. Virology 23: 291-294.
222. Freedman VH, Shin SI (1974) Cellular tumorigenicity in nude mice: correlation with cell growth in semi-solid medium. Cell 3: 355-359.
223. Diaz VM, Bachi A, Blasi F (2007) Purification of the Prep1 interactome identifies novel pathways regulated by Prep1. Proteomics 7: 2617-2623.
224. Jalal C, Uhlmann-Schiffler H, Stahl H (2007) Redundant role of DEAD box proteins p68 (Ddx5) and p72/p82 (Ddx17) in ribosome biogenesis and cell proliferation. Nucleic Acids Res 35: 3590-3601.
225. Segal E, Friedman N, Koller D, Regev A (2004) A module map showing conditional activity of expression modules in cancer. Nat Genet 36: 1090-1098.
226. Serrano M, Lin AW, McCurrach ME, Beach D, Lowe SW (1997) Oncogenic ras provokes premature cell senescence associated with accumulation of p53 and p16INK4a. Cell 88: 593-602.
227. Negrini S, Gorgoulis VG, Halazonetis TD (2010) Genomic instability--an evolving hallmark of cancer. Nat Rev Mol Cell Biol 11: 220-228.
228. Delval S, Taminiau A, Lamy J, Lallemand C, Gilles C, et al. (2011) The Pbx interaction motif of Hoxa1 is essential for its oncogenic activity. PLoS One 6: e25247.
229. Krosl J, Baban S, Krosl G, Rozenfeld S, Largman C, et al. (1998) Cellular proliferation and transformation induced by HOXB4 and HOXB3 proteins involves cooperation with PBX1. Oncogene 16: 3403-3412.
230. Fernandez LC, Errico MC, Bottero L, Penkov D, Resnati M, et al. (2008) Oncogenic HoxB7 requires TALE cofactors and is inactivated by a dominant-negative Pbx1 mutant in a cell-specific manner. Cancer Lett 266: 144-155.
231. Huang H, Rastegar M, Bodner C, Goh SL, Rambaldi I, et al. (2005) MEIS C termini harbor transcriptional activation domains that respond to cell signaling. J Biol Chem 280: 10119-10127.
232. Schroder M (2009) Human DEAD-box protein 3 has multiple functions in gene regulation and cell cycle control and is a prime target for viral manipulation. Biochem Pharmacol 79: 297-306.
233. Bessa J, Tavares MJ, Santos J, Kikuta H, Laplante M, et al. (2008) meis1 regulates cyclin D1 and c-myc expression, and controls the proliferation of the multipotent cells in the early developing zebrafish eye. Development 135: 799-803.
234. Lu Q (2005) Seamless cloning and gene fusion. Trends Biotechnol 23: 199-207.
235. Dignam JD, Lebovitz RM, Roeder RG (1983) Accurate transcription initiation by RNA polymerase II in a soluble extract from isolated mammalian nuclei. Nucleic Acids Res 11: 1475-1489.
236. Shevchenko A, Wilm M, Vorm O, Mann M (1996) Mass spectrometric sequencing of proteins silver-stained polyacrylamide gels. Anal Chem 68: 850-858.
237. Rappsilber J, Ishihama Y, Mann M (2003) Stop and go extraction tips for matrix-assisted laser desorption/ionization, nanoelectrospray, and LC/MS sample pretreatment in proteomics. Anal Chem 75: 663-670.

6. Acknowledgments

I could not succeed to finish my PhD thesis and may not have gotten to where I am today without the invaluable and admirable support of several people, especially the ones I am about to mention.

This PhD thesis was carried out in the laboratory of Professor Francesco Blasi at the IFOM-IEO campus, Milan, during the years 2009-2012. Foremost, I am extremely grateful to my supervisor Professor Francesco Blasi who gave me the opportunity to start my scientific career in his laboratory and allowed me to work on the amazing Meis1-Prep1 project. Thank you for the kind guidance, warm encouragements, valuable ideas, time, responsibility, and trust that you have given me, and for the freedom to pursue independent work, make my own mistakes, and learn.

I have been very fortunate to have Elena Longobardi in every day lab life. Her endless support, advice, and patience are deeply admirable and have been central for this work. You have always found time for me despite your busy schedule, and your help has been invaluable. I am extremely thankful to you. You are also thanked for the critical reading of the thesis.

Professor Stefano Casola and Professor Eric so, the internal and the external co-supervisors of this work, are acknowledged for the scientific support, critical review of the thesis and for the valuable comments that improved this thesis. Dr Diego Pasini from IFOM-IEO campus and Professor Gordon Peters from UK cancer research institute are thanked for accepting to act as examiners in the occasion of thesis defance.

During these years I have had chance to work with great colleagues. All former and current FB lab members are thanked for the shared times in the lab and for the advise and for the help. The former members, Luis Fernandez-Diaz and Giorgio Iotti are warmly thanked for their excellent ideas, important advices, and all the inspiring discussions. I am

especially thankful to Audrey Laurent for all the scientific and not-scientific discussions. Thank you also for the unforgettable favor you made for me on the last August.

Valentina Pirazzoli is acknowledged for her kind teaching and supporting me to my first approach into the mice handling and subcutaneous injection. I am very grateful to all the facilities at the IFOM-IEO campus. Especially, Paolo Soffientini from mass spectrometry unit is thanked for his kind help and support.

I truly appreciate all my friends outside the lab for the good times shared, which was helpful for me throughout this project by taking thoughts off work.

A very special thanks goes to Mio Sumie for her kind daily support which made the life in Italy much more easier and enjoyable. Francesca Fiore and Veronica Viscardi are warmly appreciated for their help and support of SEMM PhD students.

My heartfelt appreciation goes to my parents and to my family who have been supporting and encouraging during these years. You have always let me make my own choices and supported me in all my decisions. Thank you for always believing in me, also when I didn't.

Deeply-felt thank you goes to my husband; my companion and love. Your daily support has been crucial for me during this project. Thank you for always listening and encouraging me, for understanding me and for being patient with me.

Finally, I thank Umberto Veronesi Foundation for their generous financial support during this thesis.

Milan, November 2012

Leila Dardaei